Silver nanocomposite material as antibacterial coating on indwelling medical devices-based biomaterials

Zohra Khatoon

A thesis submitted to the Faculty of Graduate and Postdoctoral Studies in partial fulfillment of the requirements for the degree of

MASTER OF APPLIED SCIENCE

in Biomedical Engineering

Ottawa-Carleton Institute of Biomedical Engineering

University of Ottawa

Ottawa, Canada

And

Bionanomaterial Chemistry and Engineering Laboratory

University of Ottawa Heart Institute

Ottawa, Canada

Fall 2018

Abstract

The most common type of adverse events in healthcare in Canada reported by the Canadian Institute for Health Information (CIHI) are nosocomial infections. Amongst nosocomial infections, implant associated infections have been reported to be most common. Despite having the implantation surgeries carefully performed, a small, but still considerable number of devices gets colonized by bacteria resulting in implant associated infections and/or surgical site infections. The patients are then started on high dose antibiotics, which if ineffective, is followed by reimplantation surgeries that leads to long hospital stays and detrimental effects in their lives. Due to this, an alternative to antibiotics is required which could prevent and/or treat bacterial colonization on implants. The main objective of this thesis was to demonstrate the effectiveness of an antimicrobial based CLKRS peptide capped silver nanoparticle coating on a metallic and polymeric based biomaterial used in various implantable medical devices. The CLKRS peptide capped silver nanoparticle formulation was specifically engineered and tested for its antibacterial and antibiofilm properties. Silver nanoparticles were synthesised by photochemical reduction of silver ions upon photocleavage of the photoinitiator I-2959. The metal nanostructure surfaces were protected with the CLKRS peptide and tested on planktonic and biofilms of *P. aeruginosa, S. aureus* and *S. epidermidis*. The bacterial quantification was done by survival colony counting. The cytotoxicity of the silver nanoparticle formulation was also tested on human dermal fibroblast, mouse bone marrow derived macrophages, and human epithelial cells by cell proliferation assay. Results show the formation of a nanometric layer of nanosilver on the surface of the material inhibiting the growth of bacteria and eradicating pre-existing biofilms with no significant cell toxicity suggesting the prepared formulation could be a useful tool in preventing and controlling infections on implants during surgery and post implantation. This technology thus could serve as an alternative therapy for surgical site infections and/or implant associated infections.

Acknowledgments

It is my genuine pleasure to acknowledge several people who were instrumental in the completion of this thesis. Firstly, I would like to profoundly thank my thesis supervisor Dr Emilio I. Alarcon who was not only supportive and motivating, but also patient, amicable and understanding. I am very grateful to him for providing me with an opportunity to pursue research in such a fascinating field. With losing my father during the program, it has not been an easy journey for me, but with Dr Alarcon's support, encouragement and guidance, I was able to complete my thesis. His constant faith in me has helped me improve my learning curve and urged me to do better each time, despite many obstacles, for which I owe him a lot. It is not easy to find such a considerate and generous supervisor.

I would like to express my sincere gratitude to my team members whose assistance, suggestions and motivation helped me throughout the project. I would like to specially thank Dr Manuel Ahumada who was not just a postdoc in the lab but also a friend. He helped me a lot when I first joined the team and made me feel very welcomed. I would like to sincerely thank him also for his guidance (especially with formation of experiment models), suggestions and input in this project. His and the teams' previous work helped shape this project. I would like to thank Dr Christopher McTiernan, Dr Marcelo Munoz, Dr Katsuhiro Hosoyama, Dr Veronika Sedlakova, Sarah McLaughlin and Cagla Cimensi for their precious advices and skillful guidance regarding the presentation of my work and formation of the experiment models, amongst other things. I would to like to thank Caitlin Lazurko, Erik Jacques, Keshav Goel, David Cortes and everyone else in Dr Alarcon's and Dr Suuronen's team who have helped me in various ways including sharing their knowledge with me. All my lab mates have been good friends and cooperative teammates with whom I've had fun too while efficiently working as a team. It has been such a pleasure working with them.

I would like to express my gratitude to Dr Thien Fah Mah and Ms Li Zhang for sharing their valuable input in the bacteriology part of this project. I would like to also acknowledge other facility personnel for obtaining images and data used in this project.

I am also grateful to Dr Tofy Mussivand who motivated and guided me to research when I first arrived in Canada. I had taken one of his courses in the first semester and he was very

helpful at the start of my master's program. I would like to thank all my other course professors for their helpful lectures and for providing me with enough time to simultaneously work with the course projects and the research project.

I would like to acknowledge Canadian Institute of Health Research (CIHR) and Natural Sciences and Engineering Research Council of Canada (NSERC) for their funding for this project.

Last but not the least, I would like to express my profound gratitude to all my friends and family who didn't let me get discouraged and give up with my satisfactory, but not splendid performance. They have also helped me cope with the anxiety and depression and helped me remain focused on the tasks at hand.

Dr Alarcon's consistent motivation has helped me keep the passion of learning and pursing research. His wisdom and personal experience have helped me understand life and he will always be a huge and a very important part in the success of all my future academic endeavours.

Table of Contents

List of Abbreviations

1	CLKRS	A pentapeptide with sequence cys-leu-lys-arg-ser
2	CIHI	Canadian Institute for Health Information
3	CDC	Centres for Disease Control and Prevention
4	EM	Electromagnetic
5	NP	Nanoparticle
6	AgNP	Silver nanoparticle
7	CLKRS@AgNP	CLKRS capped silver nanoparticle
8	I-2959	Irgacure-2959
9	SPB	Surface plasmon band
10	SSI	Surgical site infections
11	ICD	Implantable cardioverter defibrillator
12	APTES	(3-Aminopropyl)triethoxysilane
13	PDI	Polydispersity index
14	FWHM	Full width half maximum length
15	SEM	Scanning electron microscope
16	TEM	Transmission electron microscopy
17	Cryo-SEM	Cryo-scanning electron microscopy
18	DMEM	Dulbecco's Modified Eagle Media
19	ROS	Reactive oxygen species
20	DLS	Dynamic light scattering
21	ONC	Overnight culture
22	GFP	Green fluorescent protein

List of Figures

List of Tables

Chapter 1- Introduction

The advent and extensive use of implants or indwelling medical devices today has given rise to implant associated infections. These infections are usually caused by bacterial biofilms, which are the defensive adherent state of bacteria. Biofilms are difficult to treat or eradicate as they exist on the surface of the implants within an exopolysaccharide matrix that protects them from antibiotics and the host's immune system. This mechanism has contributed towards the rise of antibiotic resistant strains, making antibiotics less effective as a treatment. Thus, an alternative treatment is required to prevent and/or control biofilm causing implant associated infections. One such technology is using silver nanoparticles that have been shown to be antimicrobial and biocompatible in previous studies. Before further discussion, a fundamental background information is provided explaining biofilms and nanoparticles.

1.1. Background

Biofilm

Bacteria, which is one of the most common microorganisms, exists in two life forms, one as single free floating cells (*a.k.a.* planktonic) and the other as a group attached to a surface called sessile aggregates or biofilm.[1] Both bacterial states have been present on earth since the first bacteria evolved, however, the first observation of surface associated bacteria was made by Anthony van Leeuwenhoek in 1684.[1] Photomicrographs of aggregating bacteria was presented by Henrici in 1933[1] and the first use of the term biofilm was done by Rogovska et al in his article on environmental microbiome in 1961.[1] In the medical field, clumps or aggregates of bacteria was described by N. Hoiby in 1977 and the term biofilm was used and defined by Costerton et al in 1978.[1] The American Society for Microbiology recognised the significance of biofilm in 1993, as a result they were studied and accepted as an important bacterial characterisic.[1] In 1999, Costerton et al defined biofilm as "a structured community of bacterial cells enclosed in a self-produced polymeric matrix, adherent to a surface".[1] Biofilms can form on both biotic (living thing such as a surface of animal tissue or organ) or abiotic surfaces (non-living thing such as a surface of biomaterial). When planktonic bacteria comes in contact

with a surface, especially in an aqueous environment, it starts attaching to the surface.[2] The attachment is commonly seen on a conditioning film consisting of nutrients such as proteins, polysaccharides etc., which is formed on living tissues or surfaces of indwelling medical devices.[3] In 2004, Jefferson described four driving forces due to which planktonic cells attach and forms biofilm, which is default mechanism, defence mechanism (to protect themselves from antibacterial agents and other pathogens), existence as community (better chances of survival), and for obtaining favourable habitat.[2] Conditioning film is usually formed on surfaces of all indwelling medical devices which in turn makes the formation of biofilm on it common.

Biofilm formation is a complex multistep cyclic process involving various bacterial species,[3-4] stages of formation, involved interactions and multiple layers, whose colonisation accounts for ≈ 80% of total microbial infections in the human body, including prosthesis and indwelling medical devices.[3, 5-8] As described by Costerton et al, biofilm resides in a self-produced exopolysaccharide matrix which decelerates diffusion of antibiotics and host immune system thereby increasing drug resistance[8], hence treating them becomes a challenge. Prosthesis and indwelling medical devices can get infected either immediately after surgery or post-surgery due to the surface characteristics of the implant (surface area, surface roughness etc.), biomaterial composition, surgical equipment, from the patient itself, contaminated disinfectants or from other persons.[3, 9] Also, due to lack of vascularization, implants are more easily infected than other tissues or organs of the body. Two major challenges in treating biofilm are the difficulty of early diagnosis due to lack of suitable biomarkers and difficulty in their eradication due to their high tolerance to antibiotics.[10] The bacterial biofilm are ≈ 1000 fold more resistant to antimicrobial agents compared to their planktonic state.[11] The biofilm is tolerant towards an antibacterial therapy when it is unable to proliferate under the therapy and is said resistant when it can grow under the therapy. There are various reasons that leads to tolerance and resistance of the bacterial biofilm which contributes in the difficulty in treating them. It has been said that the best possible solution of biofilm causing infections is prevention of initial attachment of the bacteria at the first place, that could prevent infection and their treatment.

Nanoparticles

Nanotechnology is the study of manipulating matter at a nanometer scale and according to the International Organization for standardization, nanoparticle that ranges from 1-100 nm is the fundamental component in fabrication of nanomaterials and nanostructures.[12] Metallic nanoparticles (NP) have different physical and chemical properties compared to their bulk metals such as different melting points, optical properties, mechanical strengths, catalyst function, electrical function, magnetic function, etc.[12-13] Amongst these properties, optical properties of the nanoparticles attract most investigators as they give important characteristics to the nanoparticles.[12] Metals consists of surface plasmons (collective oscillation of plasma/multiple electrons) which absorb light in the visible region of the electromagnetic (EM) spectrum when they are in size less than 100 nm.[14] The consequence of the interaction of the EM wave with the electron density of the metallic NPs give rise to an absorption band known as surface plasmon band (SPB), showing a peak at a specific wavelength of light indicating that the maximum interaction is in that region.[13]

There are various characteristics of the plasmon excitation, one being giving rise to colours.[12, 14] For example, 20 nm gold nanoparticle displays wine red colour upon absorption of light, a spherical silver nanoparticle shows a yellowish colour, while platinum and palladium nanoparticles shows black colour.[12] These colour displays are dependent on sizes and shapes of the nanoparticle and is said that change in absorbances or wavelength gives the measure of the particle size, shape and interparticle properties.[15] The other characteristic of plasmon excitation is conversion of light energy to highly localized heating at surface of nanoparticles. Plasmon excitation can be pulsed when the nanoparticle is exposed to laser and can be continuous when exposed to sunlight.[14] Metallic NPs can be used to transform light energy to chemical energy by formation of short-lived energetic electrons and enhanced electric fields which are usually generated near the surface of the nanoparticle.[13] The optical properties of the nanoparticles have driven research into studying its various potential applications in molecular sensing (using Surface Enhanced Raman Spectroscopy, surface plasmon resonance, surface enhanced fluorescence), catalysis, DNA detection, material engineering, creating ultrafast optoelectronics, targeting and killing cancer cells, treating biofilm causing infections including controlling HIV, wound healing, cardiac tissue repair, inhibition of production of

inflammatory cytokines, corneal and retinal regeneration, skeletal muscle regeneration, nerve regeneration etc.[14-20]

In metals, the excitation of electrons to higher energy levels that are largely available leads to high conductivity, which is a common property of metal.[14] When the light of a specific wavelength interacts with the surface of metal, the electric field component of the light couples with the electrons in the metal causing an instantaneous displacement of the electron density.[14] The light is absorbed forming periodic fluctuations of a positive and negative charges called surface plasmon polaritons.[14] The absorption of light differs in bulk metals and in their nanoparticles due to the flat structure and the size of the bulk metal.[14] The plasmons of nanoparticles cannot propagate since they are confined to a particle, hence they are called localized surface plasmons.[14] The SPB appears because of this collective motion of electrons upon interaction of light and surface of the nanoparticle.[15, 21] According to Mie theory, "the choice of metal, as well as size, shape, surrounding matrix, surface bound molecules and degree of aggregation of the particles determines the energy range or frequency of light that can excite the plasmons".[14, 21] For example, spherical silver nanoparticles (~4 nm) excite plasmon when light of approximately 400 nm is absorbed.[14] Similarly, colloidal solutions of spherical copper and gold nanoparticles excite plasmons when 530 nm and 560 nm light is absorbed respectively.[14] Due to the absorbances of light at these wavelength, the nanoparticles exhibit different colours, for example, when colloidal gold nanoparticle solution absorbs 560 nm upon irradiation, it absorbs light in the green region, hence displays its complementary colour which is red-purple.[12] Similarly, colloidal silver nanoparticle solution absorbs violet light (400 nm), hence displays yellow which is its complementary colour.[12] The optical properties of the nanoparticles can be modified by changing the physical property such as their size, shape, concentration etc., thereby modifying its application. The capping agent, also called as stabilizer, which is used to protect the NP surface also plays a role in determining the size of the NP, by controlling its growth and unwanted agglomeration.[15, 22]

1.2. Rationale

A medical device is an instrument, apparatus, appliance, tool or equipment used in prevention, diagnosis, treatment, mitigation, rehabilitation and/or generation of information of a disease

or medical condition (without the use of drugs).[23] The Medical Devices Bureau of Health Canada has recognized 4 classes of medical devices based on the level of control necessary to assure the safety and effectiveness of the device, which is slightly different from Food and Drug Administration that classifies the medical devices into 3 categories. Those four classes are:

1. Class I: Presents low risk to patients and do not require a license or requires lowest regulatory normative (such as surgical instruments, dental material etc.)
2. Class II: Require the manufacturer's declaration of device safety and effectiveness (such as contact lenses, ultrasound machines, medical catheters etc.)
3. Class III: Presents greater potential risk to the patient (such as orthopedic implants like bone cement, hip implant etc., hemodialysis machine, surgical meshes etc.)
4. Class IV: Presents greatest potential risk and is subject to in-depth scrutiny and premarket regulatory approval (such as cardiovascular implants like pacemakers, ventricular assist devices etc.)

The Therapeutic Products Directorate (TPD) is the governing body in Canada responsible for monitoring and evaluating the safety and effectiveness of medical devices through assurance of premarket review, post market approval surveillance and quality systems.[23] Prosthetic and indwelling medical devices are medical devices that are used to support, replace or repair a tissue, organ or any bodily functions that are lost or damaged in a trauma or disease. Prosthetic devices are usually attached to an organ of the body while indwelling medical devices are implanted within the human body. These devices may or may not be meant to be used as long as the human is surviving. Most prosthesis and indwelling medical devices are made of biomaterials which are broadly classified into metals, polymers, ceramics, composites and natural.[24] Orthopedic implants such as bone plates, wires, hip implant, screws and cardiovascular implants such as coronary stents, pacemaker and implantable cardioverter defibrillator (ICD) are usually made of metals and its alloys. Urinary catheters, heart valves, corneal implants etc. are usually made of polymers. Various other dental and orthopedic implants are made of ceramics and composites. The global implantable biomaterial market accounted for $79.1 billion in 2014 which is estimated to grow at compound annual growth rate reaching $133 billion in 2022.[24] The increase in use of biomaterial based medical devices

is associated with growing diseases and deteriorating life style (consumption of unhealthy food, increased accidents, increased demand in donor grafts and organs etc.).[24] Advancement in indwelling medical devices has also made implant associated infections common today while their treatment remains a challenge. Numerous books in the past decade have been published on biofilm causing infections, implant and biomaterials associated infections and some common strategies under research, including the use of silver nanoparticle, for its treatment, some of which is given by Barnes et al, Moriarty et al, H. Cao and G. Donelli.[25-28]

Bacterial infections including nosocomial infections (hospital acquired infections that appear within 2-30 days of hospital stay), surgical site infections (SSIs) (infections from surgeries at the exposed site of the body where surgery took place) and implant associated infections (infections from colonization of bacterial biofilm on the implant) is one of the most common and major issues in healthcare system worldwide. Today, treatment of implant associated infections involves delivery of high dose antibiotics and/or replacement of the implant. Both these treatments are not very effective as many bacterial biofilms are tolerant and/or resistant towards numerous antibiotics and if the device is surgically replaced, there is high probability for the new device to get infected too. These surgeries are costly, risky and deteriorates quality of life by increasing mortality and morbidity rates. Bacterial contamination on indwelling medical devices can also be life threatening[29] leading to chronic infections and contributing to device failure.

The first report of healthcare associated infection rates was published by Centres for Disease Control and Prevention (CDC) in 1970s, and has been published constantly since then using standards methods and definitions.[30] In early 2000s, nosocomial infections accounted for 2 million cases of infections and 90,000 deaths in the US alone,[31-32] out of which medical devices associated infections occur 50-70% of all nosocomial infections.[32-35] In 2007, CIHI reported nosocomial infections to be the most common type of adverse events in healthcare in Canada too.[36] There is an estimated 220,000 cases of nosocomial infections resulting in more than 8000 deaths every year in Canada.[36] The common post-operative complication is surgical site infections, constituting between one fourth and one third of all nosocomial infections, which accounted for 6-23% in most studies.[37-40] In the US, it is estimated that more than 500,000 SSIs occur each year, at a rate of 2.8 per 100 operations.[40] Data from the National

Cardiovascular Data Registry (NCDR)-ICD registry show that 47% of patient with the ICD implant underwent repetitions of surgeries due to device upgrade, end of battery life and systemic infections, within a year.[41] Although prosthetic joint infection is found to be rare, it has been shown that mortality rate due to infected prosthesis removal is around 2.7-18% in US.[42] In a recent Dutch multicentre surveillance study, infection rates in total hip prosthesis was found to be 3% and total knee prosthesis 4.1%.[39] Treatment of infected prosthesis removal and antibiotic therapy is often estimated to be more than $50,000.[42] Hence, urgent need of treatment to infections is required to control the morbidity and mortality rates arising from acute and chronic infections worldwide, which would be an alternative to antibiotic.

As explained below in the literature, silver has been known for its bactericidal properties since ancient times. The application of silver nanoparticles in treating biofilm causing infections has given rise to various potential therapies that are widely studied today.

The novelty of this project was the use of a pentapeptide with the following amino acid sequence: cysteine-leucine-lysine-arginine-serine, referred to as CLKRS peptide, as a capping agent to protect the silver nanoparticle (AgNP) surface. Poblete et al showed that the pentapeptide CLKRS had high affinity to bind with the surface of AgNP in comparison to other pentapeptides and citrate.[43] Thus, this peptide, which is cost effective, can be used to produce AgNP with sizes 5-45 nm by varying the concentration of the peptide from 0.5 to 5 μM.[43-44] The peptide is also shown to be stable in solution even at ~100°C for the first 45 min, which is very useful when applying the AgNP in range of temperatures.[44] Since the peptide has smaller chain of amino acids, it is also easier to produce. The CLK collagen like peptides have also shown to produce stable biocompatible hybrid materials that can allow cell proliferation of dermal fibroblasts and has been shown to prevent bacterial infection by *P. aeruginosa*.[44] Hence, the CLKRS peptide was used to stabilize, protect and control the size of the AgNPs.

1.3. Literature review

A literature review is provided further on prevalence of biofilm formation on implants, the antimicrobial properties of the AgNPs, various kinds of synthesis methods of AgNPs, along

with describing the synthesis mechanism used in this project and various studies that has used AgNPs to prevent and treat bacterial infections. This review provides an overview of studies that has been done previously, which was useful in understanding and shaping this project. Finally, the objective and hypothesis of this project has been stated at the end of chapter 1.

1.3.1. Prevalence of biofilm formation on indwelling medical devices

The current inability to effectively treat biofilms, that cause chronic infection, makes this an important research area. As mentioned above, there is no ideal treatment to deal with it today, hence there are various researches underway to address this issue, such as use of electric and electromagnetic field to dissolve the cell membrane of the bacterial cells, hence eradicate them[45], use of antibiotic and antibacterial coatings[46], use of biosensors for early diagnosis[47], ultrasonication in combination with antibiotics[48], surface modifications of biomaterials[49], antimicrobial photodynamic therapies[50] and various other studies are on-going to develop a treatment to prevent and control implant associated infections. Studying the epidemiology of implant associated infections is important as it conveys the significance and scope of the above-mentioned researches. Table 1 summarises the infection rate of some indwelling medical devices mentioning the species that colonize the corresponding biomaterials and the routes through which it is commonly colonized. Thus, this informs us on: 1) the most common implant that gets infected, 2) common routes of those infections, 3) common species that colonize the corresponding device and 4) biomaterials that are commonly used in manufacturing such devices.

Table 1: List of infection rate, infection route and biomaterials used in some common indwelling and prosthetic medical devices

Indwelling and prosthetic medical device	**Biomaterials used**	**Colonizing infectious species**	**Time taken to cause infection**	**Infection rate**	**Routes of infection**	**Ref**
Central venous catheters (Class II-Class III)	Silicone, Polytetrafluoroethylene (PTFE), Polyurethane and Polyvinyl chloride	*S. epidermidis, S. aureus, C. albicans, P. aeruginosa, K. pneumoniae*	Within 10 days	3-14%	1. Through the wound created to insert the catheter 2. Through a contaminated catheter hub 3. Directly from bloodstream (BS) infection 4. Through contaminated infusate	31, 51-52
Prosthetic heart valves (Class IV)	PTFE, pyrolytic carbon	*S. aureus,* Streptococci, gram negative bacilli, candida species, enterococci and diptheroids	Can be immediate causing surgical site infection	1-4%	1. Can be from BS infections 2. Heart valve infections are common in patients with repetitive history of endocarditis or frequent surgeries	32, 51, 53
Cardiac pacemakers and ICDs (Class IV)	Ti, metal alloys, polyurethane	Coagulase negative staphylococci, *S. aureus,* pyogenic bacteria, *P. aeruginosa,* enterococci, *P. acnes*	2 weeks to 6 months	0.13-19%	1. From skin infections by staphylococci species 2. Through BS infections and is common in elderly 3. Can also occur from endocarditis patients carrying multiple lead devices	31-32, 54-64
Ventricular assist device (VAD) (Class IV)	Ti-Al-V alloy, Ti, polyurethane, porcine heart valves, polyester, ceramic materials	Staphylococci, enterococci, pseudomonas species, candida species	1 month-1 year	13-80%	1. Colonization can be initiated by mechanical disruption of the tissue and the driveline (cable connecting the VAD and its controller) 2. From BS infections which can also be caused from VAD colonization	32, 54, 65-66
Urinary catheters (Class II-Class III)	Tubular latex, silicone	*S. epidermidis, E. coli, P. mirabilis, P. aeruginosa,*	2 days to 6 weeks	26.6-35%	1. Can be colonized from the urethral meatus or within the drainage system	31, 34, 51, 53,

		K. pneumoniae, E. faecalis			contaminating the drainage bag and disrupting the catheter tubing junction 2. It can lead to urinary tract infections	58, 67-68
Intra uterine devices (Class II-Class III)	Plastic monofilament, nylon, Cu	*L. plantarum, S. epidermidis, C. albicans,* enterococci, *S. aureus,* streptococci, *A. israelii*	3-4 weeks	1%	The tail portion of IUDs is considered the primary source of contamination	51, 53, 69-71
Contact lenses and corneal implants (Class II-Class III)	Silicone hydrogel, Polymethyl methacrylate (PMMA)	*S. epidermidis, E. coli, P. aeruginosa, S. aureus,* proteus species, serratia species, candida species	Can develop immediately to several weeks	2.5-6%	1. Either by direct contact with lenses or via lens cases 2. It is also mediated by other risk factors such as age, gender, extended wear etc.	34, 51, 53, 58, 72-73
Peri implantitis and periodontitis (dental implants – Class I-Class II)	Acrylic resin, Ti and its alloys, zirconia	Veillonella species, F. nucleatun, A. naeslundii, Streptococci, *C. albicans, S. sanguinis, P. gingivalis, E. timidum, E. brachy, P. anerobicus*	Can develop immediately to 14 years	10-56%	Dental plaque, dental caries and oral microbiome are the main sources of colonization	4, 34, 51, 53, 58, 74-81
Orthopedic implants (Class III-Class IV)	HMWPE, PMMA, ceramics, Co, Cr, Ti, stainless steel and other metals &its alloys	*S. epidermidis,* streptococci, enterococci, *P. mirabilis, E. coli, P. aeruginosa, P. acnes, MRSA*	Early infection: 3 months or less Late: 3-24 months Secondary: After 24 months	5-40%	1. At time of implantation through direct inoculation or from airborne contamination of wound or device 2. From BS infections or adjacent focus of infection	31-32, 38, 53, 58, 73, 82-90
Breast implants (Class IV)	Silicone gel within silicone rubber envelope, inflatable saline	*S. aureus,* Enterococci, *S. epidermidis, P. acnes,* diptheroids	20-280 days	1-35%	Skin microflora during surgery is the most common origin of infection, other routes include 1. Contaminated implant or surgical environment 2. Skin penetrating accidents 3. Local soft tissue infections 4. Breast trauma and seeding of implant from remote infections	27, 32, 34, 56, 65, 91

1.3.2. Antimicrobial properties of silver nanoparticles

Silver has an ancient history for its antibacterial properties, known since the ancient Romans and Phoenicians (before 5th century) stored drinking water in silver containers.[14] The first person to use silver as an antimicrobial and anti-infective agent is believed to be Vonnaegele, who contributed much to controlling and treating infections with silver until the discovery of antibiotics.[20, 92] Hippocrates (~300 BC) used silver preparations to treat ulcers and promote wound healing.[20] Before and during the 20th century, ionic silver served important antibacterial uses such as prophylactic eye drops for newborns against gonorrhea and other bacterial/fungal infections, providing 'silver baths' to prevent biofilm formation in burns patients, treating syphilis with silver salvarsan, treating brain infections etc.[18, 20] Today clinically, silver is still used for treating infection with use of silver nitrate eye drops, silver sulfadiazine ointment for topical use etc., although not globally.[18] With flourish of discovery and use of antibiotics, application of silver reduced as silver showed to be cytotoxic affecting the living animal tissues to some extent, while antibiotics seemed to be a better treatment.[20] However, in the past decade, most antibiotics have contributed to development of antibiotic resistant bacterial strains reducing the efficacy of the antibiotics.[20] Thus, the need for treatment of infections, alternative to antibiotics, rediscovered silver nanoparticles and its antibacterial properties. It has shown to be antibacterial (affecting both gram-positive and gram-negative bacteria), antiviral and antifungal that can potentially treat infections caused by bacteria, fungus and viruses, while remaining non-cytotoxic.[15, 20]

The exact mechanism of action for the antibacterial activity of silver is not clearly understood but the application has been widely studied and reported.[20] Today, researches mainly focus on determining the efficacy and safety of the AgNP so as to transfer its antibacterial application to clinical setting. However, it is important to understand the mechanism of antibacterial activity as it can help in minimising the limitations of the use of silver and AgNPs. The interactions of AgNP with the microbial organism (such as bacteria) critically depends on the surface composition of the NP and the nature of the organism, i.e., whether it is gram positive bacteria or gram negative bacteria, as they differ in their intrinsic characteristic in the outer membrane.[20] The suggested mechanism for the bactericidal effect of ionic silver is listed below:

1. Catalytic oxidation with nascent oxygen to form reactive oxygen species (ROS) that affect the membrane of the bacteria, hence disintegrating them.[20]
2. Complex formation of silver ions and thiol containing peptides present in the bacterial cell wall and cell membrane which inhibits the chain of respiratory system of the bacteria, as seen in *E.coli*, where silver inhibits the uptake of inorganic phosphate and causes efflux of phosphate, proline, glutamine, succinate and mannitol from the cells.[20]
3. Binding of silver ions to DNA and/or RNA, preventing DNA replication leading to blockage in the bacterial cell cycle and/or death.[20]

The suggested mechanism for the bactericidal effect of AgNP is listed below:

1. AgNP can not only bind to membrane bound targets but can also penetrate the bacterial cell and disintegrate them, by forming a strong complex with electron groups containing N, O, S and exhibit an elevated binding constant for thiol containing proteins on the membrane and the silver ions. Since it diffuses inside the cell, it binds with intracellular DNA and inhibits replication.[20]
2. AgNP can also attack the respiratory chain of the bacterial cell, hindering cell division, leakage of cellular metabolites and causing cell rupture.[20] This was supported by TEM images used by Sondi et al, where they showed nature of interaction between *E.coli* and AgNP of ~12 nm, providing high resolution images of accumulation of NPs in cell membranes and thus formation of pits in the membrane.[93] Moreover, Li et al provided evidence of membrane disruption and changes in permeability causing *E.coli* cell death by 5 nm AgNP.[94]
3. AgNP promotes cell disruption via hydroxyl radicals and other ROS by poisoning respiratory enzymes and components of the microbial electron transport system.[20]
4. Sometimes the AgNP undergo partial oxidation that leads to chemisorbed layer of ionic silver adsorbed onto the surface of the NP that helps in the bactericidal activity seen commonly in *E.coli*.[20]
5. Ahumada et al showed accumulation of peroxides by the human serum albumin (HSA) capped AgNP under oxidative stress along with demonstrating the NP

stability. The peroxides can potentially oxidize the cell walls of the bacteria and disrupt their chemical structures.[95]

AgNP was shown to be bactericidal when the particle size fall in narrow size range, as smaller NPs have high surface area to volume ratios and low surface energy, thus the relative release of silver maybe higher for smaller sized particles.[20] Therefore, the nature of capping agent plays a critical role in bactericidal effect as it controls the size of the NP. Not only this, the capping agent can also interact with the surrounding biomolecules followed by modification of cellular uptake and altered interaction with biological macromolecules[20], which sometimes can lead to aggregation of the NP at high ionic strength or low temperatures, as shown by Alarcon et al.[96] They showed AgNP capped with collagen type I (found to be more stable) and α-poly-L-lysine were effective in controlling *B. megaterium, S. epidermidis, E. coli* bacteria, however, AgNP coated with poly-L-lysine led to spontaneous aggregation, increasing the size of the NPs.[96]

Apart from size, concentration of silver is also important in determining the toxicity level to bacterial cells. Choi et. al. showed that AgNP of 14 nm in diameter inhibit nitrifying *E.coli* growth up to 86%, while silver colloids and silver ions inhibited the bacterial respiratory chain by 46 and 42% respectively, suggesting that at lower concentrations (seen in AgNP when compared to silver ions), AgNP can inhibit collective respiration of microbes within these communities with almost double of the efficiency, however, in this study no signs of membrane damage were observed in the bacterial wall by any silver species.[97] The total actual concentration of the AgNP in solution can be estimated by various methods and equipments (using initial silver content and other parameters), one being by the use of an algorithm called nanoparticle polydispersity corrector (NANoPoLC) that combines binding parameters of nanoparticle and reduces batch-batch variability by incorporating corrections to the total number of nanoparticles available in a sample.[98]

The antimicrobial efficacy of AgNPs has also been shown to be shape dependent in studies that utilized different shapes of AgNP and measured the toxicity level of the AgNP towards the bacteria. Studies showed that truncated triangular AgNP is most effective in inhibiting bacterial growth, as the triangular geometry needed around 1 μg of silver to exert bactericidal effect, while the spherical and rod shaped NPs needed 12.5 and 50-100 μg respectively.[20]

Another study showed that nanosilver wires significantly affected alveolar epithelial cells, while spherical NP had no effect, suggesting that shape of the NP also affects the toxicity level of mammalian cells.[99] Thus, it can be stated that bactericidal effect of the AgNP is directly dependent on the rate and location of release of silver from the NP which in turn is shape, size and physiochemical nature of capping agent dependent.[20, 22, 100-101]

In several studies, AgNP protected with different capping agents has shown to impact bacterial biofilms by killing the cells (studied when treatment is applied on pre-existing biofilm) and preventing biofilm formation (studied when treatment is applied before/during biofilm formation).[20] AgNP has also been shown to exert synergistic effect when combined by antibiotics as shown in multiple studies that used beta lactam amoxicillin, penicillin G, erythromycin, clindamycin, vancomycin in combination with 5-30 nm of AgNP to kill *E.coli* and *S. aureus* bacteria.[15, 20] Some studies have shown resistance of bacteria to silver ions; for example, McHugh et al showed *S. typhimurium* (isolated from burn patients who had been receiving topical treatment with 0.5% $AgNO_3$ solution) to be resistant to $AgNO_3$, mercuric chloride, ampicillin, chloramphenicol, tetracycline, streptomycin and sulphonamides.[102] Another study showed *P. aeruginosa* strain isolated from burn patients to be silver resistant which could have happened due to manipulation of a plasmid source.[103] Studies showing mechanism of developing of the silver resistant bacteria are quite few, which has been summarised to the formation of metal cation gene cluster consisting of periplasmic multi-metal-binding protein, chemiosmotic efflux pump and an ATPase efflux pump, which could lead to the resistance.[20] Although, resistance of bacteria to AgNP has not been shown so far and is believed that it might not be evolved, as their mechanism of attack against bacteria is through destruction of cells, preventing mutation of the bacteria[20], which was studied and supported by Zhang et al.[104]

Studies have shown toxicity of silver ions in primary skin cells and its immune supressing ability due to which use of colloidal and ionic silver is strongly ill-advised.[18] However, there is inadequate information on adverse effects of AgNPs on human health[15] which has provided hope in treating and controlling infections which can be explained due to its reduced fixed silver concentration and the ability of protecting the NPs with capping agents that helps in preventing interactions between the silver and live cells/tissues.[18] Also, while understanding

the killing mechanism of bacteria by the silver, some of those mechanism such as production of ROS can affect the living human cells as well, however, human cells (eukaryotic) are known to possess stronger protection mechanism against these species that lack in the bacterial (prokaryotic) cells.

Eukaryotic cells are usually larger and show high structural and functional redundancy compared to prokaryotic cells, hence higher silver concentrations are required to achieve comparable toxic effects than the prokaryotic cells.[105] Also, essential protein complexes of the bacterial electron transport chains are located on the cell exterior, therefore it is accessible for inactivation by reactive silver ions, whereas the same structures are found intracellularly in the mitochondrial organelles in eukaryotes, which requires higher silver concentration for comparable inactivation due to the diffusion barrier of the cell membrane.[105] The eukaryotic cells are also capable to phagocytose the AgNP subsequently degrading the particles by lysosomal fusion.[3] Furthermore, eukaryotic cells contain several mitochondria while the bacterial cells do not, thus they lack the ability to conserve their biological energy system under silver ion attack.[105] Hence, it can be suggested that a human cell can be able to defend itself from species like ROS, provided it is present in low concentrations. Moreover, silver in the metallic state gets easily oxidized by dissolved oxygen in solution which is prevented when the NP is capped with a protective agent, hence avoiding ionic silver infiltration within the mammalian cells.[18]

There are various roles of the capping agent apart from protection including attributing towards surface charge of the NP which in turn controls formation of complexes within biomolecules and dictates cell-nanoparticle interactions, thereby controlling toxicity of the NP.[18] Stability of NP can be assessed by calibrating number of live cells before and after treatment which can be done using cell membrane markers/dyes, redox activity sensors, cell proliferation assays etc.[18] There are various factors that determines the toxicity level of AgNP to primary cells including 1) NP size, concentration and polydispersity, 2) nature of capping agent and 3) NP stability in chosen cell culture media.[18] Various studies show that NP size controls the cell uptake mechanism which are divided into 2 major groups: simple and facilitated diffusion.[18] Studies have shown that AgNP can be made biocompatible or non-toxic to mammalian cells by using stable capping agents which controls cell-nanoparticle interactions. One of the benefit

of AgNP is that, it can be synthesized with control over silver concentration, NP lifetime and dose, in a way to obtain desired bactericidal effect without enhancing toxicity on host cells.[20] The delivery can be optimized with the release kinetics and by minimizing the additional release of silver ions beyond therapeutic dose.[20]

1.3.3. Mechanism of synthesis of silver nanoparticles

Properties of AgNPs differ from the bulk silver which is a noble, lustrous transition metal. As mentioned earlier, the optical properties of AgNPs depends on its size, shape, capping agent etc.[12, 106] Generally there are two approaches for synthesis of metal nanoparticles: *top down* approach (preparation of nanoparticles from break down of bulk materials) and *bottom-up* approach (combining molecules or atoms to form nanoparticles).[106] Figure 1 represents the various methods of synthesis of AgNP provided in the literature.

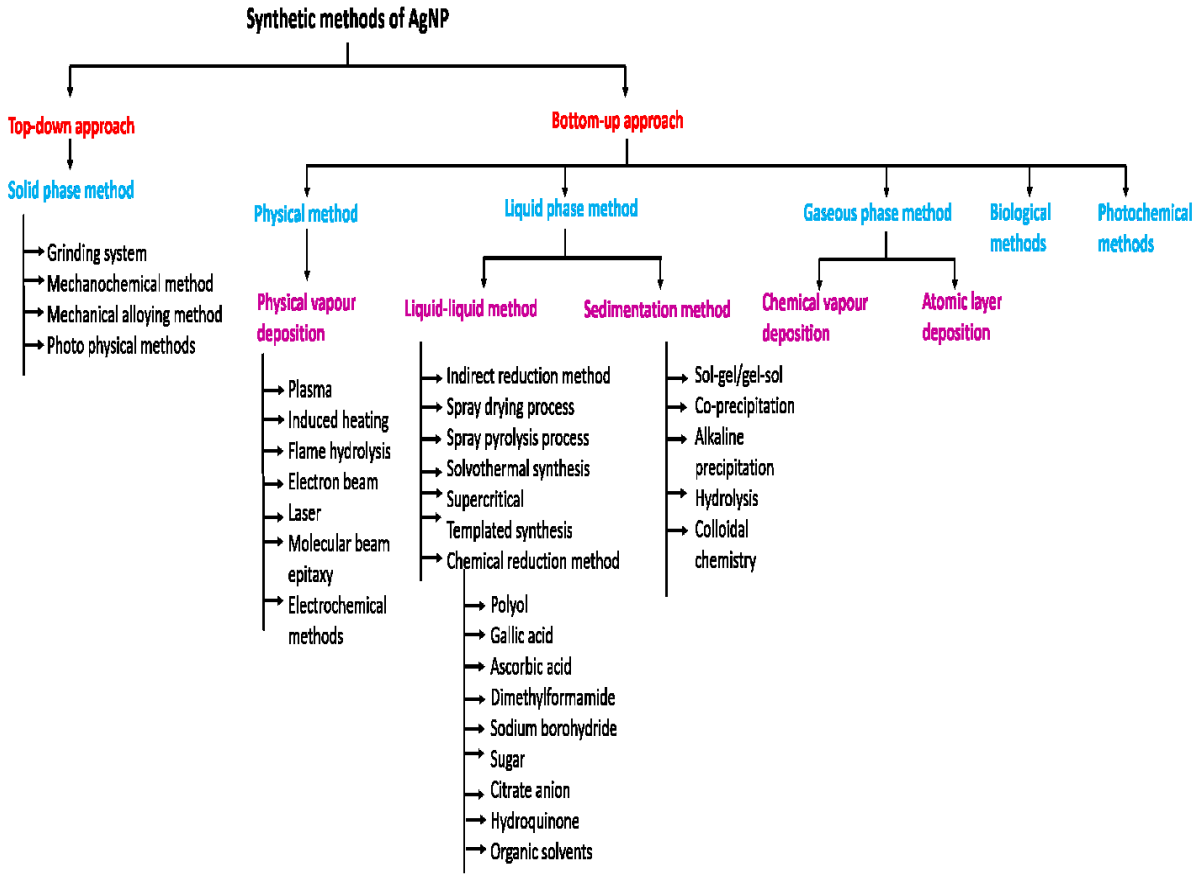

Figure 1: Some common methods of synthesis of silver nanoparticles.[12, 106]

From the various methods of synthesis provided in Figure 1, the most common and rational method to obtain AgNPs is the bottom-up approach using liquid phase, biological and photochemical methods.[106] A high quality synthesis procedure usually provides control over nanoparticle size and shape.[12] Sizes and shape of the NP affects the wavelength at which SPB occur, for instance, SPB of 5-10 nm of AgNP occurs at 400 nm while SPB of larger sizes of AgNP occur at longer wavelengths.[12]

In Dr Alarcon's lab, AgNPs are synthesized by photochemical methods by irradiating a mixture of 2-hydroxy-4'-(2-hydroxyethoxy)-2-methylpropiophenone (Irgacure-2959 or I-2959), silver nitrate and sodium citrate (stabilizer) in a UVA photoreactor with 14 UVA lamps. I-2959, which helps in the synthesis reaction, is a water soluble and highly efficient photoinitiator. A photoinitiator is a compound, usually organic, that cleaves to forms polymerization initiating species (free radical or ionic or both) upon absorbing light.[107]

Initially, the Irgacure acts as a photoinitiator upon irradiation and forms into free radicals of organic compounds including ketyl radicals by cleavage of its α-hydroxy ketone which are produced by Norrish type I photocleavage reactions.[16, 21, 106] The homolytic rupture of the α-cleavage bond of the two hydroxy groups is said to occur in picoseconds upon irradiation.[106] The ketyl radical reduces the silver ion, derived from silver nitrate, to produce silver nanoparticle seed, ketone and hydronium ions. This single seed reacts with the citrate anion to form a complex which upon aggregation forms silver nanoparticles capped with citrate as shown in Figure 2 and Figure 3.[106] The aforementioned method, promote the generation of spherical silver nanoparticle with a diameter of ~5 nm and shows yellowish colour as it absorbs light in the violet region of the visible spectrum, hence displays its complementary colour with a surface plasmon absorbance found at ~400 nm.[106] This size and shape of the silver nanoparticle is attributed to the fact that the electromagnetic field (EMF) generated at the vicinity of the silver nanoparticle is extremely high in comparison to other metal nanoparticles as their efficiency of electronic and vibration transitions increases.[21, 106] It is also stated that the size and strength of the resultant EMF induced around the particles upon excitation is proportional to the size of the particles.[21]

The benzoic radical formed from the homolytic bond scission forms into a stable carboxylic acid, i.e., 4-(2-hydroxyethoxy) benzoic acid, also called HEBA.[106] This molecule is found to contribute into stability of silver nanoparticles which don't get capped with the citrate.[106]

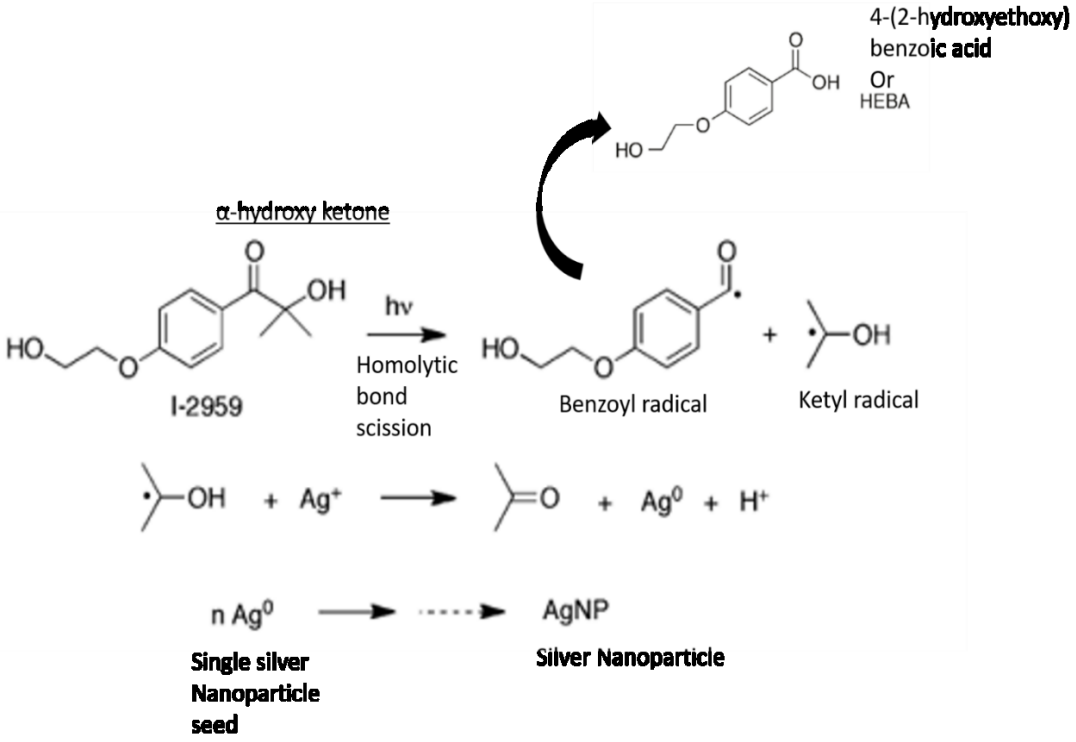

Figure 2: Mechanism of AgNP formation by reduction via photoinduced cleavage of I-2959 (figure reproduced from[16]).

From previous studies, it is shown that citrate can reduce the metal (silver) cation as well as stabilize the resulting nanoparticle.[108-109] It is also shown that it plays a role on determining the growth of the particles and its size and shape.[21, 110] One of the possible mechanism of citrate capping the silver nanoparticle was explained by Pillai et al.[110] It was described that once the silver nanoparticle seed has been formed from the reduction of silver ion, the citrate can form complexes with the metal surface, decreasing the total amount of citrate available in the bulk. Thus, fewer new seeds get capped with the citrate. The initial particles begin to grow by Ostwald ripening, in which smaller particles dissolve and redeposit onto larger particles, hence forming large stable nanoparticles as shown in Figure 3.[110]

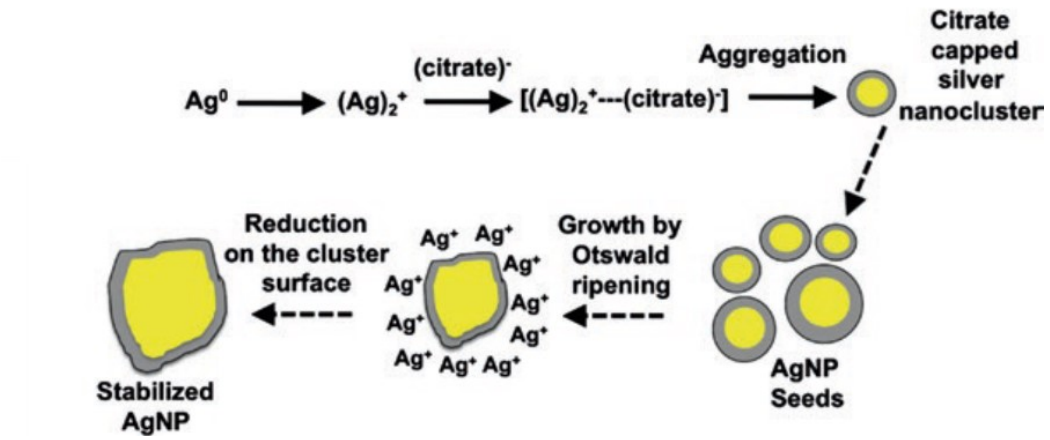

Figure 3: Mechanism of formation of citrate capped AgNP from reduced nanoparticle seed (figure reproduced from [110]).

This methodology is clean, fast, inexpensive and allows real-time kinetics monitoring by UV-vis spectroscopy,[106] that have excellent spatial and temporal control and is usually synthesized at room temperatures.[17] The yellow colour observed from the plasmon absorbance of the AgNP is also a characteristic of there being no surface oxidation of the silver.[111] This method produces a homogeneous solution of silver nanoparticles and allows modification of size and shape of the nanoparticle.[17, 106] One such example was shown by Stamplecoskie et al [21] where a broad diversity of morphologies of AgNP was achieved by simply changing the LED source to excite the plasma with different wavelength maxima. The AgNPs seeds capped with citrate (3.3 nm diameter) were irradiated with narrow band LEDs, thereby causing spectral changes and producing triangular AgNP plates with excitation of 590/627 nm LED light, larger spheres with 405 nm, decahedra shapes with 455 nm, hexagonal shapes with 505 nm and silver nanorods with 720 nm.[17, 21] Figure 4B shows the plasmon absorbance band of these shapes, which were derived from spherical AgNP seeds shown in Figure 4A.

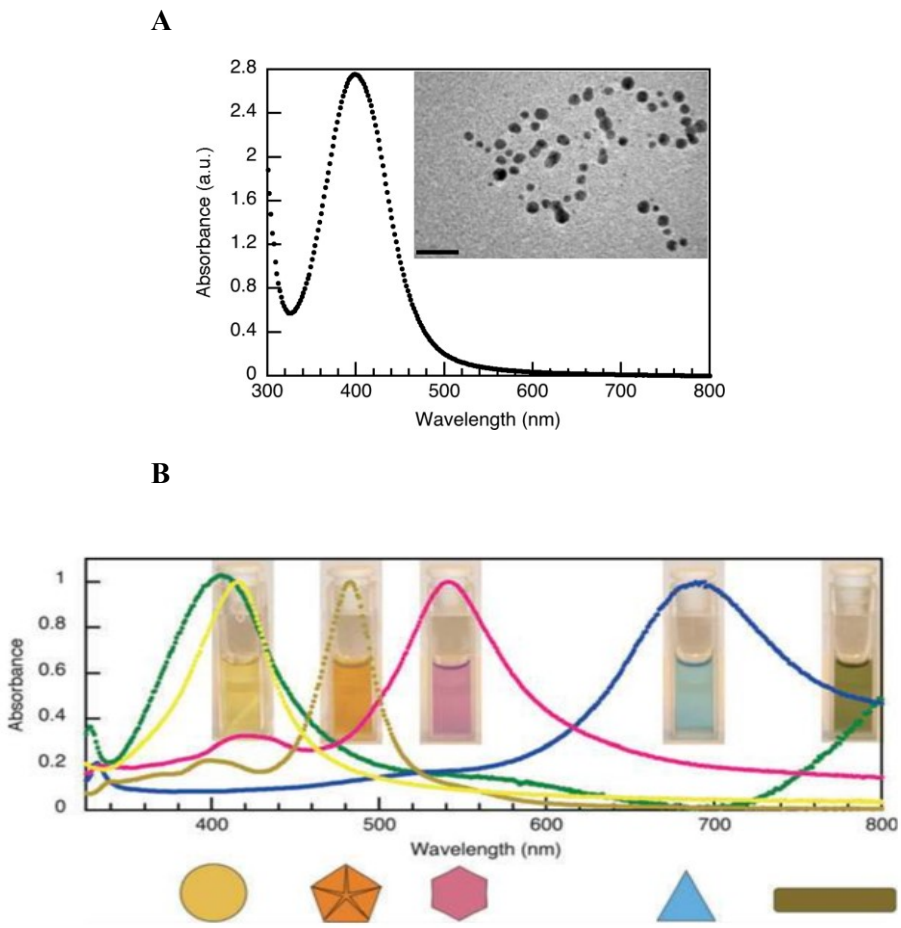

Figure 4: A) Typical plasmon band of citrate capped AgNP seed of size around 3 nm with TEM image at the side, **B)** Plasmon absorption band of each shape of AgNP produced from a solution of 3 nm of AgNP seeds by exposing to narrow band LEDs for different amount of time (figure reproduced from [17, 21]).

The above mentioned methodology allows the use of different capping agents along with citrate, such as biological materials like proteins, peptide etc.[106] From past studies, citrate has not been shown to be as stable as other peptides and collagen like proteins when used as capping agents.[96] Proteins like collagen, albumins, peptides and free amino acids with combinations of thiol in cysteine, lysine and arginine have shown to control the structure of AgNPs during synthesis and improve their stability under various conditions.[43] Thus, a high quality synthesis method is required to achieve desired characteristics of the AgNPs.

1.3.4. Treatment approaches to prevent and control biofilm on indwelling medical devices by application of silver nanoparticles

Because of the antibacterial property of the AgNPs, there has been numerous studies done to optimize the synthesis of AgNPs and its capping agent in a way to diagnose, prevent, eradicate, inhibit or/and control bacterial infections along with making it biocompatible. Application of AgNP has been extensively studied on various strains of bacteria that infect the environment (aquaculture, water, plants which in turns affects in the food industry), sewage pipes (leading to biofouling) and the human body (medical biofilms that causes acute and/or chronic infections in the clinical setting).

Table 2 summarises some studies done on applications of AgNPs on medical biofilms that can potentially infect the human body or implantable or prosthetic devices. These studies show the efficacy of AgNPs used for treating or preventing bacterial/biofilm growth. Some of these studies are reported in Table 3 that also tested on mammalian cells to study biocompatibility of the AgNPs. The synthesis method of the AgNPs, size and its capping agent has been listed in both the tables. If the study was done to prevent or treat implant associated infection, the biomaterial which was tested is also listed in Table 2. The microorganism and its state, i.e., whether the test was done on planktonic cells or biofilms or both, is listed in Table 2. Furthermore, the mammalian cells used in the cell viability test and its assay method is listed in Table 3. Finally, some main findings have been provided for each study listed.

Table 2: Summary of physical properties of AgNP, the microorganism and concluding comments of some reported studies (ND represents not done in the study and NA represents not available).

Synthesis method	**Size of NP (nm)**	**Capping agent**	**Biomaterial tested**	**Microorganism**	**Bacterial state tested**	**Conclusions**	**Ref**
Photochemical synthesis using Irgacure-2959	3 (TEM)	Human serum albumin (HSA)	ND	Kanamycin and tetracycline resistant *E. coli*	Planktonic state	1. Delay in bacterial growth observed 2. HSA showed to be stable, non-aggregating protective agent	[16]
Photochemical synthesis	19±1 (DLS)	LL37 peptide	ND	*P. aeruginosa, S. epidermidis, E. coli, S. aureus*	Planktonic state	1. LL37@AgNP showed to be stable 2. This treatment showed to be effective in preventing infection and promoting wound healing	[112]
Photochemical synthesis	50	Minimum essential alpha medium (α-MEM)	ND but potential application for orthopaedic implants	*S. epidermidis*	Planktonic state	Study showed antimicrobial efficacy of silver nanoparticles	[113]
Photochemical synthesis	4.4 ± 1 (TEM)	Type-I collagen @ rose bengal	ND	*S. epidermidis*	Planktonic state	AgNP@collagen controlled *S. epidermidis* growth	[114]
Photochemical synthesis using Irgacure	3.5 ± 0.04 (SEM)	1. Type-I collagen 2. α-Poly-L-Lysine	ND	*Bacillus megaterium, E. coli, S. epidermidis*	Planktonic state	1. AgNP prepared with type I collagen, displayed extraordinary stability 2. AgNP@collagen showed to be bactericidal against *Bacillus megaterium* and *E. coli* but only bacteriostatic against *S. epidermidis*	[96]
Photochemical method (UV light)	1. 20-25 2. 80-90 (TEM and DLS)	Gallic acid	ND	*E. coli, A. baumanii, P. aeruginosa, B. subtilis, M. smegmatis, M. bovis, S. aureus methicillin-*	Planktonic state	It showed that the 20–25 nm AgNPs have greater potential to be used as antimicrobial agents against microorganisms	[115]

				resistant,C. albicans, C. neoformans and A. niger			
Chemical reduction by ascorbic acid in chitlac solutions	33 ± 7.6 (TEM)	Chitlac	ND	*E. coli, S. epidermidis (clinical isolate), S. aureus and P. aeruginosa*	Planktonic state	1. Study showed that the NPs immobilized in the gel matrix can exert their antimicrobial activity by simple contact with the bacterial membrane, but they can not be up taken and internalized by eukaryotic cells 2. The polysaccharide Chitlac was found to be fundamental in the formation and stabilization of well-dispersed AgNPs	[116]
Chemical reduction by sodium borohydride	NA	1. Polyethylene glycol 2. Ethylenediamin etetraacetic acid 3. Polyvinyl pyrrolidone 4. Polyvinyl alcohol (PVA)	ND	*E. coli* and Pseudomonas species	Planktonic state	1. Zeta potential analysis of the PVA@AgNPs showed a value of 46.6 mV, indicating their high stability display 2. PVA@AgNP showed the highest antibacterial activity 3. PVA@AgNPs were chosen for use in an LSPR-based hydrogen peroxide sensor 4. This detection method was found to be simple, relatively inexpensive, reliable and can be suitably employed in medical and environmental monitoring	[117]
Photochemical synthesis using Irgacure	3.5 ± 0.04	Type I collagen	ND	*S. aureus, S. epidermidis, E. coli* and *P. aeruginosa*	Planktonic state and biofilms	1. Collagen capped AgNPs showed to be stable 2. Bactericidal activity was observed	[118]
Photochemical synthesis using Irgacure (Delivered as spray-on treatment)	NA	LL37-SH peptides	ND	*P. aeruginosa*	Planktonic and biofilm	1. Study showed AgNP stability 2. AgNP acts as an anti-infective and anti-biofilm 3. This is a potential application for prophylactics and infection control in infected wounds	[111]

Photochemical synthesis using Irgacure	19±1 (DLS)	CSG-LL37 peptide	ND	*P. aeruginosa, E. coli, S. epidermidis, S. aureus*	Planktonic and biofilm	1. Literature shows LL37 peptide displays antimicrobial activity but in this study LL37 did not enhance the antimicrobial effect of the AgNP which was supported by another study that showed that the antimicrobial activity and conformation of LL37 peptide is preserved in truncated peptides containing only the sequence LL7-37 2. LL37@AgNP retained the bactericidal properties of AgNP	112
Chemical reduction	8.0 ± 2.6	Pectin	ND	*E. coli, S. epidermidis*	Planktonic and biofilm	1. Result shows antimicrobial effect of pectin capped AgNP 2. Results suggests that applied treatment can be efficient for repairing wounds and/or to treat vulnerable surgical site tissues, including the pre-treatment of implants as an effective prophylaxis in implant surgery	119
Green synthesis method using glucose (in the presence of starch as stabilizing agent) and fructose	360± 17 (using fructose), 90±7 nm (DLS, TEM)	Polyacrylate-based hydrogel thin coatings on titanium	Titanium	*Staphylococcus aureus, Pseudomonas aeruginosa and E. coli*	Planktonic and biofilm	1. From this method, it was shown that the hydrogel coating can be easily fabricated on metallic implants of any size and shape through electrosynthesis 2. AgNPs can be embedded in a very simple and fast way exploiting the hydrogel film swelling properties 3. The preparation of the bio-active coating could be performed just before the implantation of medical device 4. Silver loading showed antibacterial activity	120
Green experimental methods	32 (NTA)	Cymbopogan citratus	ND	*S. aureus*	Planktonic and biofilm	1. AgNP showed enhanced quorum quenching activity against *S. aureus* biofilm and showed prevention of biofilm formation 2. Application of silver nanoparticle showed better results as compared to antibiotics Gentamicin and Chloramphenicol	121

Biogeneic synthesis/biosynthesis/ biological method	5-40 (TEM)	NA	ND	*Fungus Trichoderma viride, S. typhi, E. coli, S. aureus and M. luteus*	Planktonic	1. The antibacterial activities of ampicillin, kanamycin, erythromycin, and chloramphenicol were increased in the presence of AgNPs 2. The highest enhancing effect was observed for ampicillin against test strains	122
Ultrasonication	10-40 (TEM)	Proline functionalized graphene oxide	Graphene oxide-based biomaterials	*S. aureus, P. aeruginosa, C. albicans and S. cerevisia*	Planktonic	1. Showed effective antibacterial and antifungal property 2. Proline/graphene oxide nano-flakes demonstrated low lethality 3. This study may be a promising antibacterial and antifungal specialist for various biomedical applications	123
Chemical reduction using sodium borohydride	NA	NA	Zirconia capillaries	*E. coli*	Planktonic	It showed strong bactericidal properties with minimal silver release	124
Chemical bath based method	10.6 (TEM)	Composite films	ND	*E. coli*	Planktonic and biofilm	1. Minimal bacterial growth was detected over the first 12 h of testing 2. This study shows the development of a very thin AgNP based antibacterial coating for usage in the medical industry	125
NA	5-50	NA	Bone cement (PMMA) (applied mostly in joint arthroplasty)	*S. epidermidis,* methicillin-resistant *S. epidermidis*, and methicillin-resistant *S. aureus*	Planktonic and biofilm	1. Nanosilver bone cement completely inhibited the proliferation of *S. epidermidis*, MRSE, and MRSA 2. Gentamicin cement was not effective against MRSA and MRSE	105
Laser ablation methods	NA	Chitosan	Titanium	*S. mutans and P.gingivalis* of the oral cavity	Planktonic and biofilm	1. It showed synergistic effect with gentamicin and ceftazidime and displayed biocompatibility 2. The coating of titanium dental implants with Ag-chitosan nanoparticles may have an	126

						added advantage on the corrosion resistance of titanium dental implants	
Electrochemical anodization using a direct-current power supply	NA	NA	Titanium nanotubes	Methicillin-resistant Staphylococcus aureus (in vivo in a rat model)	Planktonic	This study showed antimicrobial and excellent bio-integration properties make it a promising therapeutic material for orthopedic application	[127]
Chemical reduction method	28-75 (DLS) 15-30 (SEM) studied on sphere, triangular and cuboidal NP	NA	ND	*Methicillin susceptible and resistant S. aureus*	Planktonic and biofilm	The geometry of the AgNPs did not significantly impact the susceptibility outcome of the attached *S. aureus* and MRSA for subsequent biofilm formation	[128]
Biosynthesis using soil bacteria under visible light	8-21	NA	Urinary catheter (polymer)	Coagulase Negative Staphylococci (*S. epidermidis and S. haemolyticus*)	Planktonic and biofilm	1. Significant antimicrobial and antibiofilm properties were observed 2. Surface engineering application of AgNPs on urinary catheter showed its excellent potential to prevent the attachment and colonization of CoNS which make this potent medical application	[129]
Wet chemical synthesis	NA	Diamond-like carbon (DLC)	Titanium discs	*S.aureus and S. epidermidis*	Planktonic and biofilm	This study indicates that the integration of silver nanoparticles into DLC prevents bacterial colonization due to a fast-initial release of silver ions, facilitating the growth of silver susceptible mammalian cells subsequently	[130]
Facile synthesis using aniline as a reducing agent	50-150	Carboxymethyl cellulose, sodium alginate (biopolymer)	ND	*S. aureus and E. coli*	Planktonic and biofilm	1. Significant antibacterial efficacy and antibiofilm activity of biopolymer capped AgNPs were demonstrated	[131]

						2. There is a potential for production of biopolymer capped AgNPs grown under microwave irradiation, which can be used for industrial and biomedical applications	
Chemical reduction	NA	Chitosan and Hyaluronic Acid	Titanium covered with phase-transited lysozyme	*S. aureus*	Planktonic and biofilm	Study demonstrated a promising strategy for fabricating long-term antibacterial multilayer coatings on titanium surfaces	[132]
Biosynthesis using Chlorellavulgaris.	9.8 ± 5.7 (TEM)	Silver chloride	ND	*S. aureus, Klebsiella pneumoniae*	Planktonic	1. Treatment showed 98% decrement in growth of the bacteria 2. It showed a potential method in treating infections with the advantage that the green synthesis of AgCl-NPs by microalgae is ecologically sound	[133]
Biogenic synthesis using gum kondagogu	5	Biopolymers	ND	*S. aureus, P. aeruginosa and E. coli*	Planktonic and biofilm	1. Treatment with nanoparticles caused cytoplasmic content leakage and membrane permeabilization in a dose dependent manner, an evidence for membrane damage of the bacterial cells 2. Study showed promising antibacterial activity	[134]
Biogenic synthesis using Coleus forskohlii	91.03 (DLS)	Coleous forskohlii	ND	*Proteus vulgaris, Micrococcus luteus*	Planktonic	Treatment was found to be stable in aqueous medium for a longer time and exhibited favorable anti-oxidant, anti-bacterial and anti-cancer activity	[135]
Biosynthesis using Syzygium cumini	NA	Syzygium cumini (S. cumini) (L.) Skeels	ND	*S. aureus, E. coli and Salmonella typhimurium*	Planktonic	Study shows that this treatment is environmentally friendly, cost effective and green approach for synthesizing AgNPs which were stable due to eugenols, terpenes, and other different aromatic compounds present in the extract that inhibited the growth of bacteria	[136]

Chemical reduction using glucose	NA	poly vinyl alcohol (PVA)	Titanium	*S. aureus*	Planktonic and biofilm	Study showed that the combination of silver nanoparticle with gallic acid and PVA on the titanium were the best performing samples in terms of antiinfection	[137]
Chemical reduction using dimethylformamide (DMF)	NA	(3-Aminopropyl) trimethoxysilane (APS)	Orthodontic resin	*S. mutans and streptococcus sobrinus*	Planktonic	1. AgNPs showed potent antimicrobial activity 2. The silver nanoparticles enables the resin to prevent oral pathogen (causing periodontitis) growth during orthodontic therapy	[138]
Photochemical synthesis	NA	NA	PMMA hydrogel	*S. aureus, E. coli*	Planktonic	The resulting hydrogels displayed good antibacterial properties	[139]
Biosynthesis using fusion of Mussel adhesive proteins (MAP) to a silver-binding peptide	NA	NA	Metal (titanium), plastic, and glass	*E. coli, Salmonella enterica subspecies enterica serotype Typhimurium, Shigella dysenteriae and S. aureus*	Planktonic	1. AgNP showed excellent antibacterial efficacy against both Gram-positive and Gram-negative bacteria 2. MAP-silver binding peptide fusion proteins provide hybrid environment incorporating inorganic silver nanoparticle and simultaneously mediate the interaction of silver nanoparticle with surroundings	[140]
Direct and indirect liquid flame spray	NA	NA	Glass, polyethylene (PE) and PE terephthalate	*E. coli and S. aureus*	Planktonic	1. Silver nanoparticle-coated polyethylene (PE) and PE terephthalate samples did not inhibit bacterial growth as effectively as glass samples 2. Study shows that it is possible to produce nanostructured large-area antibacterial surfaces which allow antibacterial effect against clinically relevant pathogens	[141]
Biosynthesis using natural polymer pine gum	NA	Pine gum	Cotton fabric and leather	*B. linens, B. cereus, P. acnes and S. epidermidis*	Planktonic	1. Among the four tested bacteria, AgNP coated cotton fabric and leather samples displayed excellent antibacterial activity against *B. linens* 2. This treatment can be effective against odor-associated and/or skin infections	[142]

Chemical reduction with sodium borohydride	3.78±1.14	Sericin	ND	*E. coli and S. aureus*	Planktonic	AgNPs-Sericin exhibited antiviral and anti-bacterial activity without significant cytotoxicity compared with free silver ions	[143]
Biosynthesis using ovalbumin, ovotransferrin, and ovomucoid of egg-white protein under direct sunlight	NA	Egg-white protein	ND	*Salmonella typhimurium and E. coli*	Planktonic and biofilm	Results showed the treatment to be non-toxic, highly stable and antibacterial	[144]
Photochemical synthesis	NA	LL37-SH	Corneal implants and lenses (polymers)	*P. aeruginosa*	Planktonic	Results showed treatment to be anti-infective and anti-inflammatory	[145]
Photochemical synthesis with UV light	10-20 (TEM)	Titania nanotubes	Titanium	*S. aureus*	Planktonic	1. Study showed the material to possess satisfactory osteoconductivity 2. It showed long-term antibacterial ability and good tissue integration 3. It has promising applications in orthopedics, dentistry, and other biomedical devices.	[146]
Biosynthesis using cocoa bean extract (CBE)	8.96-54.22	CBE	ND	*E. coli, S. aureus, K. pneumoniae, A. flavus, A. fumigatus and A. niger*	Planktonic	1. Study showed synergistic effect with ampicillin, cefuroxime, cefixime and erythromycin by 42.9–100 % 2. It showed antimicrobial and larvicidal activities	[147]
Biosynthesis using Ocimum sanctum leaf extract	4-30 (TEM)	Protein	ND	*E. coli, S. aureus*	Planktonic	1. Study showed strong dose-dependent antimicrobial activity 2. This technique provides rapid, cost effective, and ecofriendly way for the synthesis of silver nanoparticles which can be used in various industrial and medical applications	[148]

Chemical reduction by sodium borohydride	7 (TEM) and 10 (DLS)	Polyvinylpyrrolidone	Collagen-alginate biocomposite (CA)	*S. aureus and E. coli*	Planktonic	CA-AgNPs biocomposite possessed much higher antimicrobial activity than CA biocomposite	[149]

Table 3: Summary of physical properties of AgNP, the mammalian cell used and concluding comments of some reported studies (NA represents not available)

Synthesis method	**Size of NP (nm)**	**Capping agent**	**Mammalian cell**	**Cytotoxic assay**	**Conclusions**	**Ref**
Photochemical synthesis using Irgacure-2959	3 (TEM)	Human serum albumin (HSA)	Human primary dermal fibroblast monitored up to 2 days	MTS colorimetric assay	Study showed no significant toxicity to fibroblasts	[16]
Photochemical synthesis	19±1 (DLS)	LL37 peptide	Human primary dermal fibroblast	1. MTS colorimetric assay 2. Live/dead staining	Study showed no significant toxicity to fibroblasts	[112]
Photochemical synthesis	50	Minimum essential alpha medium (α-MEM)	1. Primary osteoblast 2. Primary osteoclast	1. XTT colorimetric assay 2. Alkaline Phosphatase assay 3. Tartrate resistant acidic phosphatase assay	1. Study demonstrated biocompatibility 2. Further *in vivo* studies is essential prior to the widespread clinical application of orthopaedic implant with nanoparticulate silver coatings	[113]
Photochemical synthesis	4.4 ± 1 (TEM)	Type-I collagen @ rose bengal	Human dermal fibroblast	Light microscopy imaging	AgNP@collagen were able to support fibroblasts proliferation	[114]

Photochemical synthesis using Irgacure	3.5 ± 0.04 (SEM)	1. Type-I collagen 2. α-Poly-L-Lysine	1. Human dermal fibroblast 2. Human epidermal keratinocyte	1. MTS colorimetric assay 2. Live/dead staining	AgNP@collagen showed comparable biocompatibility	[96]
Photochemical method (UV light)	1. 20-25 2. 80-90 (TEM and DLS)	Gallic acid	Human acute monocytic leukemia (THP-1)	Trypan blue exclusion assay	NP showed no significant cytotoxicity	[115]
Chemical reduction by ascorbic acid in chitlac solutions	33 ± 7.6 (TEM)	Chitlac	1. Mouse fibroblast-like (NIH-3T3) 2. Human Hepatocarcinoma (HepG2) 3. Human Osteosarcoma (MG63)	1. MTT colorimetric assay 2. LDH assay	No significant toxicity observed at tested concentrations	[116]
Photochemical synthesis using Irgacure	3.5 ± 0.04	Type I collagen	1. Primary human skin fibroblasts and 2. keratinocytes (*in-vitro*) 3. Inflammatory molecules (*in vivo* in mouse-model)	1. Microchip array analysis 2. ICP assay for silver accumulation 3. Live/dead Staining and cell counting (for *in vitro* study)	1. Results displayed limited cytotoxicity 2. Subcutaneous implants of materials in mice showed a reduction in the levels of IL-6 and other inflammation markers 3. Ag accumulation primarily occurred within the tissue surrounding the implant & was also found in the liver, kidney and spleen, but the concentration in liver & kidney decreased considerably after 72 h leaving a minimal concentration within the spleen	[118]
Photochemical synthesis using Irgacure (Delivered as spray-on treatment)	NA	LL37-SH peptides	1. Human skin fibroblasts (monitored for 2 days) 2. Mouse model used to estimate silver	Live/dead Staining and cell counting	1. It showed no detectable toxic or anti-proliferative effects on human skin fibroblasts embedded in a 3D collagen matrix	[111]

			infiltration (in vivo wound model)		2. The composite materials remained in the wound area and had minimal organ infiltration 3. This is a potential application for prophylactics and infection control in infected wounds	
Photochemical synthesis using Irgacure	19±1 (DLS)	CSG-LL37 peptide	Skin fibroblast	1. Live/dead Staining and cell counting 2. Flow cytometry	Study showed proliferation of primary skin cells	[112]
Chemical reduction	8.0 ± 2.6	Pectin	Dermal fibroblasts	Live/dead Staining and cell counting	Result shows non-cytotoxicity of pectin capped AgNP	[119]
Green synthesis method using glucose and fructose	360± 17, 90±7 nm (DLS, TEM)	Polyacrylate-based hydrogel thin coatings on titanium	MG63 human osteoblast-like cells	MTT viability assay	Silver loading was easily tuned that showed biocompatibility	[120]
Ultrasonication	10-40 (TEM)	Proline functionalized graphene oxide	L929 mouse fibroblast cells	MTT assay	Proline/graphene oxide nano-flakes demonstrated low lethality to fibroblast cells	[123]
NA	5-50	NA	Human osteoblasts	1. Elution testing qualitative method 2. Live/dead staining	Study showed biocompatibility	[105]
Laser ablation methods	NA	Chitosan	Human gingival fibroblast	MTT test assay	Study showed biocompatibility	[126]
Electrochemical anodization using a direct-current power supply	NA	NA	Bone testing	1. Immunostaining 2. Histomorphometric analysis	This study showed excellent bio-integration properties make it a promising therapeutic material for orthopedic applications	[127]
Chemical reduction method	28-75 (DLS) 15-30 (SEM) studied on sphere, triangular	NA	Human fetal osteoblast (hFOB)	AlmarBlue fluorescence assay	1. While lower AgNP concentrations did not affect the hFOB viability, it was also concluded that the presence of AgNPs results in a time dependent reduction in hFOB population	[128]

	and cuboidal NP					
Wet chemical synthesis	NA	Diamond-like carbon	1. Human endothelial cells 2. Mouse fibroblast-like cell line 3. Primary human osteoblasts	WST-1 assay	This study showed growth of silver susceptible mammalian cells	[130]
Chemical reduction	NA	Chitosan and Hyaluronic Acid	MC3T3-E1 murine preosteoblasts	1. Lactate dehydrogenase activity assay 2. Alkaline phosphatase activity cell counting kit-8 assay	Study showed biocompatibility	[132]
Biogenic synthesis using Coleus forskohlii	91.03 (DLS)	Coleous forskohlii	Liver cancer cell lines HEPG2	1. MTT assay 2. Anti-oxidant assay	Study showed anti-cancer activity	[135]
Photochemical synthesis	NA	NA	NIH-3T3 fibroblasts	MTT assay	*In vivo* study showed biocompatibility	[139]
Biosynthesis using Mussel adhesive proteins (MAP)	NA	NA	Mouse preosteoblast MC3T3-E1 cells	Cell Counting Kit-8 assay	AgNP showed good cytocompatibility with mammalian cells	[140]
Chemical reduction with sodium borohydride	3.78 ±1.14	Sericin	Human genital epithelial cells	CCK-8 kit assay Anti-HIV-1 assay	AgNPs-Sericin exhibited non-significant cytotoxicity compared with free silver ions	[143]
Biosynthesis using ovalbumin, ovotransferrin and ovomucoid of egg-white protein	NA	Egg-white (EW) protein	Chicken blood	MTT assay	Study revealed that the AgNPs-EW did not induce any hemolytic effect or structural damage to the cell membranes of chicken erythrocytes, suggesting biocompatibility	[144]
Photochemical synthesis	NA	LL37-SH	1. Subcutaneous grafts in mice	Cell proliferation assays	Results showed treatment to be anti-inflammatory and non-cytotoxic	[145]

			2. Human umbilical vein endothelial cells 3. Human corneal epithelial cells			
Photochemical synthesis with UV light	10-20 (TEM)	Titania nanotubes	Primary rat osteoblasts	Lactate dehydrogenase activity assay	Study showed the material to possess satisfactory osteoconductivity and good tissue integration	[146]
Chemical reduction by sodium borohydride	7 (TEM) and 10 (DLS)	Polyvinylpyrrolidone	Mouse embryonic fibroblasts	Cell Counting Kit-8 assay	1. AgNPs biocomposite possessed negligible cytotoxicity at low AgNPs concentration 2. It showed strong potential as wound dressing	[149]

From Table 2 and Table 3, it is evident that AgNPs are a very useful tool to prevent and treat bacterial infections, while remaining biocompatible. Most of the studies have shown to use photochemical synthesis, chemical reduction and biosynthesis/biological synthesis methods to synthesize the AgNPs. The most common capping agent used were various proteins like human serum albumin, collagen etc., various peptides, different polymers such as PEG, PVA etc., gallic acid, chitosan, pectin and various biopolymers. There could be more studies done or on-going that can support the fact that AgNP protected with a capping agent can be antimicrobial and non-cytotoxic to mammalian cells. These studies show that AgNP is a promising tool to prevent and/or treat chronic infections, however the main limitation with the studies is that they have been majorly studied *in vitro*, with only some studied *in vivo* (animal models). These studies are needed to be extended to clinical trials which seems a challenge as certain limitations such as limited information on extent of biocompatibility, demands the study to be further optimized. Hence, a major focus for these studies should be taking the therapy forward to clinical trials and introducing it in clinical applications.

This project was also based on *in vitro* tests, as the capping agent has not been tested previously. Thus, the study needs to be extended to *in vivo* models and clinical trials. However, the capping agent selected in this project gives advantages to other capping agents used in the studies reported in Table 2, as it is expected to be much cheaper and effective in comparison to various other peptides, collagen and citrate.

1.4. Objective and hypothesis

The overall objective of this project was to prepare a biocompatible CLKRS peptide capped silver nanoparticle (CLKRS@AgNP) that could be used to coat biomaterial based indwelling medical devices for prevention and treatment of bacterial infections during/post-implantation of indwelling medical devices. It was hypothesized that surface modification with CLKRS@AgNP will be effective at preventing and treating biofilms causing infections on implants without significantly affecting surrounding tissues.

Two biomaterials were used in the project to show the efficacy of the prepared silver nanoparticle formulation coated on it, *i.e.* titanium discs and collagen hydrogels (collagen like

corneal gels). These two biomaterials were selected for specific reasons as discussed in Results and Discussion section (Chapter 3).

Our aims were: 1) To optimize the surface coating, 2) To assess the antimicrobial and antibiofilm performance, and 3) To evaluate the toxicity and cell compatibility using primary cells.

Chapter 2- Materials and methods

The materials and experimental set-up will be explained in this section. The bacterial strains and other materials used will be stated. All methods were conducted using sterile techniques and most experiments were based on Alarcon's group's standard operating procedures (SOP) as mentioned and cited.

2.1. Materials used

Various chemical reagents were used in this project including sodium citrate, silver nitrate, Iragcure-2959, glutaraldehyde and 3-aminopropyltriethoxysilane (APTES), all of which were purchased from Sigma Aldrich.

Major biological components used in the project were Corning Rat tail type I collagen solution (purchased from Fisher Scientific), Theracol porcine type I collagen solution (purchased from Sewon Cellontech Co Ltd), DMEM media, (purchased from Gibco Fisher Scientific), keratinocyte media, (purchased Gibco Fisher Scientific), fetal bovine serum, (purchased from Gibco Fisher Scientific), lysogeny broth (purchased from Sigma Aldrich) and tryptic soy broth (generously provided by Dr Thien Fah Mah, University of Ottawa).

2.2. Preparation and optimization of CLKRS peptide capped silver nanoparticles

Citrate protected silver nanoparticles (80 nM) were first prepared by irradiating a mixture of deoxygenated silver nitrate (200 μM), Irgacure-2959 (200 μM) and sodium citrate (1 mM) dissolved in milli Q water for 30 minutes in a UVA photoreactor (Luzchem) at room temperature. Deoxygenation of the mixture was important as silver is known to easily oxidize and form a very stable silver oxide which would prevent the synthesis of AgNP seeds. The methodology for preparing the peptide capped silver nanoparticle spray-on treatment was based on the protocol established by McLaughlin et al.[111] Since the LL37-SH peptide was replaced with CLKRS, the protocol was optimized by changing the concentration of the peptide and the incubation time after 4-spray treatment.

To prepare the CLKRS capped silver nanoparticle, 60 µl of a known concentration of the CLKRS peptide was added to 6 mL of citrate protected silver nanoparticle, which was crosslinked with rat tail type I collagen (192 µl of 0.1 mg/mL) by adding 174 µl of 1.5% w/v glutaraldehyde solution. The solution was allowed to cross link on ice for 30 min covered from light. The excess glutaraldehyde was then quenched by adding 426 µl of 20% w/v glycine solution which was incubated for another 30 min on ice covered from light. 138 µM of CLKRS capped silver nanoparticle is obtained.

For the spray-on treatment, the obtained solution was diluted in sterile 1X PBS. The solution was added to the cup of an airbrush make-up system device (Figure 5A), which was used to spray the AgNP solution on the centre of an objective (in a well of a plastic cell culture 6-well plate). The device was kept at a distance of 8-10 cm from the objective, covering other wells with a filter paper to ensure the treatment goes only to the well of choice as shown in Figure 5B. The treatment was sprayed for 10 seconds and incubated for 10 minutes at 37°C until 4 treatments were reached and after that incubated for a known amount of time at 37°C.

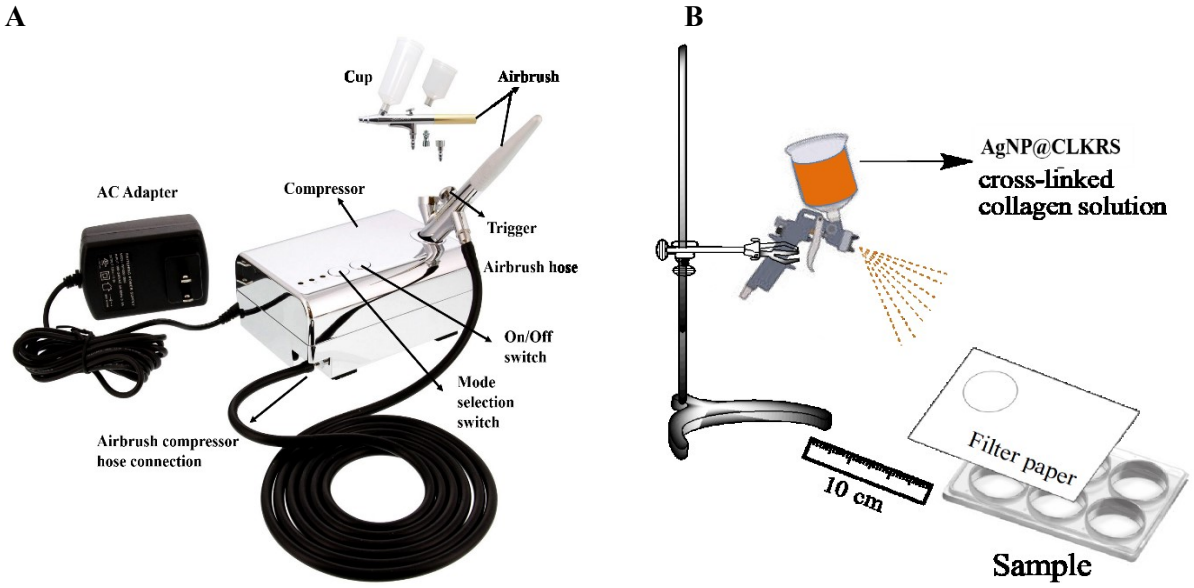

Figure 5: A) Airbrush make-up system device[150], **B)** Spray-on treatment set-up.

The tested concentrations of the peptide were 5, 10, 20, 50 and 100 µM and the tested incubation times were 1, 2 , 3 , 6 , 12 and 24 hours. Surface plasmon band was measured in a

Biotek plate reader (spectrophotometer) (SynergyMx). 20 μM and 6 hours were selected as final formulation parameters, as described in the results.

2.3. Planktonic bacteria and biofilm preparation

Pseudomonas aeruginosa is a gram negative bacterium known for rapidly adapting to harsh environments and antibiotics. [151] *P. aeruginosa* biofilm readily attach to indwelling medical devices leading to nosocomial infections that have become a worldwide healthcare issue.[151] PA14 and PAO1 strains were used in this project initially obtained from by Dr Thien Fah Mah, an Associate Professor at the Faculty of Medicine, University of Ottawa. PAO1 is a standard laboratory strain which is a derivative of PAO strain isolated from an infected wound in 1954 in Melbourne.[152] PA14 was first reported by Professor Milton Schroth in 1977 where he described PA14 as one of the most virulent clinical isolate to cause extensive plant rot.[153] He obtained the strain from Dr Spyros Kominos who isolated it from burn patients in the 1970s.[153]

Staphylococcus epidermidis ATCC 35984 and *Staphylococcus aureus* ATCC 25923 were also used in this project. Staphylococci species is a gram positive bacteria that mostly inhabit skin and mucous membranes of most mammals and can grow both in aerobic and anaerobic conditions.[10] *S. aureus* and *S. epidermidis* are reported to be a major source of nosocomial infections and common causes of surgical site infections and catheter associated bloodstream infections.[10] About two-third of implant associated infection is found to be caused by either *S. aureus* or coagulase negative staphylococci.[32] Hence, in many studies, including this project, staphylococci species were used to test the antibacterial property of the AgNP. *S. epidermidis* 35984 strain and *S. aureus* 25923 were obtained directly from American Type Culture Collection (ATCC). ATCC 35984 was isolated from a catheter related bloodstream infection in 1982 in Tennessee[154], while ATCC 25923 was isolated in 1945 in Seattle.[155] All the strains were stored in -80°C dissolved in 25% glycerol.

Planktonic bacteria were prepared using a protocol from Scaiano's group, Department of Chemistry, University of Ottawa. 10 μL of the bacterial suspension initially stored in -80°C was streaked on a LB (lysogeny broth) agar plate in a zig-zag 2-phase streaking pattern and incubated for 16 hours at 37°C. After single colonies had grown on the agar plate, a single

colony was resuspended in a 2 mL of 100% LB agar broth and incubated in an orbital shaker incubator for 16-18 hours at 225 rpm and 37°C. This overnight culture (ONC) is found to yield approximately 10^9 cfu/mL.

Alarcon's group protocol was used to grow biofilms. Briefly, after placing sterile glass slips on a 12-well plate, the plate was placed in a Tupperware at an angle of 40-45˚ to ensure the biofilm formation on a liquid-air interface. 650 µL of 10^7 cfu/mL of ONC was added on the glass slips. The surrounding of the Tupperware was filled with sterile milli Q water and the whole setup was incubated for 6-24 hours at 37˚C. PAO1 and PA14 ONC was diluted in supplemented M63 broth and incubated for 6 hours, while *S. aureus* and *S. epidermidis* was diluted in tryptic soy broth and incubated for 24 hours. These conditions were selected from studies performed by Alarcon's and Mah's groups.

2.4. Methods of cell culture

Human dermal fibroblast culturing:

The fibroblast cells were primary cultures transfected with GFP obtained from human skin. These cultures were purchased and stored in liquid nitrogen storage tanks.

To grow and inoculate them within collagen hydrogels, type 1 rat tail collagen hydrogels were prepared on two 6-well plates. To prepare the hydrogels, 1mL of 10X Dulbecco's modified eagle's medium (DMEM) (collagen medium) was added to 6 mL of type 1 rat tail collagen. After neutralizing (pH-7.5) the collagen solution, 520 µL of 20% chondroitin-6-sulphate solution was added to the solution. 100 µL of 1.5% glutaraldehyde mixture was then added to crosslink the solution. The solution was allowed to crosslink for an hour on ice protected from light. 500 µL of 20% glycine was added to quench the excess glutaraldehyde and left for another 1 hour on ice protected from light. Once the fibroblasts cells were obtained (see below) they were added to the gel and mixed such that 200,000 cells are added to each well. The gels with the cells were plated dropwise on a 6-well plate ensuring even spread on the bottom of each well. (1mL /well). The well plate was placed in a cell incubator for 20 minutes at 37˚C to allow the gel to set. 2 mL of the DMEM media was then added and changed every 2nd day.

1 mL of dermal fibroblasts were obtained from the liquid nitrogen vessel which was mixed in a 7 mL of 1X DMEM media with 10% fetal bovine serum and 1% penicillin/streptomycin. It was then centrifuged at 1000 rpm for 5 min. The media was removed, and fresh media was added. In a flask, 10 mL of DMEM was added with the 5 mL of the cells. The cells were allowed to grow for 7 days in a 37˚C cell incubator and every second day, half the media was changed. The media was taken out on the 7^{th} day and 5 mL of trypsin was added. The trypsin allowed the cells to detach from the surface of the flask. After a couple of minutes, 8 mL of 1X DMEM media was added and centrifuged in a falcon tube for 5 min at 1000 rpm. The media was removed and fresh 1 mL DMEM was added. With a cell counting slide and trypan blue stain, the cells were counted on a live cell movie analyser (NanoEnTek- Juli Br&FL station). The cells were added to the gels (as described above) and kept in the incubator. The media (2 mL/well) was changed twice that very day and was changed half of it every 2^{nd} day. The cells were allowed to grow and spread out within the hydrogels to mimic the extracellular structure of the human body.

Human epithelial corneal cell culturing:

The epithelial cells were primary cultures transfected with GFP obtained from human cornea tissue. These cultures were purchased and stored in liquid nitrogen storage tanks.

To grow the epithelial cells, they were mixed in a 7 mL of keratinocyte serum free media (K-SFM) media with 20% fetal bovine serum and centrifuged at 1000 rpm for 5 min. The media was removed and fresh media of K-SFM without the FBS was added. It was transferred to a flask and grown for 5 days at 37˚C. The cells were then trypsinized as previously described and added directly on the collagen like corneal gels in a 96-well plate (25,000 cells/well), which was previously treated with sterile PBS for 12 hours (to remove byproducts from the silver nanoparticle synthesis) and K-SFM without the FBS for 3 hours (to allow the cells to readily attach and grow on the corneal gels). Images were captured and quantified at day 1 and day 3 and half the media was changed every 2^{nd} day.

Isolation of bone marrow derived macrophages:

To culture primary macrophage cells, a pair of mouse legs were obtained after euthanizing a mouse. Using tweezers and scissors, the muscle and surrounding tissue were removed, and the fibula was discarded. The four tibia and femur bones were separated. The bone marrow from each bone was flushed using a syringe with 2.5 mL of 1X DMEM high glucose media with heat inactivated FBS, penicillin-streptomycin (1%) and L929 conditioned medium (containing colony stimulating factor harvested from L929 cells). After collecting the bone marrow from each bone, the media with the cell suspension was plated in a flask and the bone marrow cells were allowed to grow for 7 days. The cells were trypsinized and added directly to the collagen like corneal gels in a 96-well plate (2800 cells/well) which was previously treated with sterile PBS for 12 hours and macrophage DMEM media for 3 hours. Images were captured and quantified at day 1, day 3 and day 7.

As mentioned in chapter 1, two biomaterials were used to test the antibacterial and biocompatibility properties of CLKRS@AgNP. For titanium, CLKRS@AgNP was prepared and transferred to the air brush make-up system, from which the treatment was delivered to a cell culture well plate referred to as spray-on treatment. These treated and non-treated well plates were tested for antibacterial and biocompatibility properties and then a method was adapted to coat the formulation on titanium discs.

For the collagen like cornea gels, the CLKRS@AgNP was *in situ* synthesised on the gels. These treated and non-treated gels were directly tested for the antibacterial and biocompatibility properties.

The final concentrations of CLKRS peptide used were 0.2 µM for the spray-on treatment and 15, 20 and 100 µM for coating the AgNP synthesized on collagen like corneal gels.

2.5. Bacterial experiment for the spray-on treatment

Type I porcine collagen hydrogels were prepared on two 6-well plates (Plate 1 and Plate 2). To prepare the hydrogels, 1 mL of 10X Dulbecco's Modified Eagle Medium (DMEM) collagen

medium was added to 6 mL of Type I medical grade porcine collagen (Theracol purified collagen solution). After bringing the pH of the solution to 7 using sodium hydroxide (1M), 200 µL of 1.5% glutaraldehyde solution was added to the solution. Finally, 500 µL of 20% glycine solution and 500 µL of 40% chondroitin solution were added to the solution and kept covered from light for an hour on ice. The final solution (400 µL) was added dropwise to the 6-well plates and incubated for an hour at 37˚C to allow the hydrogel to set.

The spray-on treatment was sprayed on Plate 1 for 10 seconds and incubated for 10 minutes up to 4 treatments (4-spray). The well-plate with the hydrogel and spray-on treatment was incubated for 6 hours and the surface plasmon band was measured. Then 3 mL of PA14 (10^5 cfu/mL) was added in each well and the surface plasmon band was measured. The well-plate with the hydrogel, spray on treatment and the planktonic bacteria was incubated for 16 hours and again the surface plasmon band was measured. Finally, bacteria plating and counting were performed. This test was done to calibrate the preventative ability of the prepared spray-on formulation from *P. Aeruginosa* planktonic bacterial cells.

On the other 6-well plate (Plate 2), 3 mL of PA14 (10^5 cfu/mL) were added on the hydrogel and the surface plasmon band was measured. The bacteria were incubated for 16 hours and were plated on agar plates for quantification. The agar plates were incubated for 16 hours at 37˚C. After growing the PA14, the spray-on formulation was sprayed by the same protocol as mentioned above and incubated for 6 hours. This solution was plated on agar plate too and quantified. The surface plasmon band was measured of the well plate. This test was done to calibrate the treatment ability of PA14 planktonic bacteria by the spray-on formulation.

To test the biofilm growth, one 12-well plate and two 6-well plates were taken, and three glass slips were placed in three well in each of the plates after sterilizing it. The 12-well plate was considered the control and PA14 biofilms were grown on the glass slips. Plating and quantification of the biofilms were done.

In one of the 6-well plate, the glass slips were sprayed with the spray-on formulation until 4 treatments were reached. After 6 hours of incubation, the solution was taken out and biofilms were grown. Plating and quantification were done. This test was done to calibrate the preventative ability of the prepared spray-on formulation from *P. Aeruginosa* PA14 biofilm.

In the other 6-well plate, the biofilm was grown on the glass slips first. Then after discarding the bacterial solution, it was sprayed by the spray-on formulation. After 6 hours of incubation, plating and quantification was done. This test was done to calibrate the treatment ability of PA14 biofilm by the spray-on formulation.

These tests were repeated with *S. aureus* and *S. epidermidis* planktonic and biofilm cells. PA14 and *S. aureus* planktonic concentrations were also tested from 10^5 cfu/mL to 10^8 cfu/mL to check up to what concentration can the spray-on formulation be effective. For this, the planktonic bacteria were added to treated wells and quantified.

2.6. Cell viability experiment for the spray-on treatment

Two 6-well plates were taken, one to perform the bacterial test on fibroblast cells and the other to test toxicity of the spray-on formulation on fibroblast cells.

In the first 6-well plate (plate 1), rat tail collagen hydrogel was formed on the wells of the plate with the fibroblast cells seeded and grown for 7 days. On the 7^{th} day the media was removed and the spray on treatment was performed in a biosafety cabinet (1 well with control and 3 wells with 4-spray treatments). After incubation of 3 h, the DMEM media was added and incubated for 16 h after removal of nanoparticle solution. Images were captured and 3 mL of planktonic PAO1 and *S. aureus* (10^5 cfu/mL) were added separately in different well plates, which was incubated for another 16 h. Images were taken, plating of bacteria on LB agar plate and further quantification of the bacteria were performed. The bacterial solution was removed, and the wells were washed with 1X PBS thrice and plating was done again. Images were captured once again. This test was performed to test the prevention of *S. aureus* bacteria on a hydrogel seeded with the fibroblast cells.

In the other plate (plate 2), the cells were seeded within the rat tail hydrogel and the spray-on treatment was done. The well plate was incubated for 3 hours and then the media was added and incubated for 16 hours, after removing the solution. Day 1, day 2 and day 3 images were captured and quantified manually using the ImageJ software. The media was changed on the 2^{nd} day. This test was performed to test the cytotoxicity.

2.7. Coating of the spray-on formulation on titanium discs

Preparation of the CLKRS capped AgNP was done and tested on bacteria and fibroblast cells. Now, the challenge lied in coating this formulation onto the titanium discs which is a very common biomaterial used to manufacture indwelling medical devices.

Titanium discs with 1 mm of thickness and 1.5 cm of diameter were obtained and tested for coating of AgNP formulation. The mentioned spray-on treatment of the AgNP alone showed to be ineffective in coating the discs, hence an additional step was done to stimulate a coating of AgNP on the titanium discs.

A technique of silanization was used to coat the silver nanoparticle onto the titanium discs. Silanization of the treated discs with 3-aminopropyltriethoxylsilane (APTES) led to exposed amino groups that bonded with the silver nanoparticle by coordinate bonds. To perform the experiment, the protocol was adapted and modified from Xiao et al.[156] Briefly, the titanium discs were abundantly washed with water, sonicated for an hour and cleaned in boiling water for 30 min. The discs were then soaked in methanol/HCl (1:1) for 30 min at room temperature, followed by rinsing 5 times with water. Then, they were soaked in sulphuric acid for 20 min at room temperature, followed by rinsing 5 times with water and soaking in boiling water for 10 min. Finally, they were rinsed with acetone 3 times and dried in a desiccator for 12 hours. This was done to etch the surface of the disc for the APTES attachment. By etching, the surface of the titanium exposed to the hydroxyl groups derived from the acid reaction with methanol. The discs were then put on a hot plate with a temperature of 110-130°C to warm it. 100 µL of APTES were dropped every 10-15 min onto the discs for 3 hours at 110-130°C. The hydroxyl group at the surface of titanium reacted with the tri-ethoxy silane from the APTES leaving the amine group exposed. The discs were then washed with acetone 3 times and water 5 times and dried for another 10-15 hours. 4-spray treatment was done with the CLKRS@AgNP formulation on the discs and incubated for 6 hours at 37°C. The valence electrons in the amine group were believed to be shared with the exposed silver forming weak coordinate bonds, thereby providing attachment of AgNP to the titanium surface.

Pictures were taken and compared with the control titanium discs and then washed with sterile PBS 10 times and then taken again.

2.8. Preparation and optimization of *in-situ* formed CLKRS@AgNPs on collagen-based cornea-like gel

Collagen based cornea like gel was prepared using Alarcon group's SOP. It was prepared using medical grade porcine type I collagen with 200 µm thickness. Briefly, 10% w/v collagen solution were obtained from 0.1% collagen and crosslinked using 1,4-butanediol diglycidyl ether after neutralizing the collagen solution. They were then dropped onto hemispherical moulds with known thickness and allowed to set in a humidity chamber at 2-4°C for 16-18 hours. After solidification, they were stored in sterile PBS at 4°C. The obtained cornea-like gels are currently studied in clinical trials as a potential corneal implant that can replace corneal transplant surgeries.

In-situ formation of CLKRS@AgNP on the collagen based corneal like gel was prepared using Alarcon group's SOP. Briefly, collagen-based cornea like gels previously washed with nanopure water were placed in a plastic boat. It was dried as much as possible and 2 mL of selected formulation (mixture of CLKRS peptide, silver nitrate and Irgacure-2959) were added in the boat and irradiated in a UVA photoreactor (Luzchem) for 1-5 minutes. The synthesized cornea gel was washed with milli Q water and sterile PBS 3 times.

A single corneal gel was punctured to small pieces (around diameter of 0.4-0.5 cm) so that a single gel can be divided into multiple pieces and tested differently. 18 different formulations were tested with different concentration of CLKRS, Irgacure-2959 and silver nitrate, without the corneal gels. Physical observations were made and surface plasmon band was measured using Biotek Plate reader (SynergyMx). The zeta potential and size of the nanoparticles were measured by dynamic light scattering (Malvern zetasizer systems). The first 3 formulations to give a yellow colour (due to strong plasmon absorbance at around 400 nm[106]) at earliest time were selected by mere observation as listed in the results, referred to as F1, F2 and F3. These 3 formulations were then used to synthesize the AgNPs on the corneal gels which were freeze-dried in a lyophilizer for 6-7 days and were given to Emmanuel Yumvihoze, a research associate at the laboratory for the Analysis of Natural and Synthetic Environmental Toxins, University of Ottawa, for obtaining the silver content in each corneal gel by inductively coupled plasma test. The Cryo-SEM, SEM and TEM images were also obtained with the help of Dr Jianqun Wang, in the nanoimaging facility at Carleton University.

To obtain the SEM and TEM images, CLKRS@AgNP solution was synthesized using F1, F2 and F3 formulations. For obtaining the TEM images, they were diluted 10 times with milli Q water. 10 µL of each of the formulation was dropped on the shinier side of the carbon mesh copper grids and was allowed to rest for 10 min. The solution was removed, and the copper grids were dried in a desiccator for 2-3 days. These copper grid samples were then taken to obtain the SEM and TEM images.

2.9. Bacterial experiment for treated corneal gels

In-situ CLKRS@AgNPs formed corneal gels were prepared as described previously with the selected F1, F2 and F3 formulation. The peptide concentration for these formulations were 100, 15 and 20 µM respectively. The treated corneal gel was placed in a 24-well plate and 1.5 mL of 10^5 cfu/mL of PA14 and *S. epidermidis* (separate well-plates) were added in each well and incubated for 16 hours. Plating on LB agar plate and quantification was done. 250 µL was added in a 96- well plate and SPB was measured in the spectrophotometer.

2.10. Cell viability experiment for treated corneal gels

In-situ CLKRS@AgNPs formed corneal gels were prepared as described previously with the selected F1, F2 and F3 formulation. They were transferred to a 96-well plate and soaked in sterile PBS for 12 hours protected from light. Then the PBS was removed, and keratinocyte serum free media (for growing epithelial cells) and 1X DMEM high glucose media (for growing bone marrow derived macrophages) were added and left for 3 hours. GFP epithelial cells and macrophages were prepared prior in a flask as described previously. They were trypsinized and 25,000 cells (epithelial cells) or 2800 cells (macrophages) were added per well on the cornea gels. Images were captured and quantified at day 1, day 3 and day 7 and half the media was changed every 2nd day.

2.11. Imaging

The images of the silver nanoparticle precipitate and the cells were captured by a live cell movie analyzer (NanoEntek Juli Br&Fl station). These images were quantified in ImageJ. Cryo-SEM images were taken at −50°C using a Tescan (Model: Vega II – XMU) equipped with a cold stage sample holder and backscatter electron detector (BSE) and a secondary electron detector (SED). SEM images were taken from the Tescan Vega-II XMU machine, while the TEM images were taken from a FEI Technai G2 F20 machine by Dr Wang from the nanoimaging facility at Carleton University.

2.12. Statistical analysis

All tests mentioned above were repeated minimum 3 times in a set/batches of 3 (n=3), where 'n' denotes the number of times an experiment was repeated. This was done to obtain standard deviation and demonstrate repeatability and reproducibility.

The statistical analysis for this project experiments were evaluated using 2-tail student's T-test in Microsoft Excel 2016 by showing significance when p-value is less than or equal to 0.05.

Chapter 3- Results and Discussions

The results of the above experiments are shown, analyzed and explained in this section. The possible suggestion/conclusions comprehended from the results are stated. They are presented in the same order as the above methods.

3.1. Optimization of CLKRS peptide capped silver nanoparticles

The concentration of the CLKRS peptide was optimized by testing concentrations between 5 μM to 100 μM. For this project, we wanted high precipitation of the AgNPs onto the surface of a material as it will scatter more on the surface indicating a formation of a layer (coating) on it, which is helpful in efficiently delivering the antibacterial properties of the AgNP on the surface of the material.

The amount of precipitation is related to degree of supersaturation,[157] which when increased, shows high absorbances and high polydispersity index (PDI).[17] The high polydispersity index given by larger full width half maximum (FWHM) length suggests heterogenous nature of the formed nanoparticles in a solution. Formation of larger nanoparticles attributed to initial high concentration of silver nanoparticle seeds that combine to make large particles has shown the absorption of light at higher wavelength.[17] Hence, larger precipitation of the silver nanoparticles is normally correlated with higher absorbances at longer wavelength. We screened for a formulation with higher absorbance at longer wavelengths.

As mentioned earlier, the AgNP formulation was needed to be optimized in terms of peptide concentration and treatment delivery in order to produce a stable AgNP formulation that can deliver it antibacterial properties. The spray-on treatment was adapted from the study done by McLaughlin et al, that described 4 sprays to be the maximum limit for the delivery of AgNP required.[111] Firstly, 5 different formulations with different concentration of the peptide were prepared and the spray-on treatment was done on a cell-culture well plate. The SPB were measured from which various information were derived, whose results are represented in Figure 6. Four sprays suffice to produce a maximum absorption of the SPB and scattering region (Figure 6A and B). The absorbance in SPB were observed to be highest in position and

width in the formulation with 20 µM, as shown in Figure 6C & D, hence 20 µM of the CLKRS peptide was selected to be used in the formulation. It ensured the best ratio of precipitation of the AgNP that indicated its level of coating on the surface. The final peptide concentration used in the spray-on treatment was 0.2 µM according to its protocol.

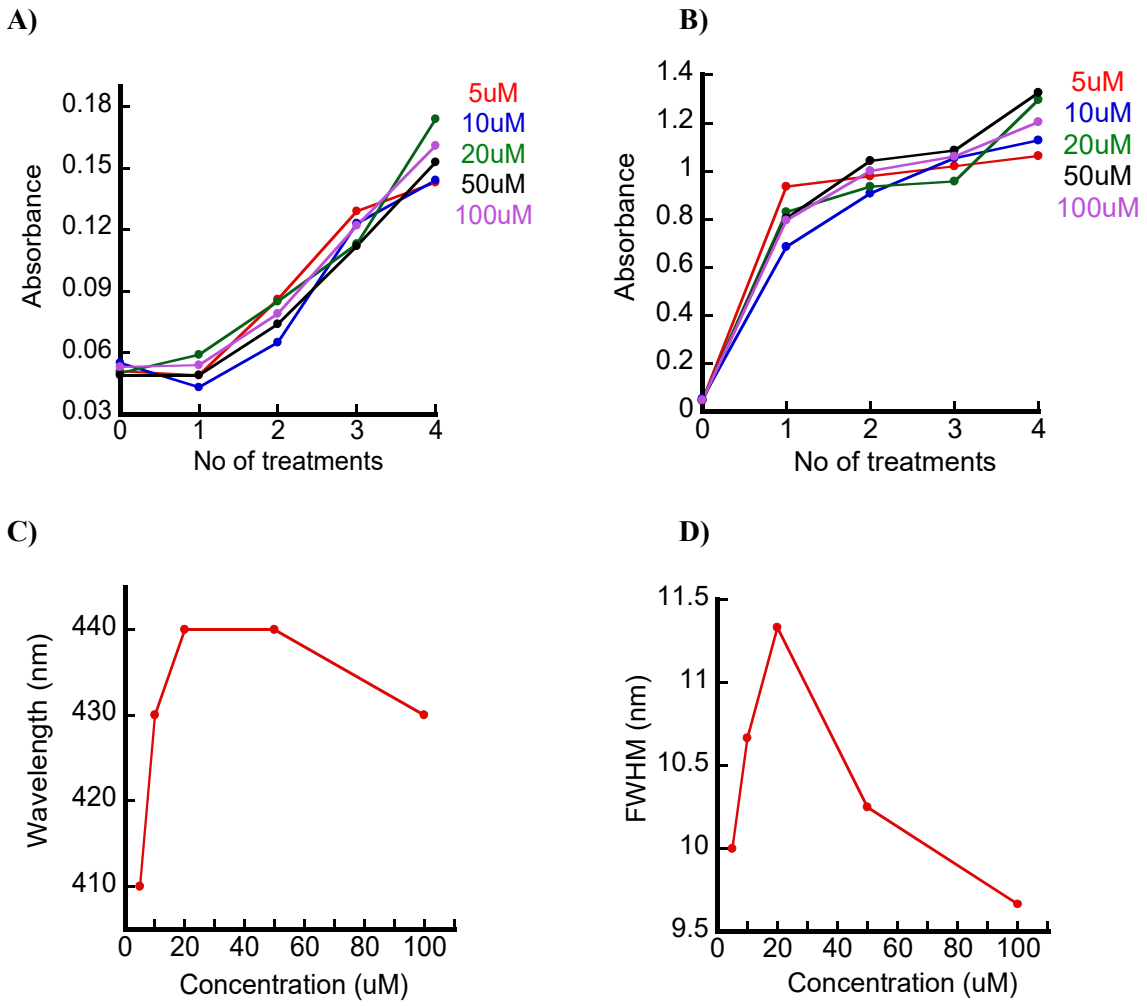

Figure 6: A) Maximum absorbances at 440 nm at different CLKRS concentration (with solution); B) Maximum absorbances at 570-590 nm at different CLKRS concentrations; C) Plasmon band shift at increasing concentrations of CLKRS showing 20 µM and 50 µM has the highest wavelength at which absorbance occur; D) FWHM of different CLKRS concentrations showing 20 µM has the highest PDI ['with solution' denotes the measurements done when there was AgNP solution in the well plate, while 'without solution' or when it is not specified, it denotes the measurements done when the AgNP solution was removed].

Now the next step was to determine the treatment delivery parameters, *i.e*., how many spray treatments to be used and how much time should the formulation be incubated at 37°C, as mentioned in the protocol. Thus, incubation time was evaluated from 1-24 hours with different spray-on treatment (1-4 sprays), while fixing the 20 µM concentration of the peptide. Again, the formulation with maximum absorbance and maximum wavelength was to be selected. The maximum absorbance was given by the formulations with 6, 12 and 24 hours with small differences as shown in Figure 7A. The shortest time was selected as the treatment delivery should be quick and effective. This data was supported while measuring the maximum wavelength which was given by 6 hours as shown in Figure 7B. Now, while keeping the incubation time constant, the SPB were measured for 1-spray treatment, 2-spray treatment, 3-spray treatment and 4-spray treatment. The plasmon absorbances seemed to increase from 0 to 4 sprays (Figure 7C) suggesting 4 spray treatment to be most effective. However, in this regard 1-4 spray treatments were done until the planktonic bacterial test to confirm that 4-spray treatment works best.

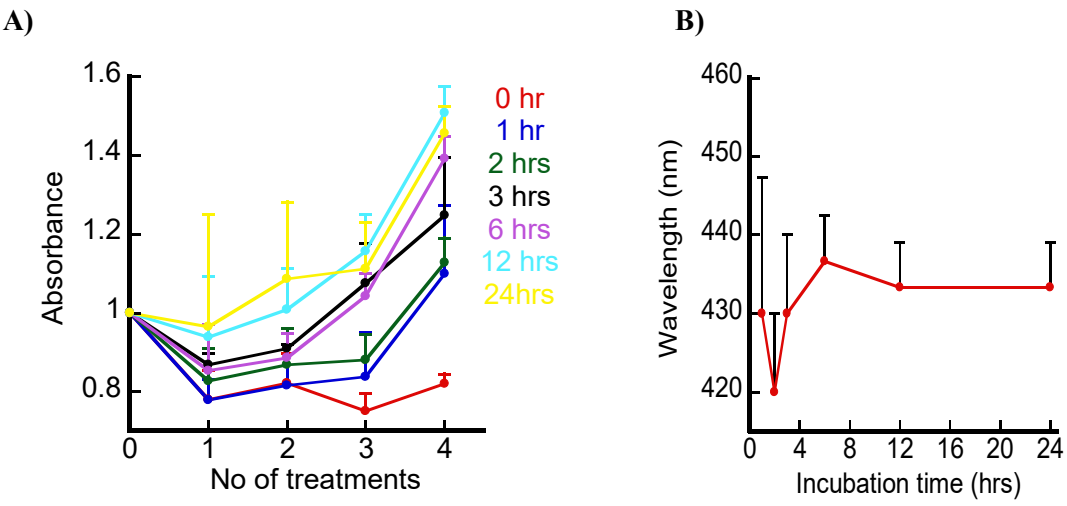

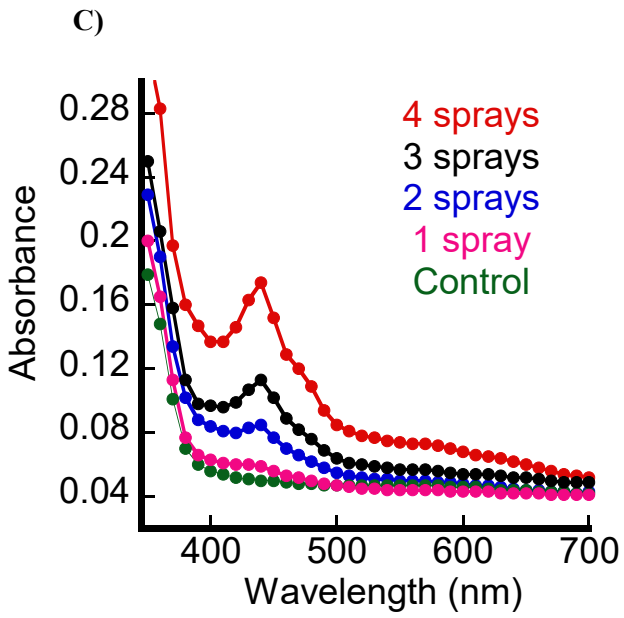

Figure 7: **A)** Maximum absorbances at 557-587 nm at different incubation time; **B)** Plasmon band shift at increasing incubation time showing 6 hours has the highest wavelength at which plasmon absorbance occur; **C)** Plasmon absorption spectra at different treatments with optimized parameters (with solution) at 440 nm (control denotes no spray).

Photographic and microscopic images were taken to justify the above plots. After the 4-spray treatments in a well plate, a yellow colour solution was observed which was the AgNPs as shown by the SPB measurement. Figure 8A shows the AgNP solution from 0 to 4 sprays which was removed, and the picture was taken again as shown in Figure 8B. A thin yellow film was observed at the surface of the well plate indicating the AgNP precipitate or the coating of it on the surface. As mentioned, the increase in size of AgNP (given by longer wavelength) indicates precipitation that would allow the AgNP to coat the surface of a material which is translated with the yellow colour as shown in Figure 8B. Microscopic images were taken to prove the coating of AgNP on the surface which is represented by Figure 8C (0 spray), 8D (1 spray), 8E (2 spray), 8F (3 spray) and 8G (4 spray). It is clear from this figure that as the treatment increases, the amount of precipitation of the AgNPs also increases suggesting the 4-spray treatment can be expected to be more effective.

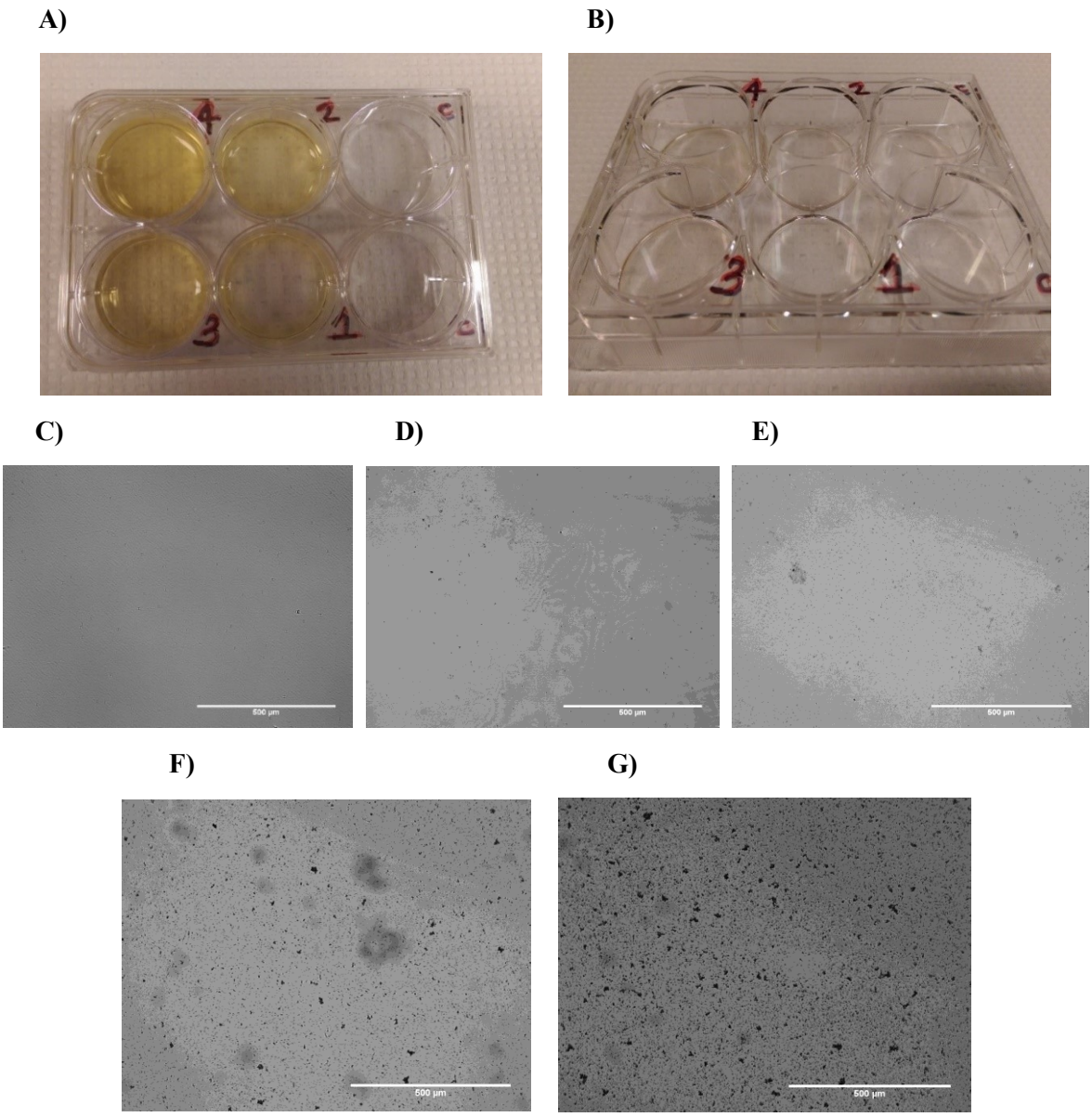

Figure 8A-B: Figure shows the photographic image of the AgNP solution in the treated well-plate**; C-G:** Microscopic images of AgNP precipitate at different treatments with optimized parameters where C) refers to control, D) 1-spray treatment, E) 2-spray treatment, F) 3-spray treatment and G) 4-spray treatment.

3.2. Antibacterial activity of the spray-on treatment

P. aeruginosa PA14, *S. aureus* (ATCC 25923) and *S. epidermidis* (ATCC 35984) were used to test the planktonic and biofilm formation. For the planktonic test, the spray-on treatment with 1 spray, 2 spray, 3 spray and 4 sprays of the optimized AgNP formulation were tested and for the biofilm experiment, only 4-spray treatment was tested. PA14*, S. aureus* and *S.*

epidermidis planktonic bacteria formation was shown to be prevented by the spray-on formulation, and the counts of the existing planktonic cells were also shown to be reduced by the treatment as shown in Figure 9, Figure 10 and Figure 11. The spray-on treatment was shown to prevent PA14, *S. aureus* and *S. epidermidis* biofilm formation as well and treat preformed biofilm as shown in Figure 12, Figure 13 and Figure 14. The p-value was determined to test significant differences between the treatment and control (no treatment) that indicated the spray-on treatment of the AgNP formulation to be antibacterial and antibiofilm. In all the experiments, the p-values were found to be less than 0.05 in comparison to control, suggesting that the colony forming units in the treatment were significantly lower than control showing the potential of the treatment and its effectiveness.

When PA14 was tested, the 1, 2, 3 and 4-spray treatments showed the tendency to prevent PA14 growth, but only 3 and 4-spray treatment showed the tendency to eradicate the PA14 bacteria as shown in Figure 9A and B. The 4-spray treatment showed to be 95-100% effective in preventing and eradicating the planktonic bacteria. This suggests that 4-spray treatment is most effective in preventing and eradicating the planktonic PA14 cells.

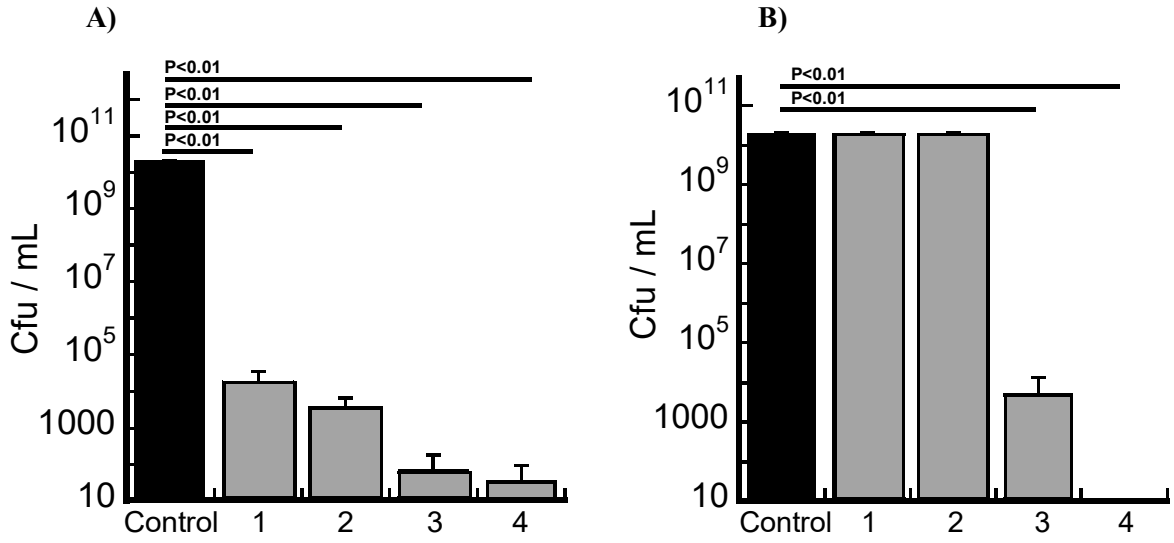

Figure 9A: PA14 planktonic bacterial counts on treated well plate showing the preventive ability of the spray-on treatment, **B**: Plot shows the planktonic counts when the spray-on treatment was applied on the existing grown bacteria showing the therapeutic effect (1,2,3 and 4 represents 1-spray, 2-spray, 3-spray and 4-spray treatments).

As mentioned earlier, Staphylococci species are found to be the most common bacterial species to cause nosocomial and implant associated infections. Two common strains of staphylococci were used to confirm the antibacterial property of the AgNP formulation. For *S. aureus*, 4-spray treatment showed preventative ability of the AgNP formulation whereas, 2, 3 and 4 spray treatment showed the treatment ability as shown in Figure 10A and B. Amongst all the spray treatment, 4-spray treatment was found to be most effective.

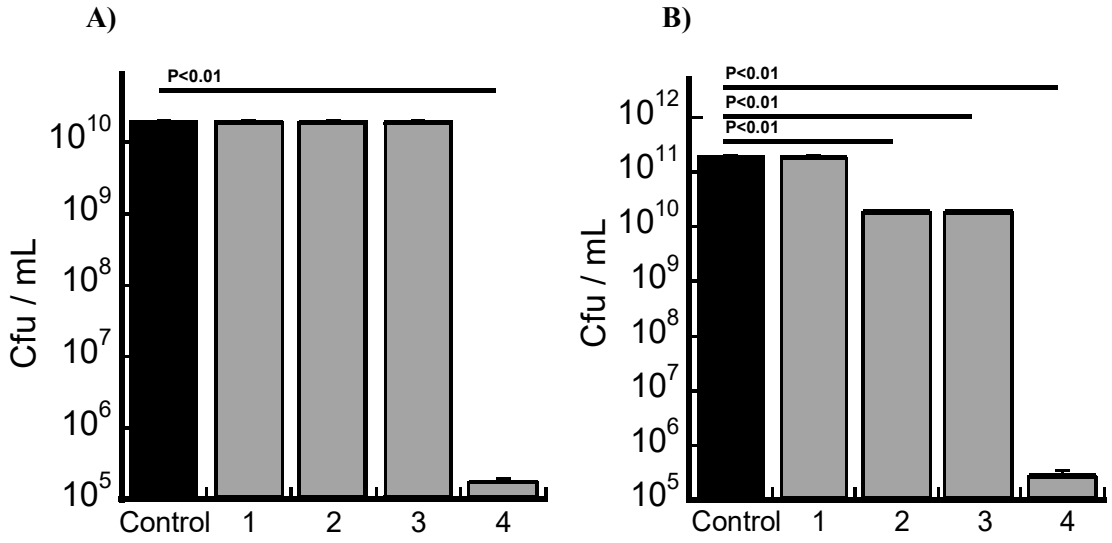

Figure 10A: *S. aureus* planktonic bacterial counts on treated well plate showing the preventive ability of the spray-on treatment, **B**: Plot shows the planktonic counts when the spray-on treatment was applied on the existing grown bacteria showing the therapeutic effect.

S. epidermidis presented similar results where 3 and 4-spray treatment showed to be preventative and 4-spray treatment to be therapeutic as shown in Figure 11A and B. As seen in the other 2 strains, *S. epidermidis* also showed 4-spray treatment to work best of all. Hence, 4-spray treatment was considered to be the best effective spray-on treatment amongst the other spray treatments.

It is interesting to note how all the three strains showed different preventative and therapeutic effect of the same AgNP spray-on treatment. This could be attributed to the fact that staphylococci species are found to be more robust than *P. aeruginosa*, thus requiring stronger

treatment to eradicate them, hence at least 3 or 4-spray treatment was required to treat them, whereas 1-spray treatment was sufficient to prevent the *P. aeruginosa* growth.

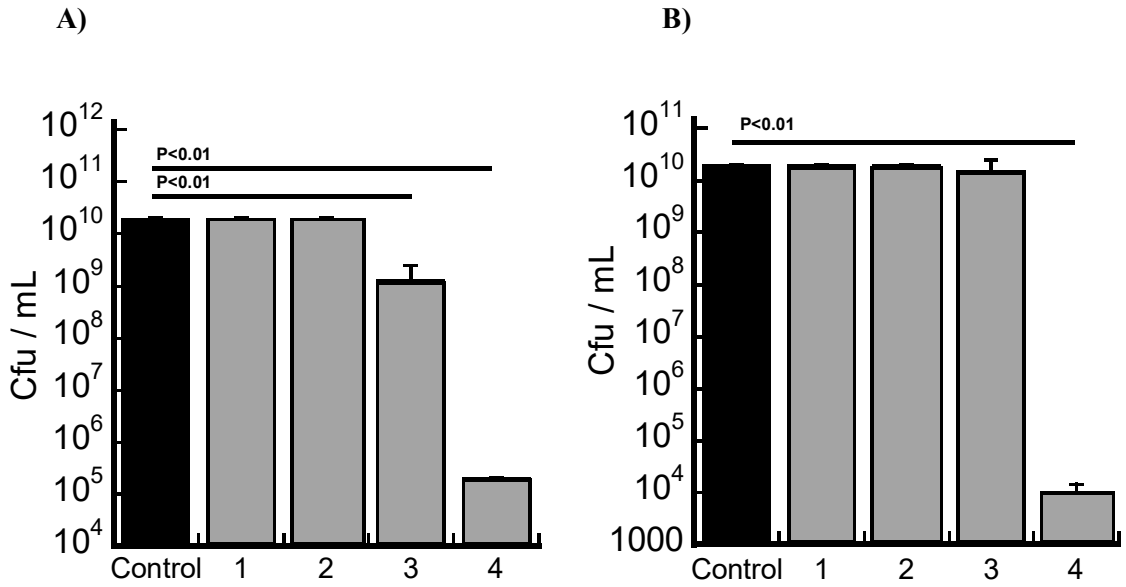

Figure 11A: *S. epidermidis* planktonic bacterial counts on treated well plate showing the preventive ability of the spray-on treatment, **B**: Plot shows the planktonic counts when the spray-on treatment was applied on the existing grown bacteria showing the therapeutic effect.

Biofilms are the dangerous state of bacteria as explained earlier since it is more difficult to eradicate. Thus, to show that the AgNP formulation is also antibiofilm, the 4-spray treatment was done on all the 3 strains. The biofilm was grown on pre-treated well plates to see if the spray-on formulation can prevent the biofilm growth (prevention). The spray-on treatment was also done on pre-existing biofilm to see if the spray-on formulation can eradicate the biofilms (treatment). This was measured with the bacterial solution used to grow the biofilm (solution) and the scraped-out bacteria from the biofilm which was attached to a glass cover slip (scrape).

For PA14, the spray on formulation showed to be most effective in preventing the biofilm growth. There was a significant eradication in the pre-formed biofilms as well (Figure 12A) which was supported by the microscopic image as shown in Figure 12B and C.

A)

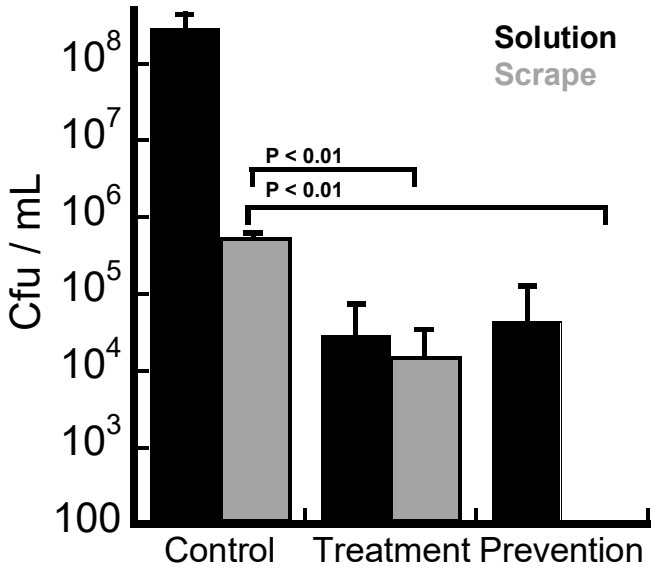

B)

C)

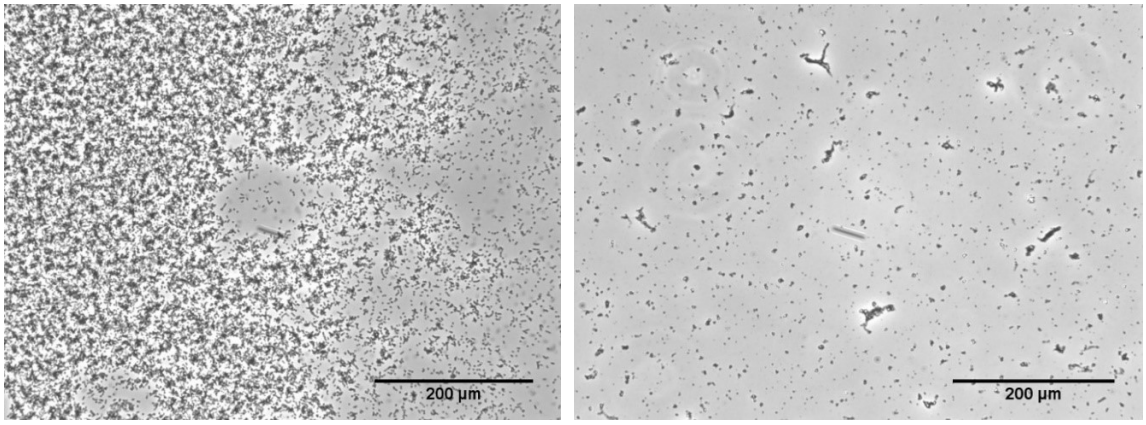

Figure 12A: Comparison of surviving PA14 biofilms ['Treatment' refers to no. of surviving preformed biofilms after treatment and 'Prevention' refers to growth of biofilms on treated glass slips. 'Solution' refers to counts of the bacteria from the solution culture which was the source of biofilm formation on the glass cover slips, whereas, 'Scrape' refers to the actual bacteria count scraped from the biofilm attached to the surface of the glass slips]; **B**: Microscopic image of preformed biofilms; **C:** Microscopic image of those biofilms after 4-spray treatment.

Staphylococci biofilm strains were found to be more difficult to prevent and treat, however, *S. aureus* biofilms were successfully prevented by the spray-on treatment and eradicated by the treatment (Figure 13A-C). Here, treatment of pre-formed biofilm showed better results

suggesting preventing *S. aureus* biofilm could be little more difficult and needs further attention in terms of optimization of treatment.

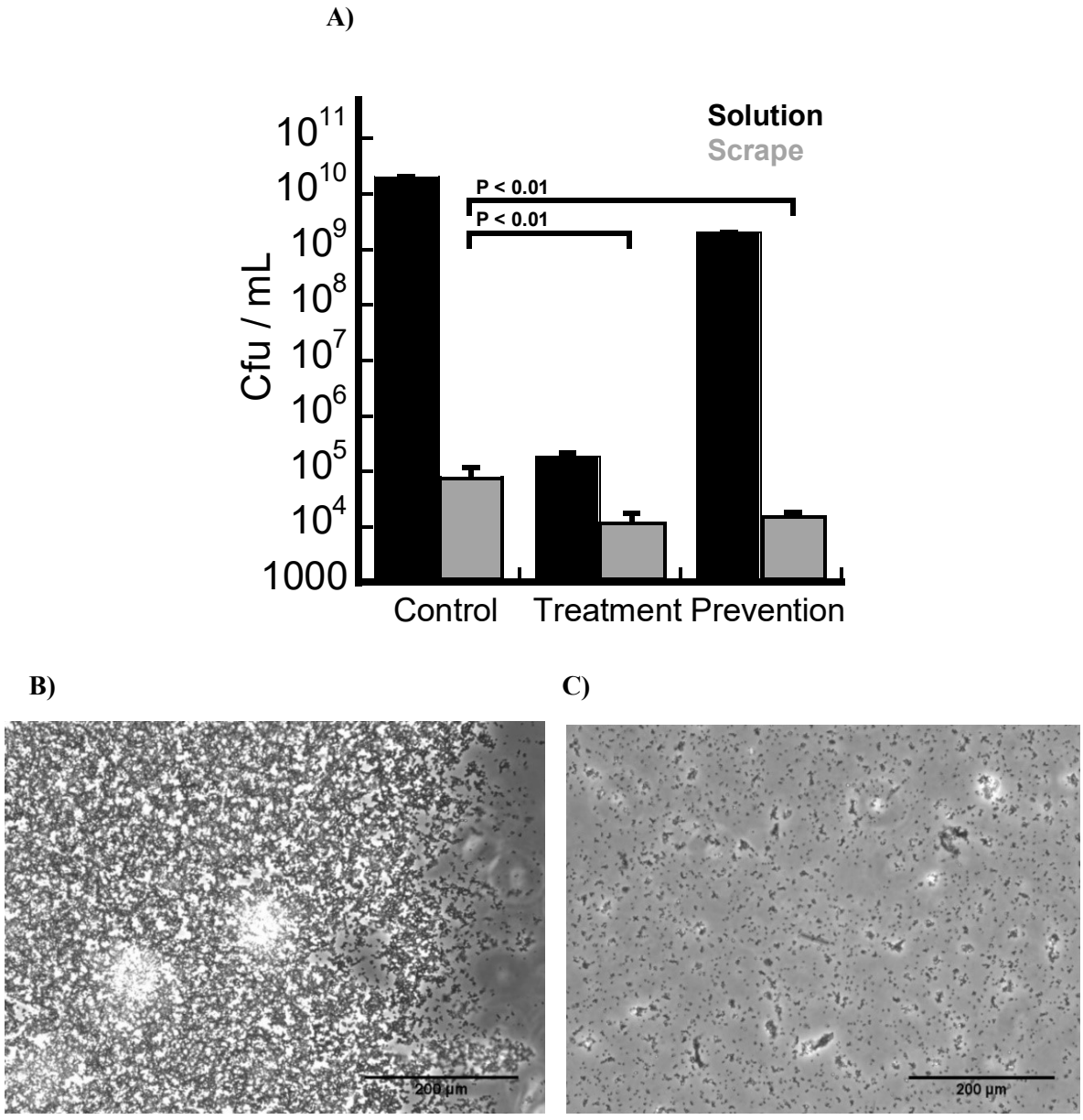

Figure 13A: Comparison of surviving *s. aureus* biofilms, **B**: Microscopic image of preformed biofilms, **C:** Microscopic image of those biofilms after 4-spray treatment.

The AgNP formulation, on the other hand, showed to be more effective in preventing the *S. epidermidis* biofilm but also successfully eradicated the preformed biofilm (Figure 14A-C).

Even for the biofilms, there was a slight difference in the obtained results of the biofilm tests with all the 3 strains by using the same AgNP formulation, suggesting the treatment can be optimized as per the bacterial strain used.

The prepared AgNP formulation can be easily modified, thus can be personalized according to the bacterial strain used for the *in-vitro* or *in-vivo* experiments or the specific bacterial strain causing the infection in the clinical setting. For instance, to prevent and treat Staphylococci causing infections, 5 or 6-spray treatments can be done to further achieve better results, or the CLKRS peptide and silver concentrations can be further optimized. Longer incubation times can also help the surface of the material to be better coated with the AgNP precipitates, hence better antibacterial results can be obtained.

A)

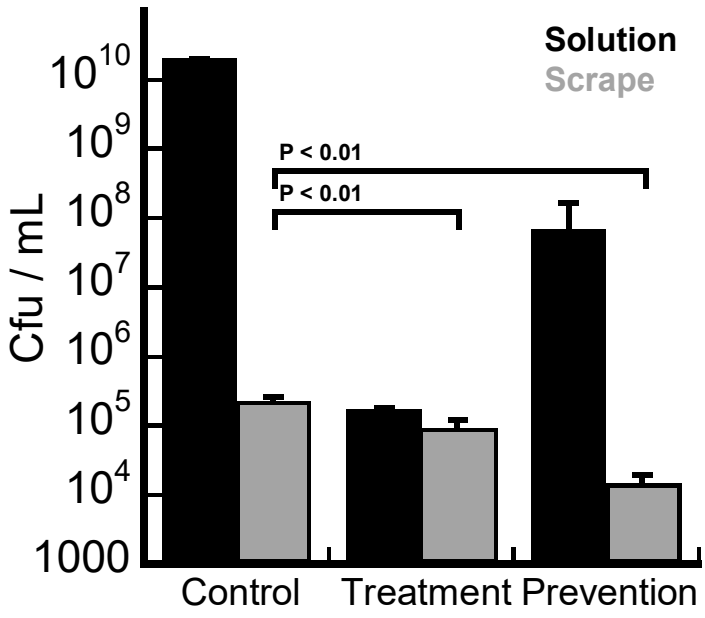

B) **C)**

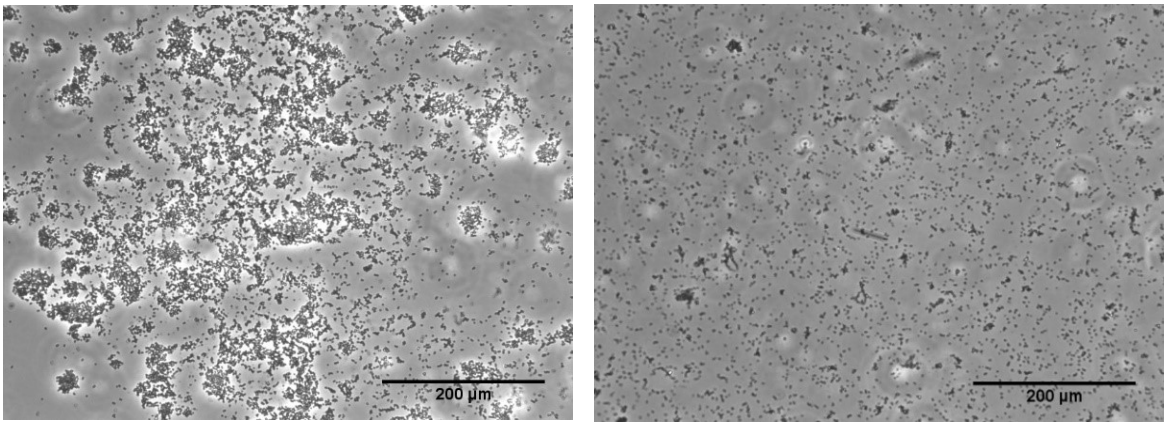

Figure 14A: Comparison of surviving *s. epidermidis* biofilms, **B**: Microscopic image of preformed biofilms, **C:** Microscopic image of those biofilms after 4-spray treatment.

The microscopic images of the biofilms shown were obtained by Ms Li Zhang from Dr Mah's lab using Leica CTR 6000 microscope. Both sets of images, i.e., pre-sprayed glass coverslips and biofilms grown on it and pre-formed biofilms and spray-on treatment done on it, were obtained. All the images supported the plots and showed significant prevention and eradication of biofilms. The images of preformed biofilms and treatment done on it are shown in the above figures that exhibits the eradication of biofilms after treatment on preformed biofilms. Similar images were obtained when biofilms were grown on pre-treated glass cover slips.

Different concentrations of the planktonic cells were also tested for PA14 and *S. aureus* that showed the 4-spray treatment is effective in preventing the planktonic growth only when the initial planktonic concentration tested is 10^5 cfu/mL (for both), 10^6 cfu/mL (for both) and 10^7 cfu/mL (for PA14 only), as shown in Figure 15A (PA14) and Figure 15B (*S. aureus*). This suggests that the AgNP spray-on treatment is ineffective to planktonic bacteria with initial concentrations above 10^8 cfu/mL.

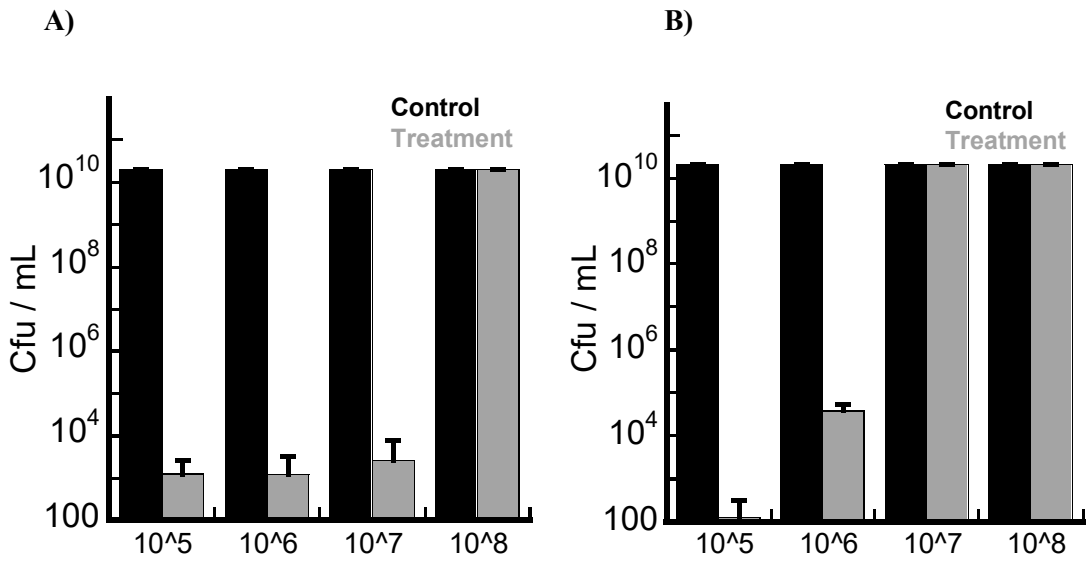

Figure 15: Plot showing bacterial growth on control and treated wells with different initial concentrations of **A)** PA14 and **B)** *S. aureus* (n=3).

From the bacterial and biofilm results, it is evident that CLKRS@AgNP is effective in preventing and treating planktonic and biofilm growth of *P. aeruginosa, S. aureus and S. epidermidis.*

3.3. Cell viability result of the spray-on treatment

To perform the cytotoxicity test, the experiment was divided into two parts: First, the planktonic PAO1 and *S. aureus* were grown on the control and treated wells that consisted of the rat tail collagen hydrogels incorporated by the primary human dermal fibroblasts. Second, the fibroblasts in the control and treated well were counted in ImageJ at 24, 48 and 72 hours. The first part of the experiment was done to show if there's any bacterial growth on the treated wells in the presence of fibroblast cells. The second test was to show the toxicity level of the spray-on formulation on the fibroblasts.

For the first part of the experiment, there was no PAO1 growth at all in treated wells and the planktonic growth in the control wells were completely washed away with PBS as shown in Figure 16A and B. This could have been due to various reasons. Majorly, the calibration/assay method for quantifying the bacteria affects the cell count and since this experiment was done

on grown fibroblast, the DMEM media used for the growth of the fibroblast cells could have affected the prevention of PAO1 planktonic growth. Similar results were obtained when tested with *S. aureus* which could be attributed to the same conclusion that the cell culture media used, contributed in the preventing of the planktonic growth. All in all, it can be said that the spray-on treatment helped in preventing the planktonic bacteria growth since there was a growth in control but none at all in the treated wells.

The main part of this experiment was to show non-cytotoxicity towards the fibroblast which was successfully obtained as shown in Figure 16C. This test was evaluated up to 3 days and it was observed that the fibroblasts proliferate in the presence of spray-on treatment suggesting that the AgNP formulation is non-cytotoxic. The p value of control cells to treated cells at 48 hours showed significance suggesting the number of cells in treated wells were significantly lower than control wells. But, by the next day at 72 hours, the cells had grown back in the treated wells and the p value showed non-significance, suggesting the 4-spray treatment of CLKRS@AgNP is not toxic to the fibroblast cells. Proliferation of cells was confirmed by the p value assessed between the treated cell counts of day 1 and day 2; day 2 and day 3; day 1 and day 3, all of which was found to be less than 0.05, showing significant increase of cells in the treated wells compared with the cell count from the previous day. At day 3, the cells were also found to become confluent.

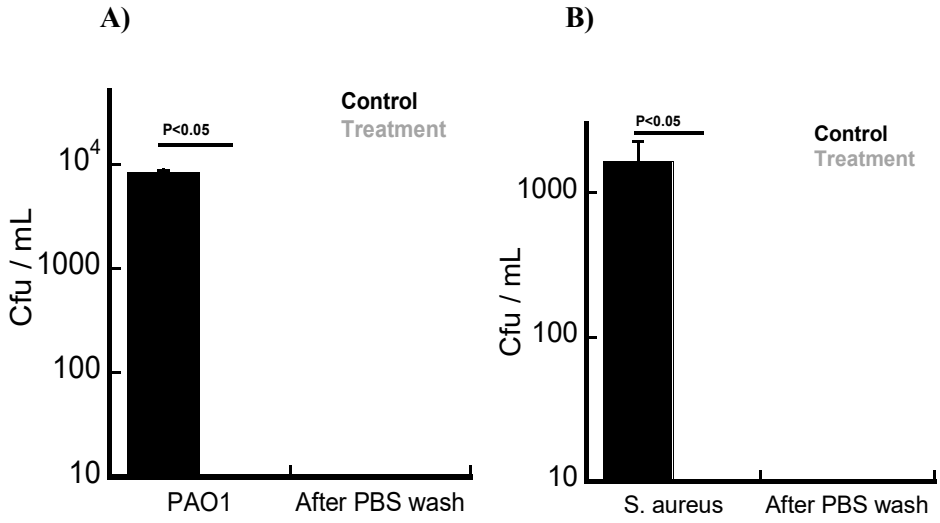

C)

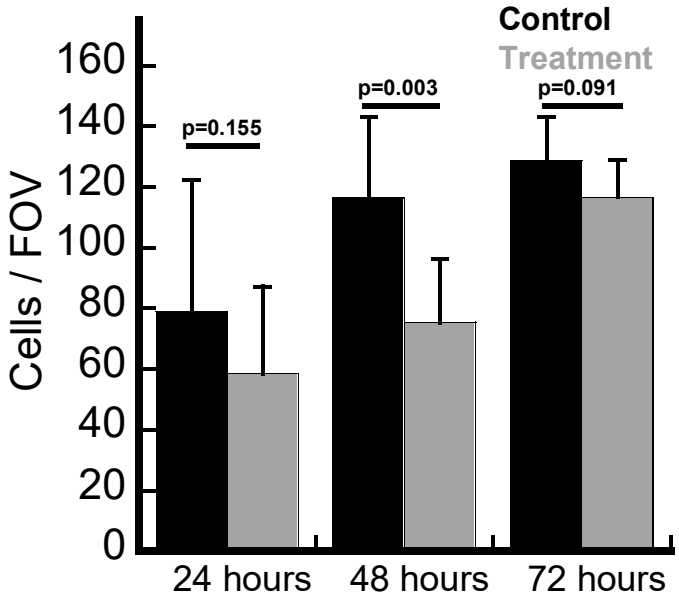

Figure 16: Plot showing surviving planktonic count of **A)** PAO1 & **B)** *S. aureus* on dermal fibroblasts seeded in rat tail hydrogels, **C)** shows no. of fibroblast cells in control and treated wells at 24, 48 and 72 hours (n=3).

Microscopic images were taken of the control and treated wells for both part of the experiment. The non-cytotoxicity of the spray on formulation was supported by the images shown in Figure 17. The fibroblasts had the GFP protein that provided the fluorescence and was found to proliferate in control and treated wells. The green colour in the background indicates the collagen hydrogel showing the 3D matrix where the cells are seeded that mimics the extracellular matrix in a human body. Figure 18 represents the fibroblast cells in the control and treated wells in the presence of *s. aureus* bacteria, and after the pbs washes. It showed the live fibroblasts in the control and treated wells suggesting the planktonic growth of *S. aureus* were not as much to affect the viability of the fibroblast cells significantly. It showed that the fibroblast cells survived in the control and treated wells in the presence of *S. aureus*, that couldn't grow at all in the treated wells.

Control

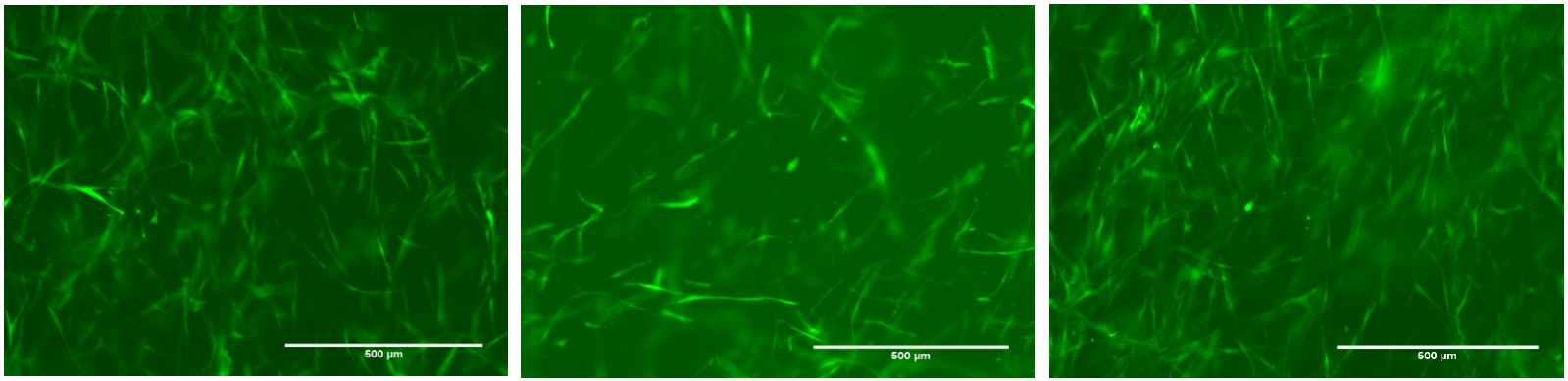

Treated

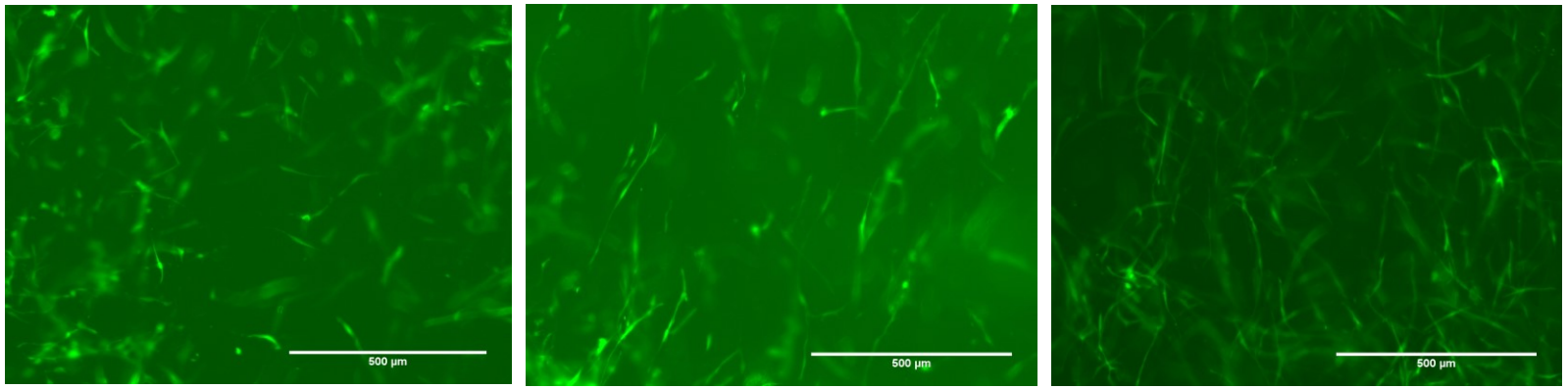

Figure 17: Fluorescent microscopic images of fibroblast cells seeded in rat tail collagen hydrogels at 24 (left), 48 (middle) and 72 hours (right).

Control

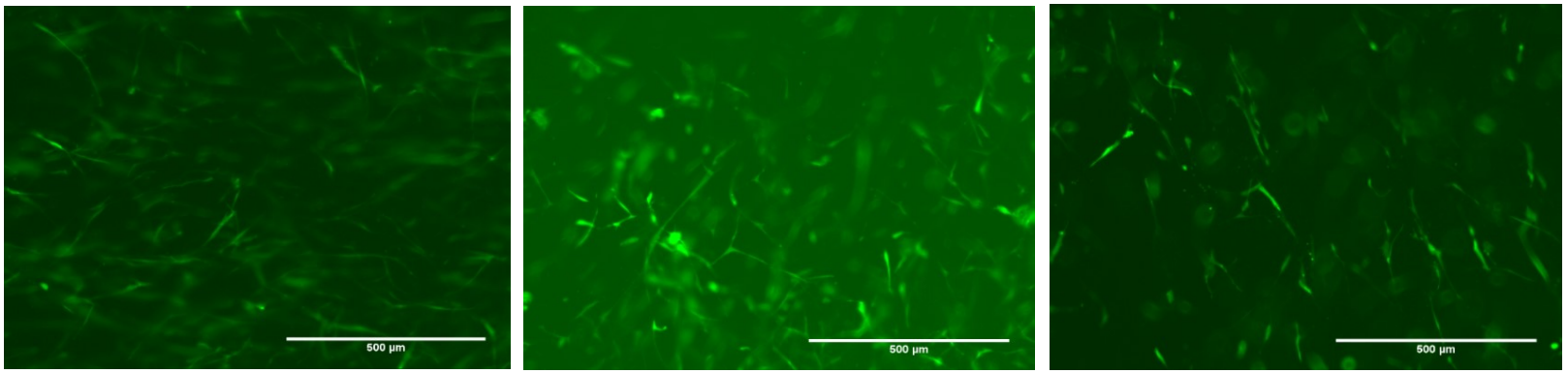

Treated

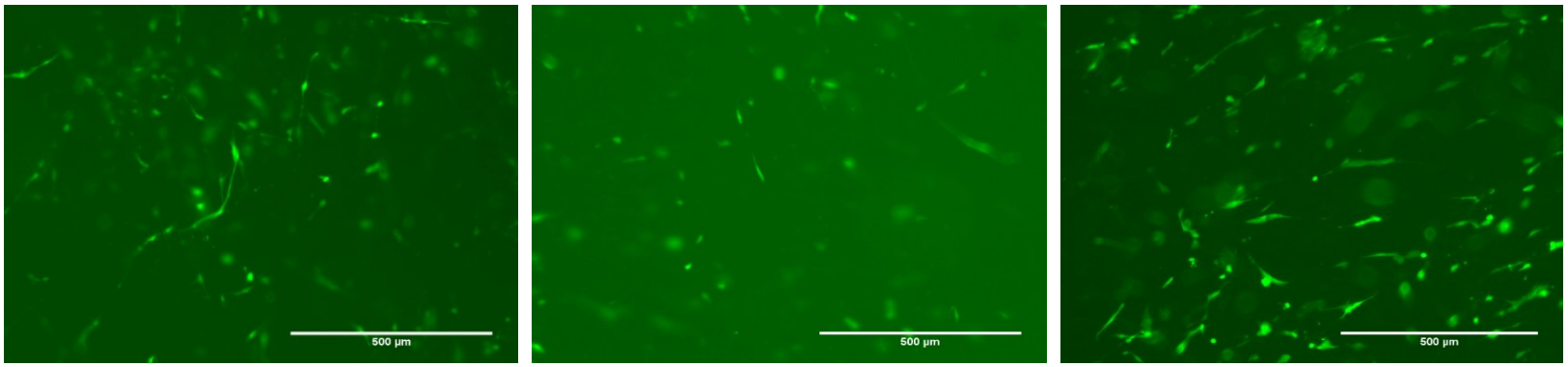

Figure 18: Fluorescent microscopic image of control and treated fibroblast cells seeded in rat tail collagen hydrogels before inoculation of *s. aureus* bacteria (left), after 16 hours incubation of bacteria (middle) and after PBS washes (right).

3.4. Results obtained from the proposed method for coating the spray-on formulation on titanium discs

The biomaterials used in manufacturing indwelling medical devices are biocompatible and manufactured according to its application (whether the implant needs to be soft like polymer or strong like metal). Most orthopedic (artificial hip joints, knee joints, bone plates etc.), dental (dental screws, bridges etc.) and cardiovascular implants (cardiac valve prosthesis, artificial heart, pacemakers etc.) are made of metals, commonly by titanium and its alloy for its excellent physical and mechanical properties such as high biocompatibility, high resistance to corrosion, high durability, low modulus of elasticity corresponding to low stiffness, high strength to specific weight ratio etc.[158-160] Titanium is one of the most successful metallic biomaterial which is extensively used today for manufacturing various devices as mentioned above.[156] Hence, titanium discs were obtained and tested for coating the spray-on formulation for this project.

The APTES used as explained in the methods, was found to effectively promote silanization, thereby linking the amine groups of the APTES to the exposed surface of the silver by dipole/coordinate bonds. Physical observations were made, and the photographic images taken are provided in Figure 19.

A prominent yellow colour was observed after the 4-spray treatment of the AgNP, however, there was a very slight change in colour after 10 consecutive PBS washes, suggesting the coating developed is not strong and can eventually wear out. However, as an initial preliminary test, coating of AgNP formulation via silanization was done to see if it is effective or not. The formation of yellow film suggests the AgNP precipitate (coating) on the surface which indicates potential in this method of coating. Further tests are needed to be done to ensure:

1. A sufficiently strong adhesion of AgNP on the titanium surface
2. Bacterial and biofilm tests on the treated titanium to confirm the delivery of antibacterial and antibiofilm properties seen on the plastic cell culture well plate
3. A method to evaluate the toxicity of human cells on the treated titanium surface

These are important tests that needs to be done in future to suggest that prepared antimicrobial and biocompatible CLKRS@AgNP formulation can be effectively used as a coating on metallic based biomaterials which are used to manufacture various indwelling medical devices.

Figure 19: Photographic images of the titanium discs before treatment (left), after treatment (middle) and after 10 PBS washes (right) (Disc diameter=1.5cm).

3.5. Optimization of *in-situ* formed CLKRS@AgNPs on collagen-based cornea-like gel

Corneal transplantation is a common therapeutic approach to replace or protect a damaged, ulcerated or diseased cornea (which sometime leads to blindness[161]) that cannot be healed with drugs or surgeries. To overcome its limitation of graft failure, graft rejection or unavailability of donor grafts, corneal implantations are done using synthetic corneal implant.[162-163] Reasons of implant failure include extrusion, rejection, glaucoma and retinal detachment.[162] Another reason for implant failure is infection and its unavailability of effective treatment, as mentioned in the literature, and thus comes the need of alternative approach.

The other biomaterial tested with the AgNP formulation was the collagen-based cornea like gels as mentioned earlier, which is a potential corneal implant as studied by various investigators. *In-situ* preparation of AgNP on the corneal gels ensured more rapid, cheaper and user-friendly synthesis of AgNP, hence, instead of CLKRS@AgNP spray-on treatment, a different method was used to synthesize and prepare the CLKRS@AgNP formulation which was tested on the corneal gels. The method used, as explained in the methodology also ensures *in-situ* synthesis of AgNP protected with the desired capping agent on different types of

polymeric material, hence can be used to synthesize on other polymeric biomaterials used not only for corneal implants but also in other applications.

To test the AgNP coating on corneal gels, first the synthesis method was optimized by preparing different formulations with different concentration of silver, Irgacure-2959 and the CLKRS peptide. Once the formulation was selected, it was synthesized on clean and dry corneal gels producing a coating of CLKRS@AgNPs on it.

For optimization of the formulation, physical observations were made, and the first 3 formulations (F1, F2, F3) to provide a yellow colour solution (indication of formation of AgNP with absorption of around 400 nm) were selected and are listed below in Table 4. Each of the three formulation were irradiated for 5 min in the UVA photoreactor. This was the best possible way to evaluate rapid synthesis of AgNP as it was not feasible to take SEM/TEM images to calibrate the presence of AgNP during optimization for the best formulation. The reason to select the formulation that give quicker yellow colour solution was to obtain a synthesis method which is rapid and have low photolysis time. There are various benefits of having an effective and rapid AgNP synthesis method including being cost effective and user-friendly.

Table 4: List of concentration of silver, I-2959 and CLKRS peptide of the formulations selected for corneal gel experiments (5 min irradiation in all cases).

Formulations (F)	**$AgNO_3$ Conc. (mM)**	**I-2959 Conc. (mM)**	**CLKRS Conc. (mM)**
1	0.5	0.5	0.1
2	0.55	0.55	0.015
3	0.6	0.6	0.02

The above 3 formulations were selected and tested for antibacterial and biocompatibility properties. But before that, various AgNP characteristics were important to be determined to ensure the stability of the AgNP formulation, such as AgNP size (measured from SEM, TEM and DLS), SPB (showing maximum absorbance at specific wavelength), zeta potential and silver content in each of the formulation. The SPB (Figure 20) showed F1 to have the maximum absorbance suggesting that it is the most stable of all the 3 formulations. This can

be attributed to the fact that the peptide concentration was highest in F1 indicating high amount of capping agent available to protect the surface of the AgNP, thereby producing stable solution, as we already know the affinity of the CLKRS peptide to bind with the AgNP surface is high. However, there are various other factors that determine the stability of the AgNP, hence other parameters were also evaluated.

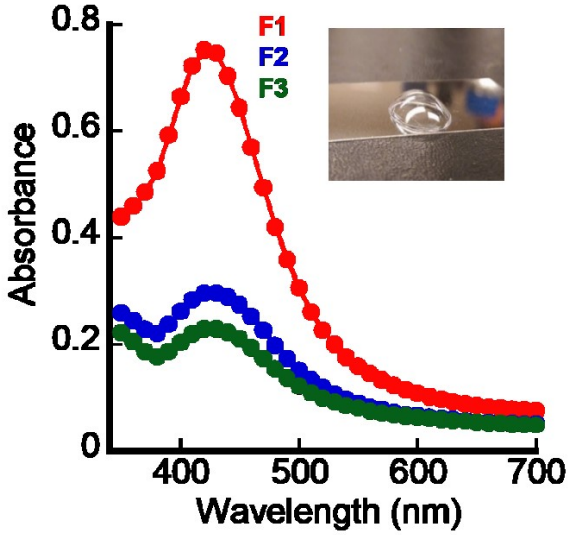

Figure 20: Surface plasmon band of AgNP with F1, F2 and F3 formulation synthesized on collagen like corneal gels shown at the top right side with diameter around 1.2-1.3 cm.

There are various methods to determine the size of the NPs. In this project the size of the AgNPs were characterised using dynamic light scattering (DLS) in a Malvern DTS-nano and were measured from SEM and TEM images using ImageJ software. Cryo-SEM images were also obtained, but since the AgNPs were not as clear, the sizes of the NPs were not able to be measured. The summary of the size, zeta potential, maximum absorbance and maximum wavelength at SPB of all the 3 formulations are given in Table 5. The variation in size of the NPs evaluated by DLS, SEM and TEM could be attributed to the fact that the DLS measures hydrodynamic size of the NP hence it appears to be larger than actual.[148] Also, the NP in DLS is measured in an aqueous solution with concentrated amount of NPs, thus the NP have the tendency to aggregate and show large sizes.[164] From the known fact, the order of the size of the AgNPs was expected to be DLS >SEM&TEM, however the order obtained was SEM >DLS >TEM. This can be explained by the fact that the batch-batch variability causes changes

in parameters of the AgNP, such as its size. In SEM images, many NPs were observed to be larger as they seemed to aggregate. It could have happened due to various reasons, one being the concentration of the AgNP solution used were higher than the concentration used in TEM. The zeta potential of the AgNPs in F1 and F3 formulations were found to be greater than 30 mV which is a characteristic for stability as it has sufficient electrostatic repulsion to remain stable in solutions.[165] The wavelength at SPB of all the 3 formulations were observed to be similar, hence not much information could be derived from the wavelength alone.

Table 5: Characterization of the AgNPs in F1, F2 and F3 formulations

Parameters	Instrument	F1	F2	F3
Size of the NP (mean diameter in nm)	DLS	9.9±0.4	21±4.4	50±22
	SEM	16±11	65±37	29±13
	TEM	8.2±9	11.4±7	15±14
Zeta potential in mv	DLS	+33±1	+28±1.7	+37±0.6
Absorbance	Spectrophotometer	0.752	0.297	0.23
Wavelength at SPB in nm	Spectrophotometer	420	430	430

Figure 21A represents the SEM images of F1, F2 and F3 formulation and the plot (Figure 21B) shows the size distribution of the AgNPs observed in the SEM images. The images obtained appeared to be blurred and due to high concentration of AgNPs in the sample, it was difficult to evaluate, nevertheless evaluation using ImageJ was done and plotted. From the SEM images, AgNPs in the F2 formulation appeared to be largest and F1 to be the smallest, suggesting F1 formulation could better serve as antibacterial coating, as previously mentioned that smaller NPs are more bactericidal.

A)

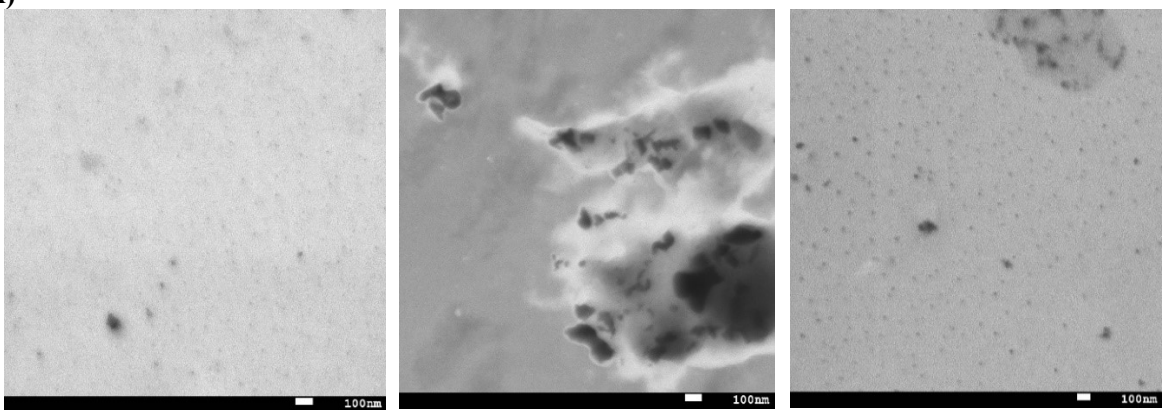

B)

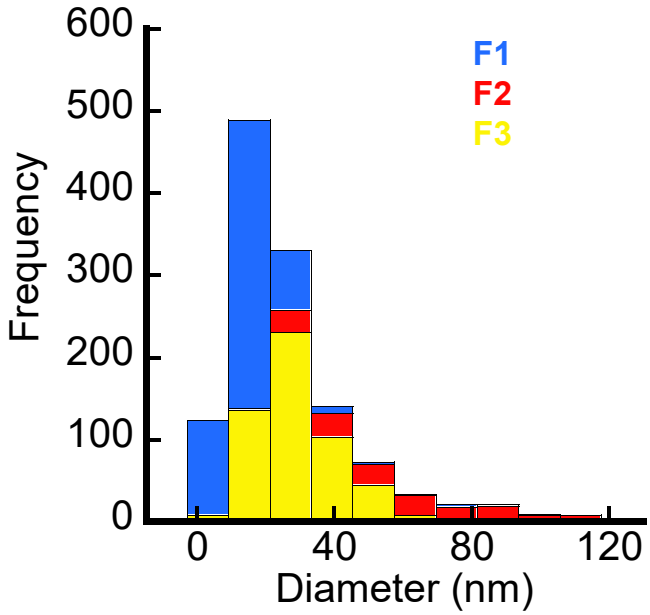

Figure 21: A) SEM images of CLKRS@AgNP of F1 (left), F2 (middle) and F3 (right), **B**) Size of silver nanoparticles vs frequency from the SEM images of CLKRS@AgNP samples (n=556 for F1, 165 for F2 and 533 for F3).

Similar evaluation was done from the TEM images obtained which were clear and easily perceived. From the size distribution plot as shown in Figure 22B, AgNPs in the F3 formulation were observed to be the largest and F1 to be the smallest. The TEM images are provided in Figure 22A.

By determining the size of the AgNPs from the DLS, SEM and TEM, it was observed that NPs in the F1 formulation has the smallest size, thereby it can be used as an effective antimicrobial coating in comparison to the other 2 formulations, since smaller AgNPs are found to be more bactericidal as mentioned earlier.

A)

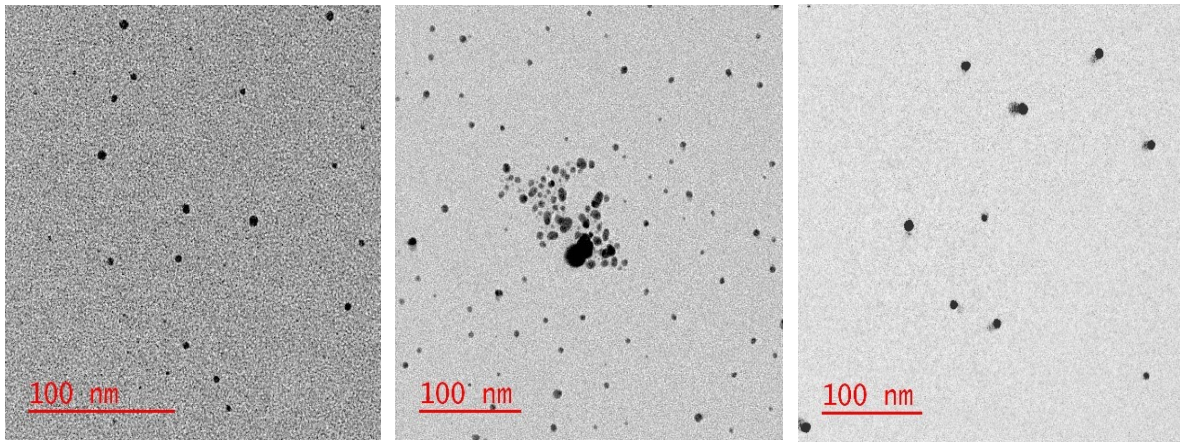

B)

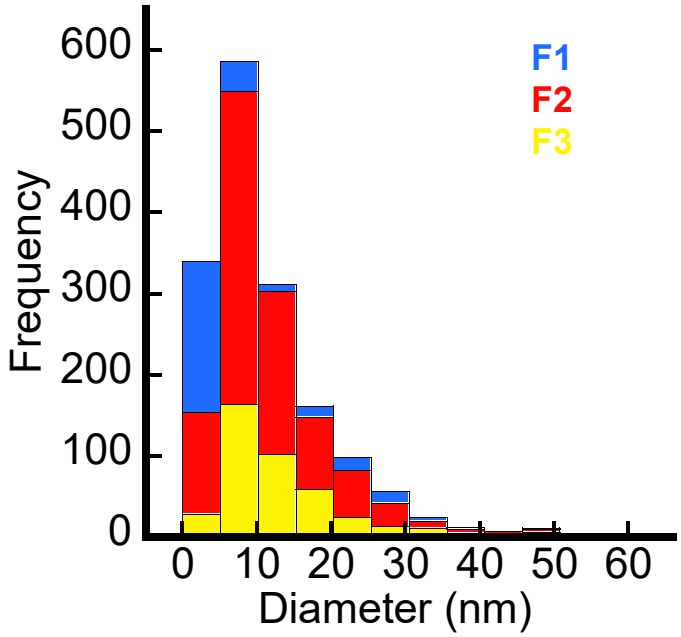

Figure 22: A) TEM images of CLKRS@AgNP of F1 (left), F2 (middle) and F3 (right), **B)** Size of silver nanoparticles vs frequency from the TEM images of CLKRS@AgNP samples (n=282 for F1, 906 for F2 and 424 for F3).

Finally, silver content was evaluated by ICP test to determine which of the formulation has the highest concentration of silver. From the results shown in Figure 23, it was observed that AgNPs in the F1 formulation has the least silver content suggesting it to be the best formulation of all the 3. This can be explained by the initial concentration of silver used (concentration of silver nitrate) which was least in F1 formulation.

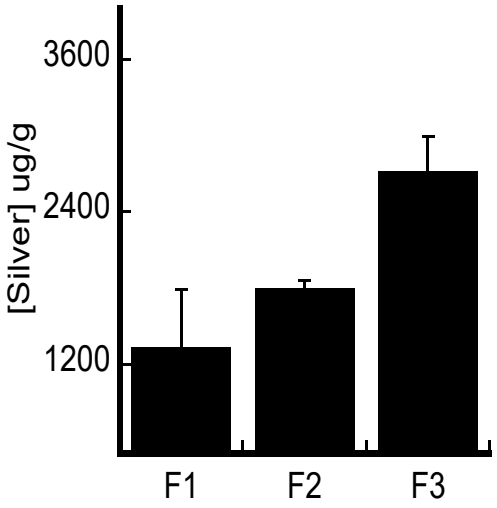

Figure 23: Inductively Coupled Plasma test results for F1, F2, F3 formulations. Data expressed in µg of total silver per g of dry hydrogel (n=3)

From the above evaluated parameters, it can be concluded that F1 formulation of CLKRS@AgNP can be expected to show good antimicrobial and non-cytotoxicity results, however, these tests were done with all the 3 formulations to confirm the hypothesis.

3.6. Bacterial experiment result for treated corneal gels

As mentioned in Table 1, the most common pathogen to colonize the contact lenses and corneal implants are *P. aeruginosa, S. epidermidis, S. aureus, E. coli* and species of Candida, Proetus and Serratia. For this experiment *P. aeruginosa* and *S. epidermidis* were used and inoculated on the treated corneal gels and quantified for testing the inhibition rate of the planktonic bacteria. All the 3 formulations showed significant difference in the growth of bacteria in the treated wells when compared to control (Figure 24). The F1 formulation inhibited the PA14 and *S. epidermidis* growth to 99% while F2 formulation inhibited the *S. epidermidis* growth to

99%. F3 formulation also significantly inhibited the planktonic bacteria, but F1 showed to work best for the both the strains. This result suggested that CLKRS@AgNP is effective in preventing the planktonic bacterial growth on the treated corneal gels.

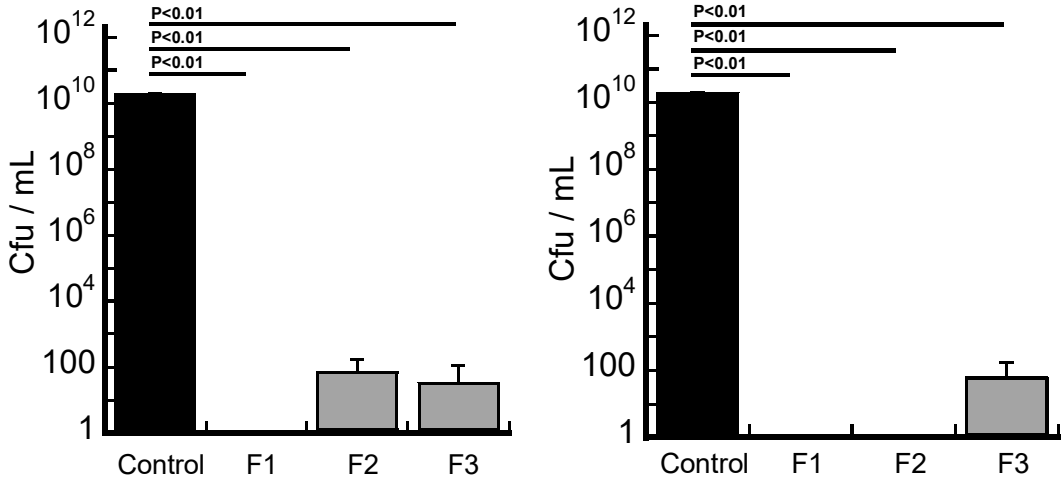

Figure 24: Surviving planktonic cells of *P. aeruginosa* PA14 (left) and *S. epidermidis* (right) on control and treated corneal gels (n=3)

3.7. Cell viability results for treated corneal gels

Cell viability test was done with human cornea epithelial cells and mouse bone marrow derived macrophages. Epithelial cells were monitored up to 3 days beyond which the cells became too confluent. There was a significant increase in cells in the treated wells when compared to control, which indicated the epithelial cell growth on AgNP treated gels, suggesting the AgNP formulation was not only non-cytotoxic but also induced proliferation of the epithelial cells (Figure 25A). The proliferation was confirmed by the p value assessed between day 1 and day 3 in treated wells, which was less than 0.05 showing significant increase in cell counts in the treated wells compared to the previous day. All the 3 formulations had similar results with F3 being the best of all. The data was supported by the microscopic images of epithelial cells on the control and treated corneal gels as shown in Figure 25B.

A)

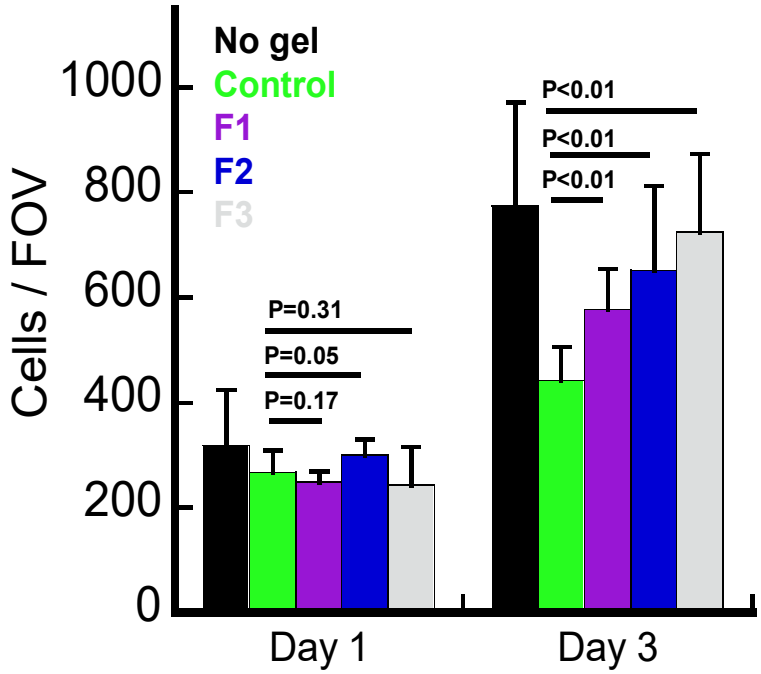
No gel
Control
F1
F2
F3
Cells / FOV
1000
800
600
400
200
0
P=0.31
P=0.05
P=0.17
P<0.01
P<0.01
P<0.01
Day 1
Day 3

B)

DAY 1:

No gels

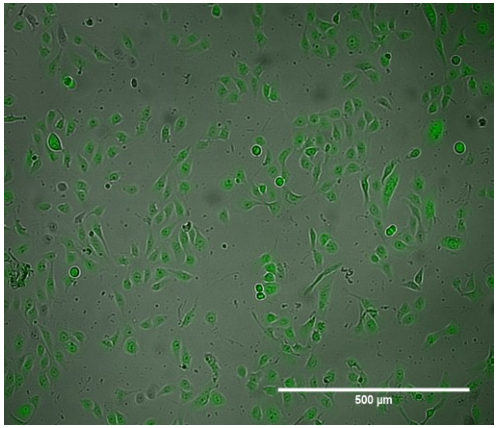

Control

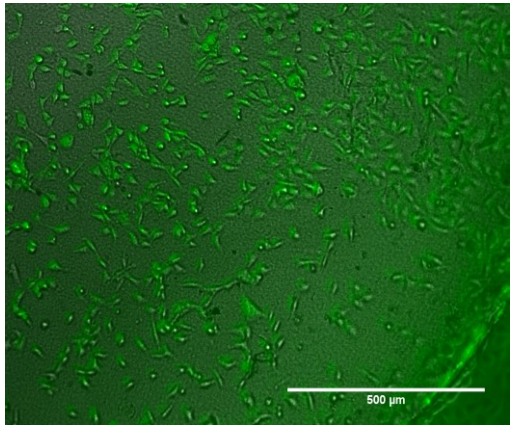

F1

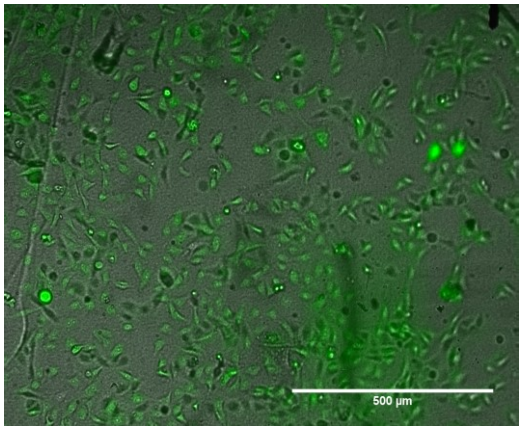

F2

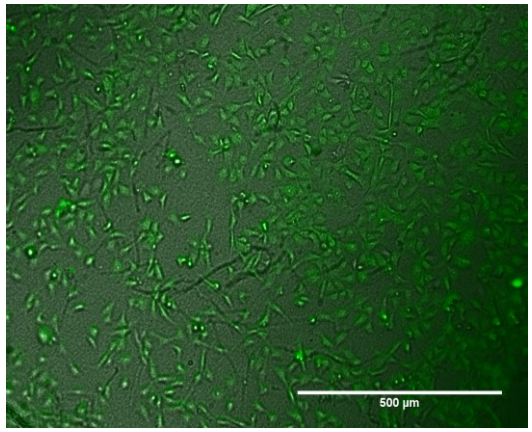

F3

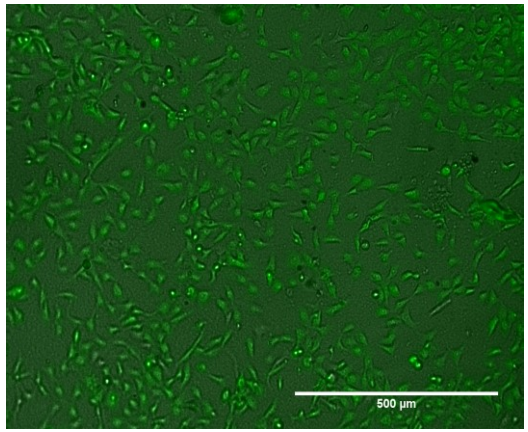

DAY 3:

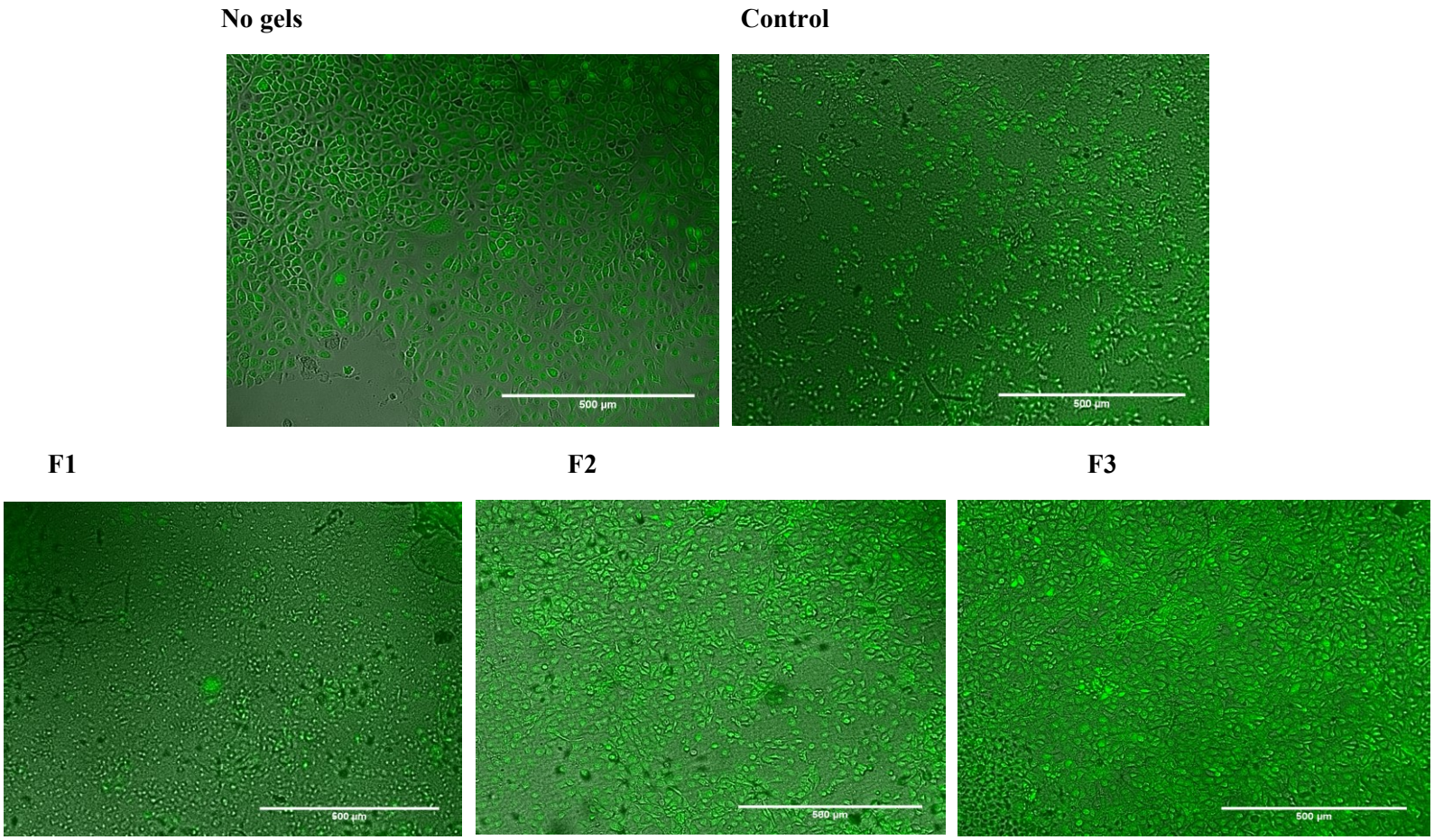

Figure 25: A) Plot shows epithelial cell counts on plastic cell culture plates (no gel), corneal gel (control) and treated cornea gels with F1, F2 and F3 formulation, **B)** Microscopic image of control and treated epithelial cells at Day 1 and Day 3 (n=4).

While testing the toxicity with macrophages, there was a significant decline in cell count after day 3 compared to control as shown in Figure 26A. This does not necessarily mean that the AgNP formulations are cytotoxic, since the cells used here were macrophages. We know the 2 most common type of macrophages that exist are M1 and M2 which grows on different situations. In this test, it was not determined whether the cells observed were M1 or M2. There was a difference in the phenotype observed in the microscopic images of the macrophages on the control and treated wells as shown in Figure 26B, suggesting there were two possible populations of the macrophages growing on the corneal gels. The way M1 and M2 would grow and react on the corneal gels is expected to be different. The counting of the cells was done altogether which could attribute to errors in the results of the cell counting. Hence, a follow-up experiment on macrophages is required by identifying and counting the M1 and M2 types through immunostaining that could provide better insight of the toxicity and immunological aspect of the AgNP formulations in a living body.

From the results obtained so far, it can be suggested that the CLKRS@AgNP formulation is not toxic to epithelial and macrophages cells.

A)

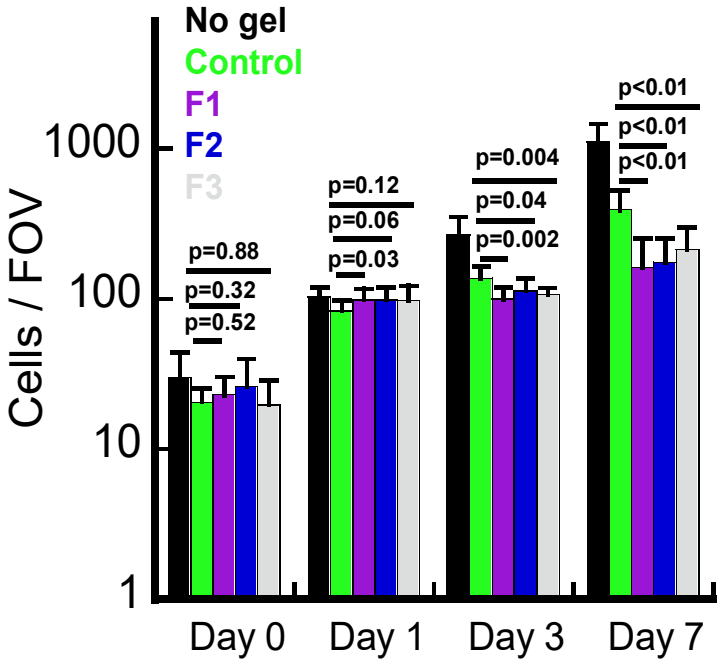

B)

DAY 0

No gels

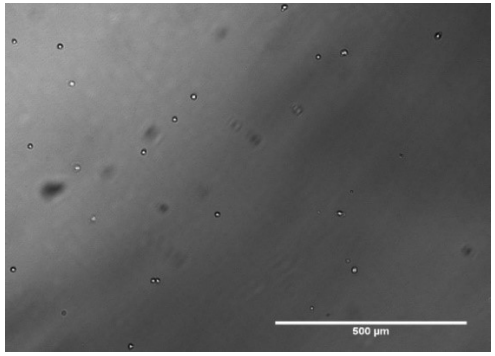

Control

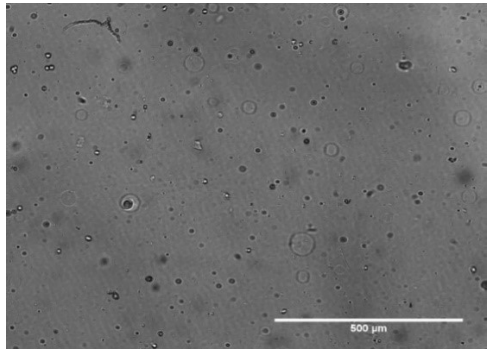

F1

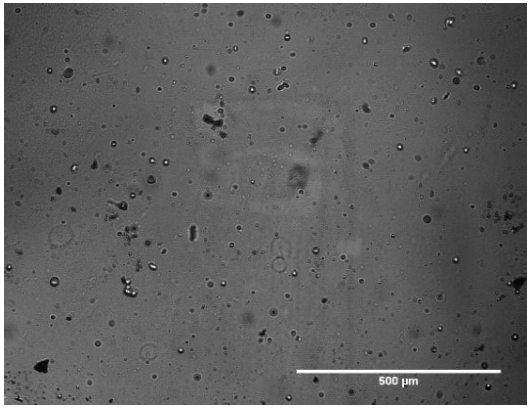

F2

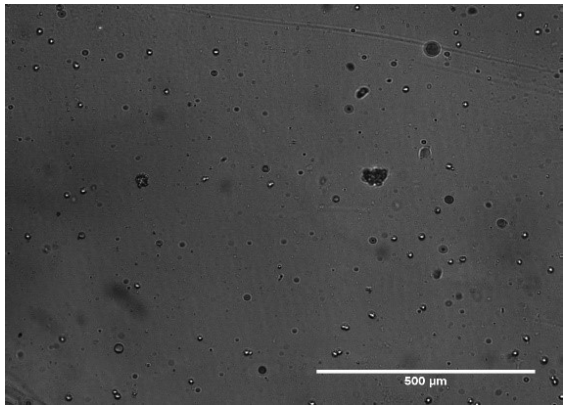

F3

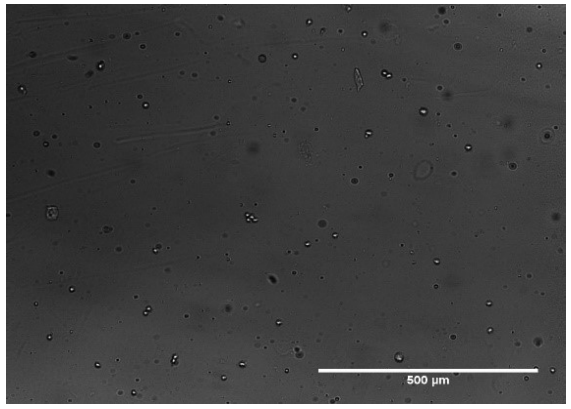

DAY 1

No gels

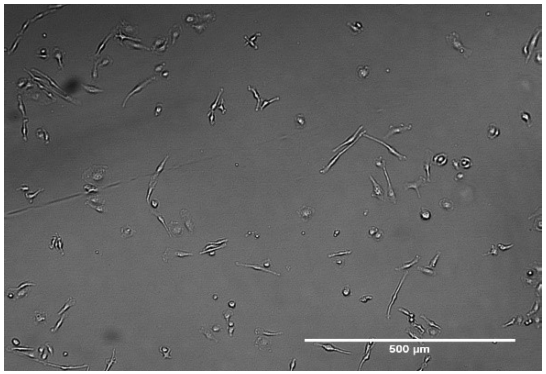

Control

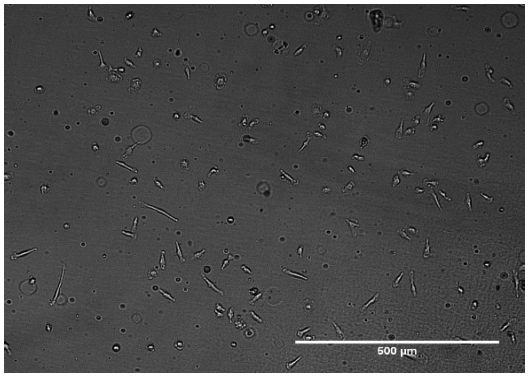

F1

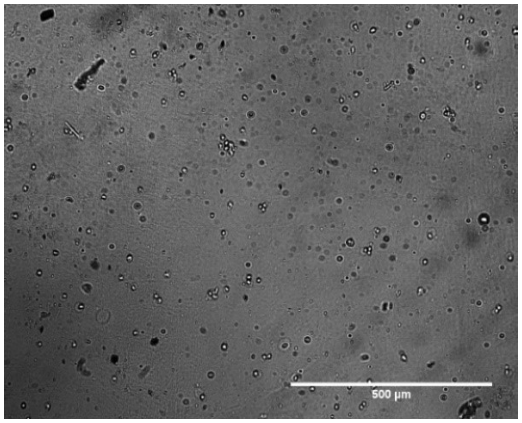

F2

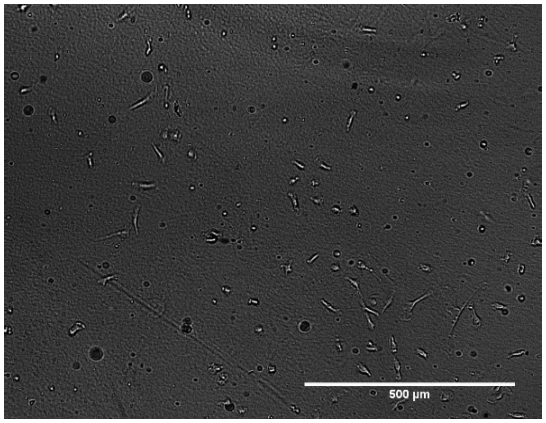

F3

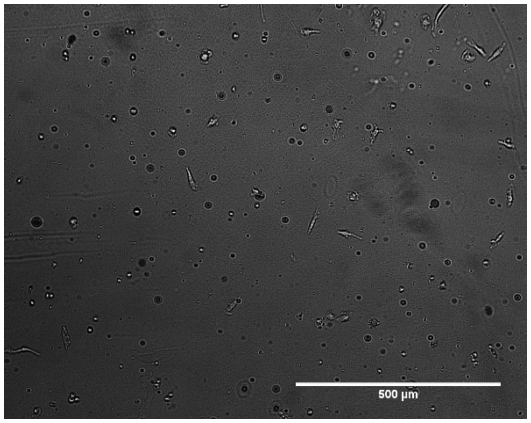

DAY 3

No gels

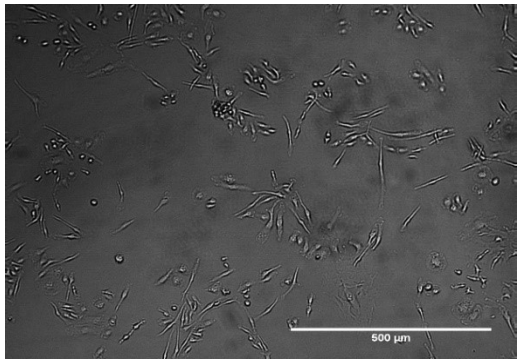

Control

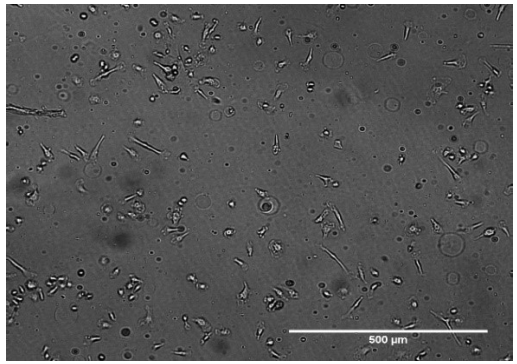

F1

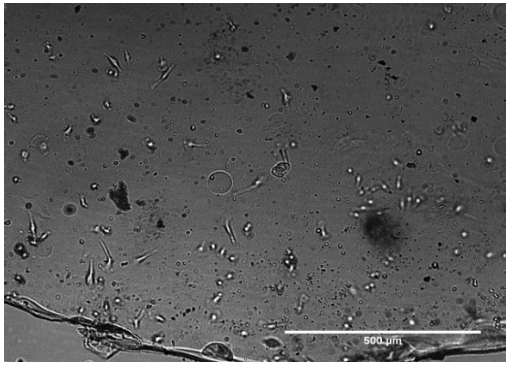

F2

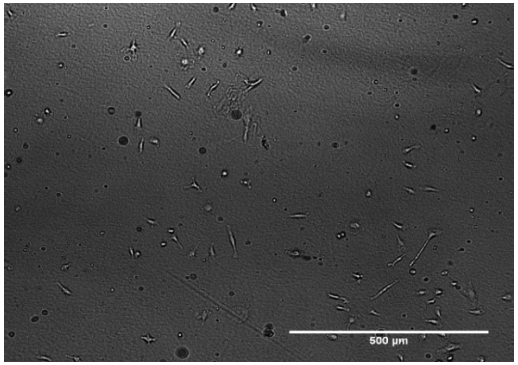

F3

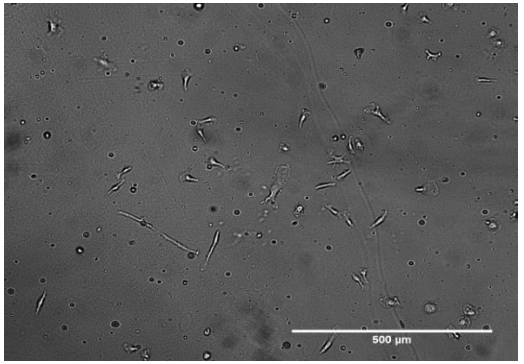

DAY 7

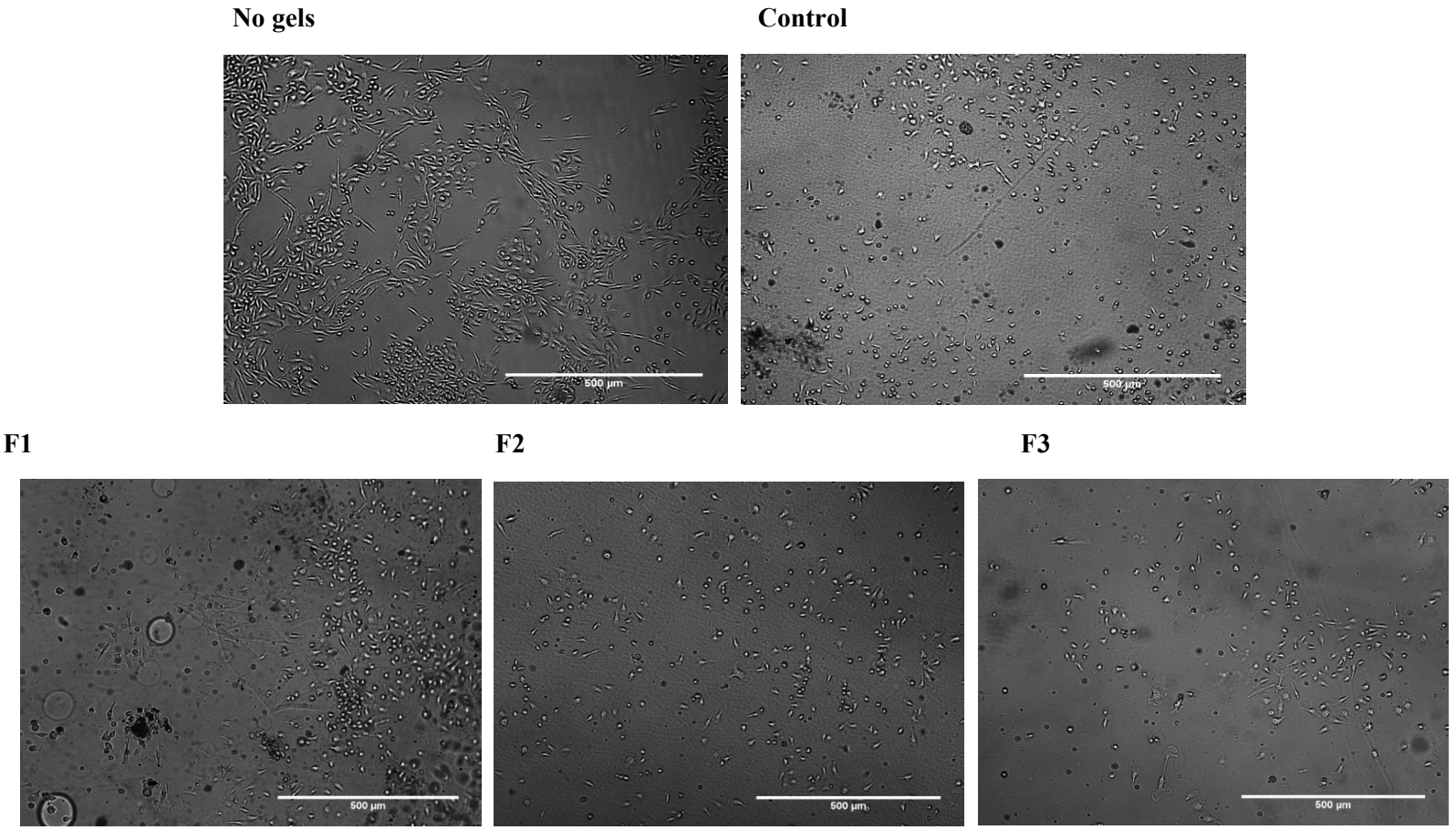

Figure 26: A) Plot shows macrophage cell counts on plastic cell culture plates (no gel), corneal gel (control) and treated cornea gels with F1, F2 and F3 formulation, **B)** Microscopic image of control and treated macrophage cells at Day 0,1,3 and 7 (n=3).

Chapter 4- Conclusions and Future work

4.1. Limitations

Even though AgNP has shown to be antimicrobial and biocompatible, there are some limitations to it and some limitations with this project. Firstly, not all forms of silver possess antimicrobial properties. Efficacy depends upon silver species, its delivery system, duration of release, size, shape and concentration of silver content.[20] Ionic and colloidal metallic silver has shown to possess a number of side effects in comparison to AgNP, as it is more toxic to mammalian cells especially to keratinocytes and fibroblasts. Specifically, due to silver deposition, it can cause cosmetic abnormalities upon prolonged use, transient skin discolouration, allergic response, leucopenia, bone marrow toxicity, renal or hepatic damage.[20] Silver ions are highly reactive species that bind with negatively charged proteins, DNA, RNA, inflammatory related molecules and other anions that leads to formation of complexes and complicates delivery.[20] The limitation of topical silver antimicrobial is that it cannot penetrate deeply in the tissue, it lacks control over silver release, it limits release of reactive species which reduces the efficacy of antimicrobial effect and slows wound healing.[20]

Evidence also exists for toxicity of AgNP towards mammalian germline stem cell which decreases the function of mitochondria, increases membrane leakage, induces apoptosis and necrosis, however it displays significantly less systemic toxicity and has found to be in organs like liver, spleen and kidney in low concentrations.[20, 166] One of the main limitation of AgNP therapeutic application is limited knowledge of long term effects of AgNPs in living organisms. [19] They have found to lack long term stability in solution,[44] thereby found to be effective only for a small period of time in a living organism. Hence, it can be said that although studies show AgNP to be biocompatible, it is still yet to be determined at what extent does the biocompatibility lie.

Some highlights and drawbacks of this thesis can be summarized as follows:

1. Since AgNP is known to be biocompatible for short amount of time, the CLKRS@AgNP formulation can be used as a coating on indwelling medical devices

to treat surgical site infections and implant associated infections which arises almost immediately after the surgery or within few days.

2. The method used to coat the titanium discs needed further evaluation to strongly suggest that the method can successfully coat the AgNP formulation on metals like titanium and ceramics-based biomaterials.
3. While spraying the formulation onto an objective using the airbrush make up system, one drawback related directly to this was the spray intensity was not monitored and controlled or kept constant throughout the project. There were different airbrushes used thereby making the delivery of treatment slightly different suggesting a possibility that some wells were treated more than others, however with a matter of solution less than 0.6 mL.
4. While calibrating the macrophage viability assay, the macrophages cells displayed different morphology after 3rd day and did not proliferate on the treated gels as much as in control, suggesting a need to further analyze and identify the M1 and M2 types.

4.2. Future work

This study was an *in-vitro* assessment of the CLKRS@AgNP coating on plastic cell culture well plate which can be transferred to titanium-based materials and on collagen like corneal gels. This was the first and initiative step in delivering this treatment to a clinical setting. From here, animal infection models are needed to be studied. Silver infiltration in organs of the animal needs to be measured. Biofilm assays needs to be run on corneal gels, as biofilm causing infections are way more common than planktonic causing infections. Inflammatory and further cell viability assays are needed to be done to further support the biocompatibility of the formulation. Finally, this formulation needs to be effectively coated on various biomaterials, such as different polymer (HDPE, PVC etc.), ceramics (zirconia, hydroxyapatite etc.), and other metals and its alloys including titanium, used widely in implant device manufacturing, to effectively apply the treatment on implants.

4.3. Conclusions

In conclusion, the objectives of the project were obtained, and the hypothesis was proved showing CLKRS@AgNP formulation to be antibacterial and antibiofilm. The formulations showed to be non-cytotoxic to human dermal fibroblast, human epithelial cells and mice macrophages. This was obtained by the preparation of an effectively optimized formulation used as a spray-on treatment and direct synthesis on collagen like corneal gels. A method to coat the AgNP spray-on treatment on titanium discs was proposed which showed potential for successful coating and delivery of the antimicrobial properties of AgNP on titanium-based implants. By working on the limitations and future work mentioned earlier, CLKRS@AgNP can be effectively utilised in clinical settings, thereby providing an alternative treatment to antibiotics and expensive re-implantation surgeries for implant associated infections.

References

1. Bjarnsholt, T., Introduction to Biofilms. In *Biofilm Infections*, Bjarnsholt, T.; Jensen, P. Ø.; Moser, C.; Høiby, N., Eds. Springer New York: New York, NY, 2011; pp 1-9.10.1007/978-1-4419-6084-9_1
2. Bjarnsholt, T., The role of bacterial biofilms in chronic infections. *APMIS* **2013,** *121*, 1-58.10.1111/apm.12099
3. Veerachamy, S.; Yarlagadda, T.; Manivasagam, G.; Yarlagadda, P. K., Bacterial adherence and biofilm formation on medical implants: a review. *Proc. Inst. Mech. Eng. H* **2014,** *228* (10), 1083-99.10.1177/0954411914556137
4. Al-Ahmad, A.; Wiedmann-Al-Ahmad, M.; Faust, J.; Bachle, M.; Follo, M.; Wolkewitz, M.; Hannig, C.; Hellwig, E.; Carvalho, C.; Kohal, R., Biofilm formation and composition on different implant materials in vivo. *J. Biomed. Mater. Res. Part B* **2010,** *95* (1), 101-9.10.1002/jbm.b.31688
5. Jamal, M.; Ahmad, W.; Andleeb, S.; Jalil, F.; Imran, M.; Nawaz, M. A.; Hussain, T.; Ali, M.; Rafiq, M.; Kamil, M. A., Bacterial biofilm and associated infections. *J Chin. Med. Assoc.* **2018,** *81* (1), 7-11.10.1016/j.jcma.2017.07.012
6. Karatan, E.; Watnick, P., Signals, regulatory networks, and materials that build and break bacterial biofilms. *Microbiol. Mol. Biol. Rev.* **2009,** *73* (2), 310-47.10.1128/MMBR.00041-08
7. Davies, D., Understanding biofilm resistance to antibacterial agents. *Nat. Rev. Drug Discovery* **2003,** *2* (2), 114-22.10.1038/nrd1008
8. Gupta, P.; Sarkar, S.; Das, B.; Bhattacharjee, S.; Tribedi, P., Biofilm, pathogenesis and prevention--a journey to break the wall: a review. *Arch. Microbiol.* **2016,** *198* (1), 1-15.10.1007/s00203-015-1148-6
9. Lorite, G. S.; Rodrigues, C. M.; De'Souza, A. A.; Kranz, C.; Mizaikoff, B.; Cotta, M. A., The role of conditioning film formation and surface chemical changes on Xylella fastidiosa adhesion and biofilm evolution. *J. Colloid Interface Sci.* **2011,** *359* (1), 289-95.10.1016/j.jcis.2011.03.066
10. Paharik, A. E.; Horswill, A. R., The staphylococcal biofilm: adhesins, regulation, and host response. *Microbiol. Spectr.* **2016,** *4* (2).10.1128/microbiolspec.VMBF-0022-2015
11. Vergidis, P.; Patel, R., Novel approaches to the diagnosis, prevention, and treatment of medical device-associated infections. *Infect. Dis. Clin. North Am.* **2012,** *26* (1), 173-86.10.1016/j.idc.2011.09.012
12. Horikoshi, S.; Serpone, N., Introduction to Nanoparticles. *Microwaves in Nanoparticle Synthesis* **2013**.doi:10.1002/9783527648122.ch1

10.1002/9783527648122.ch1
13. González-Béjar, M., Silver Nanoparticles in Heterogeneous Plasmon Mediated Catalysis. In *Silver Nanoparticle Applications: In the Fabrication and Design of Medical and Biosensing Devices*, Alarcon, E. I.; Griffith, M.; Udekwu, K. I., Eds. Springer International Publishing: Cham, 2015; pp 71-92.10.1007/978-3-319-11262-6_4
14. Stamplecoskie, K., Silver Nanoparticles: From Bulk Material to Colloidal Nanoparticles. In *Silver Nanoparticle Applications: In the Fabrication and Design of Medical*

and Biosensing Devices, Alarcon, E. I.; Griffith, M.; Udekwu, K. I., Eds. Springer International Publishing: Cham, 2015; pp 1-12.10.1007/978-3-319-11262-6_1
15. Sharma, V. K.; Yngard, R. A.; Lin, Y., Silver nanoparticles: Green synthesis and their antimicrobial activities. *Advances in Colloid and Interface Science* **2009,** *145* (1), 83-96.https://doi.org/10.1016/j.cis.2008.09.002
16. Alarcon, E. I.; Bueno-Alejo, C. J.; Noel, C. W.; Stamplecoskie, K. G.; Pacioni, N. L.; Poblete, H.; Scaiano, J. C., Human serum albumin as protecting agent of silver nanoparticles: role of the protein conformation and amine groups in the nanoparticle stabilization. *Journal of Nanoparticle Research* **2013,** *15* (1).10.1007/s11051-012-1374-7
17. Stamplecoskie, K. G.; Scaiano, J. C., Light Emitting Diode Irradiation Can Control the Morphology and Optical Properties of Silver Nanoparticles. *J. Am. Chem. Soc.* **2010,** *132*, 1825–1827
18. De Alwis Weerasekera, H.; Griffith, M.; Alarcon, E. I., Biomedical Uses of Silver Nanoparticles: From Roman Wine Cups to Biomedical Devices. In *Silver Nanoparticle Applications: In the Fabrication and Design of Medical and Biosensing Devices*, Alarcon, E. I.; Griffith, M.; Udekwu, K. I., Eds. Springer International Publishing: Cham, 2015; pp 93-125.10.1007/978-3-319-11262-6_5
19. McLaughlin, S.; Podrebarac, J.; Ruel, M.; Suuronen, E. J.; McNeill, B.; Alarcon, E. I., Nano-Engineered Biomaterials for Tissue Regeneration: What Has Been Achieved So Far? *Frontiers in Materials* **2016,** *3*.10.3389/fmats.2016.00027
20. Griffith, M.; Udekwu, K. I.; Gkotzis, S.; Mah, T.-F.; Alarcon, E. I., Anti-microbiological and Anti-infective Activities of Silver. In *Silver Nanoparticle Applications: In the Fabrication and Design of Medical and Biosensing Devices*, Alarcon, E. I.; Griffith, M.; Udekwu, K. I., Eds. Springer International Publishing: Cham, 2015; pp 127-146.10.1007/978-3-319-11262-6_6
21. Stamplecoskie, K. G.; Scaiano, J. C., Silver as an example of the applications of photochemistry to the synthesis and uses of nanomaterials. *Photochem Photobiol* **2012,** *88* (4), 762-8.10.1111/j.1751-1097.2012.01103.x
22. Phan, C. M.; Nguyen, H. M., Role of Capping Agent in Wet Synthesis of Nanoparticles. *J Phys Chem A* **2017,** *121* (17), 3213-3219.10.1021/acs.jpca.7b02186
23. Canada, H. S. M. D. i. C., https://www.canada.ca/en/health-canada/services/drugs-health-products/medical-devices/activities/fact-sheets/safe-medical-devices-fact-sheet.html. **2014**,
24. Reportlinker, Global Implantable Biomaterials Market Outlook (2014-2022). *PR Newswire* 24 September 2015, 2015.
25. Barnes, L.; Cooper, I. R., Biomaterials and Medical Device - Associated Infections. *Woodhead Publishing in Biomaterials* **2015**.https://doi.org/10.1016/C2013-0-16323-4
26. Cao, H., Silver Nanoparticles for Antibacterial Devices Biocompatibility and Toxicity. *CRC Press* **2017**,
27. Donelli, G., Biofilm based health care associated infections. *Springer* **2015,** *831*.10.1007/978-3-319-09782-4
28. Moriarty, T. F.; Zaat, S. A. J.; Busscher, H. J., Biomaterials Associated Infection: Immunological Aspects and Antimicrobial Strategies. Springer New York: New York, NY, 2013.10.1007/978-1-4614-1031-7
29. Sohns, J. M.; Bavendiek, U.; Ross, T. L.; Bengel, F. M., Targeting cardiovascular implant infection: multimodality and molecular imaging. *Circ. Cardiovasc. Imaging* **2017,** *10* (12).10.1161/CIRCIMAGING.117.005376

30. Rosenthal, V. D.; Al-Abdely, H. M.; El-Kholy, A. A.; AlKhawaja, S. A. A.; Leblebicioglu, H.; Mehta, Y.; Rai, V.; Hung, N. V.; Kanj, S. S.; Salama, M. F.; Salgado-Yepez, E.; Elahi, N.; Morfin Otero, R.; Apisarnthanarak, A.; De Carvalho, B. M.; Ider, B. E.; Fisher, D.; Buenaflor, M.; Petrov, M. M.; Quesada-Mora, A. M.; Zand, F.; Gurskis, V.; Anguseva, T.; Ikram, A.; Aguilar de Moros, D.; Duszynska, W.; Mejia, N.; Horhat, F. G.; Belskiy, V.; Mioljevic, V.; Di Silvestre, G.; Furova, K.; Ramos-Ortiz, G. Y.; Gamar Elanbya, M. O.; Satari, H. I.; Gupta, U.; Dendane, T.; Raka, L.; Guanche-Garcell, H.; Hu, B.; Padgett, D.; Jayatilleke, K.; Ben Jaballah, N.; Apostolopoulou, E.; Prudencio Leon, W. E.; Sepulveda-Chavez, A.; Telechea, H. M.; Trotter, A.; Alvarez-Moreno, C.; Kushner-Davalos, L., International Nosocomial Infection Control Consortium report, data summary of 50 countries for 2010-2015: Device-associated module. *Am J Infect Control* **2016,** *44* (12), 1495-1504.10.1016/j.ajic.2016.08.007

31. Peter, J.; Guggenbichler.; Assadian, O.; Boeswald, M.; Kramer, A., Incidence and clinical implication of nosocomial infections associated with implantable biomaterials – catheters, ventilator-associated pneumonia, urinary tract infections. *GMS J. Med. Educ.* **2011,** *6* (1),

32. Darouiche, R. O., Treatment of infections associated with surgical implants. *N. Engl. J. Med.* **2004,** *350* (14), 1422-1429.10.1056/NEJMra035415

33. Darouiche, R. O.; Farmer, J.; Chaput, C.; Mansouri, M.; Saleh, G.; Landon, G. C., Anti-infective efficacy of antiseptic coated intramedullary Nails. *J. Bone Joint Surg. Br.* **1998**,

34. Bryers, J. D., Medical biofilms. *Biotechnol. Bioeng.* **2008,** *100* (1), 1-18.10.1002/bit.21838

35. VanEpps, J. S.; Younger, J. G., Implantable Device-Related Infection. *Shock* **2016,** *46* (6), 597-608.10.1097/SHK.0000000000000692

36. Leatherman, S.; Sutherland, K., Quality of healthcare in Canada. *Canadian Health Services Research Foundation* **2010**,

37. Hovis, J. P.; Montalvo, R.; Marinos, D.; Joshi, M.; Shirtliff, M. E.; O'Toole, R. V.; Manson, T. T., Intraoperative vancomycin powder reduces Staphylococcus aureus surgical site infections and biofilm formation on fixation implants in a rabbit model. *J. Orthop. Trauma* **2018,** *32* (5), 263-268.10.1097/BOT.0000000000001136

38. Ikeanyi, U. O.; Chukwuka, C. N.; Chukwuanukwu, T. O., Risk factors for surgical site infections following clean orthopaedic operations. *Niger. J. Clin. Pract.* **2013,** *16* (4), 443-7.10.4103/1119-3077.116886

39. Mathijs D. Kalmeijer; Ella van Nieuwland-Bollen; Diane Bogaers-Hofman; Gerard A.J. de Baere; Jan A.J.W. Kluytmans, Nasal Carriage of Staphylococcus aureus: Is a Major Risk Factor for Surgical-Site Infections in Orthopedic Surgery. *Infection Control and Hospital Epidemiology* **2000,** *21* (5), 319-323

40. James D. Whitehouse; N. Deborah Friedman ; Kathryn B. Kirkland ; William J. Richardson ; Sexton, D. J., The Impact of Surgical-Site Infections Following Orthopedic Surgery at a CommunityHospital and a University Hospital: Adverse Quality of Life, Excess Length of Stay, and Extra Cost. *Infection Control and Hospital Epidemiology* **2002,** *23* (4), 183-189

41. Boersma, L.; Burke, M. C.; Neuzil, P.; Lambiase, P.; Friehling, T.; Theuns, D. A.; Garcia, F.; Carter, N.; Stivland, T.; Weiss, R.; Effortless; Investigators, I. D. E. S., Infection and mortality after implantation of a subcutaneous ICD after transvenous ICD extraction. *Heart Rhythm* **2016,** *13* (1), 157-64.10.1016/j.hrthm.2015.08.039

42. Berbari, E. F.; Hanssen, A. D.; Duffy, M. C.; Steckelberg, J. M.; Ilstrup, D. M.; Harmsen, W. S.; Osmon, D. R., Risk Factors for Prosthetic Joint Infection: Case-Control Study. *Clinical Infectious Diseases* **1998,** *27* (5), 1247-1254.10.1086/514991
43. Poblete, H.; Agarwal, A.; Thomas, S. S.; Bohne, C.; Ravichandran, R.; Phospase, J.; Comer, J.; Alarcon, E. I., New Insights into Peptide-Silver Nanoparticle Interaction: Deciphering the Role of Cysteine and Lysine in the Peptide Sequence. *Langmuir* **2016,** *32* (1), 265-73.10.1021/acs.langmuir.5b03601
44. Ahumada, M.; Jacques, E.; Andronic, C.; Comer, J.; Poblete, H.; Alarcon, E. I., Novel specific peptides as superior surface stabilizers for silver nano structures: role of peptide chain length. *J. Mater. Chem. B* **2017,** *5* (45), 8925-8928.10.1039/c7tb02349a
45. Haddad, P. A.; Mah, T. F.; Mussivand, T., In Vitro Assessment of Electric Currents Increasing the Effectiveness of Vancomycin Against Staphylococcus epidermidis Biofilms. *Artificial Organs* **2015,** *40* (8), 804-810.10.1111/aor.12678
46. Qin, S.; Xu, K.; Nie, B.; Ji, F.; Zhang, H., Approaches based on passive and active antibacterial coating on titanium to achieve antibacterial activity. *J. Biomed. Mater. Res. Part A* **2018**.10.1002/jbm.a.36413
47. Raghavachari, R.; Kim, D.-H.; Kim, M. S.; Hwang, J.; Liang, R., Monitoring of biofilm formation on different material surfaces of medical devices using hyperspectral imaging method. In *Design and quality for biomedical technologies V*, 2012.10.1117/12.909980
48. Freebairn, D.; Linton, D.; Harkin-Jones, E.; Jones, D. S.; Gilmore, B. F.; Gorman, S. P., Electrical methods of controlling bacterial adhesion and biofilm on device surfaces. *Expert Rev. Med. Devices* **2013,** *10*, 85.10.1586/erd.12.70.
49. Neoh, K. G.; Wang, R.; Kang, E. T., Surface nanoengineering for combating biomaterials infections. In *Biomaterials and medical device - associated infections*, 2015; pp 133-161.10.1533/9780857097224.2.133
50. Varela Kellesarian, S.; Abduljabbar, T.; Vohra, F.; Malmstrom, H.; Yunker, M.; Varela Kellesarian, T.; Romanos, G. E.; Javed, F., Efficacy of antimicrobial photodynamic therapy in the disinfection of acrylic denture surfaces: A systematic review. *Photodiagnosis Photodyn Ther* **2017,** *17*, 103-110.10.1016/j.pdpdt.2016.12.001
51. Kokare, C. R.; Chakraborty, S.; Khopade, A. N.; Mahadik, K. R., Biofilm: Importance and applications. *Indian J. Biotechnol.* **2009,** *8*, 159-168
52. Zhang, L.; Gowardman, J.; Rickard, C. M., Impact of microbial attachment on intravascular catheter-related infections. *Int. J. Antimicrob. Agents* **2011,** *38* (1), 9-15.10.1016/j.ijantimicag.2011.01.020
53. Rodrigues, L.; Banat, I. M.; Teixeira, J.; Oliveira, R., Strategies for the prevention of microbial biofilm formation on silicone rubber voice prostheses. *J. Biomed. Mater. Res. B Appl. Biomater.* **2007,** *81* (2), 358-70.10.1002/jbm.b.30673
54. Viola, G. M.; Darouiche, R. O., Cardiovascular implantable device infections. *Curr. Infect. Dis. Rep.* **2011,** *13* (4), 333-42.10.1007/s11908-011-0187-7
55. Rohacek, M.; Baddour, L. M., Cardiovascular implantable electronic device infections: associated risk factors and prevention. *Swiss Med. Wkly.* **2015,** *145*, w14157.10.4414/smw.2015.14157
56. Okuda, K. I.; Nagahori, R.; Yamada, S.; Sugimoto, S.; Sato, C.; Sato, M.; Iwase, T.; Hashimoto, K.; Mizunoe, Y., The composition and structure of biofilms developed by propionibacterium acnes isolated from cardiac pacemaker devices. *Front. Microbiol.* **2018,** *9*, 182.10.3389/fmicb.2018.00182

57. Durante-Mangoni, E.; Mattucci, I.; Agrusta, F.; Tripodi, M. F.; Utili, R., Current trends in the management of cardiac implantable electronic device (CIED) infections. *Intern. Emerg. Med.* **2013,** *8* (6), 465-76.10.1007/s11739-012-0797-6
58. Darouiche, R. O., Device-associated infections: a macroproblem that starts with microadherence. *Clin. Infect. Dis.* **2001,** *33*, 1567–72.10.1086/323130
59. Clementy, N.; Carion, P. L.; Leotoing, L.; Lamarsalle, L.; Wilquin-Bequet, F.; Brown, B.; Verhees, K. J. P.; Fernandes, J.; Deharo, J. C., Infections and associated costs following cardiovascular implantable electronic device implantations: a nationwide cohort study. *Europace* **2018,** *0*, 1–7.10.1093/europace/eux387
60. Steckman, D. A.; Varosy, P. D.; Parzynski, C. S.; Masoudi, F. A.; Curtis, J. P.; Sauer, W. H.; Nguyen, D. T., In-hospital complications associated with reoperations of implantable cardioverter defibrillators. *Am. J. Cardiol.* **2014,** *114* (3), 419-26.10.1016/j.amjcard.2014.05.010
61. Phadke, V. K.; Hirsh, D. S.; Goswami, N. D., Patient Report and Review of Rapidly Growing Mycobacterial Infection after Cardiac Device Implantation. *Emerging Infect. Dis.* **2016,** *22* (3).10.3201/eid2103.150584
62. Rodriguez, D. J.; Afzal, A.; Evonich, R.; Haines, D. E., The prevalence of methicillin resistant organisms among pacemaker and defibrillator implant recipients. *Am. J. Cardiovasc. Dis.* **2012,** *2* (2), 116-122
63. Palraj, B. R.; Farid, S.; Sohail, M. R., Strategies to prevent infections associated with cardiovascular implantable electronic devices. *Expert Rev. Med. Devices* **2017,** *14* (5), 371-381.10.1080/17434440.2017.1322506
64. Baddour, L. M.; Epstein, A. E.; Erickson, C. C.; Knight, B. P.; Levison, M. E.; Lockhart, P. B.; Masoudi, F. A.; Okum, E. J.; Wilson, W. R.; Beerman, L. B.; Bolger, A. F.; Estes, N. A.; Gewitz, M.; Newburger, J. W.; Schron, E. B.; Taubert, K. A., Update on cardiovascular implantable electronic device infections and their management: a scientific statement from the American Heart Association. *Circulation* **2010,** *121* (3), 458-77.10.1161/CIRCULATIONAHA.109.192665
65. Laverty, G.; Gorman, S. P.; Gilmore, B. F., Biofilms and implant-associated infections. In *Biomaterial and medical device associated infection*, 2015; pp 19-45.10.1533/9780857097224.1.19
66. Padera, R. F., Infection in ventricular assist devices: the role of biofilm. *Cardiovasc. Pathol.* **2006,** *15* (5), 264-70.10.1016/j.carpath.2006.04.008
67. Stoodley, P.; Hall-Stoodley, L.; Costerton, B.; DeMeo, P.; Shirtliff, M.; Gawalt, E.; Kathju, S., Biofilms, biomaterials, and device-related infections. In *Handbook of polymer applications in medicine and medical devices*, 2013; pp 77-101.10.1016/b978-0-323-22805-3.00005-0
68. Singhai, M.; Malik, A.; Shahid, M.; Malik, M. A.; Goyal, R., A study on device-related infections with special reference to biofilm production and antibiotic resistance. *J. Global Infect. Dis.* **2012,** *4* (4), 193-8.10.4103/0974-777X.103896
69. Fux, C. A.; Stoodley, P.; Hall-Stoodley, L.; Costerton, J. W., Bacterial biofilms: a diagnostic and therapeutic challenge. *Expert Rev. Anti-infect. Ther.* **2003,** *1* (4), 667–683
70. Farley, T. M. M.; Rosenberg, M. J.; Rowe, P. J.; Chen, J.-H.; Meirik, O., Intrauterine devices and pelvic inflammatory disease: an international perspective. *The Lancet* **1992,** *339*, 785-788
71. Bendig, J. W. A.; Barker, K. F.; Driscoll, J. C. O., Purulent salpingitis and intra-uterine contraceptive device-related infection due to Haernophilus influenzae. **1990**,

72. Steele, K. R.; Szczotka-Flynn, L., Epidemiology of contact lens-induced infiltrates: an updated review. *Clin. Exp. Optom.* **2017,** *100* (5), 473-481.10.1111/cxo.12598
73. Stoica, P.; Chifiriuc, M. C.; Rapa, M.; Lazăr, V., Overview of biofilm-related problems in medical devices. In *Biofilms and implantable medical devices*, 2017; pp 3-23.10.1016/b978-0-08-100382-4.00001-0
74. Rimondini, L.; Cochis, A.; Varoni, E.; Azzimonti, B.; Carrassi, A., Biofilm formation on implants and prosthetic dental materials. In *Handbook of bioceramics and biocomposites*, 2016; pp 991-1027.10.1007/978-3-319-12460-5_48
75. Hahnel, S., Biofilms on dental implants. In *Biofilms and implantable medical devices*, 2017; pp 117-140.10.1016/b978-0-08-100382-4.00005-8
76. Laosuwan, K.; Epasinghe, D. J.; Wu, Z.; Leung, W. K.; Green, D. W.; Jung, H. S., Comparison of biofilm formation and migration of Streptococcus mutans on tooth roots and titanium miniscrews. *Clin. Exp. Dent. Res.* **2018,** *4* (2), 40-47.10.1002/cre2.101
77. Gokmenoglu, C.; Kara, N. B.; Belduz, M.; Kamburoglu, A.; Tosun, I.; Sadik, E.; Kara, C., Evaluation of Candida Albicans biofilm formation on various parts of implant material surfaces. *Niger. J. Clin. Pract.* **2018,** *21* (1), 33-37.10.4103/1119-3077.224793
78. Shah, S. R.; Tatara, A. M.; D'Souza, R. N.; Mikos, A. G.; Kasper, F. K., Evolving strategies for preventing biofilm on implantable materials. *Mater. Today* **2013,** *16* (5), 177-182.10.1016/j.mattod.2013.05.003
79. Roehling, S.; Astasov-Frauenhoffer, M.; Hauser-Gerspach, I.; Braissant, O.; Woelfler, H.; Waltimo, T.; Kniha, H.; Gahlert, M., In vitro biofilm formation on titanium and zirconia implant surfaces. *J. Periodontol.* **2017,** *88* (3), 298-307.10.1902/jop.2016.160245
80. Roos-Jansaker, A. M.; Renvert, H.; Lindahl, C.; Renvert, S., Nine- to fourteen-year follow-up of implant treatment. Part III: factors associated with peri-implant lesions. *J. Clin. Periodontol.* **2006,** *33* (4), 296-301.10.1111/j.1600-051X.2006.00908.x
81. Frisch, E.; Ziebolz, D.; Vach, K.; Ratka-Kruger, P., Supportive post-implant therapy: patient compliance rates and impacting factors: 3-year follow-up. *J. Clin. Periodontol.* **2014,** *41* (10), 1007-14.10.1111/jcpe.12298
82. Johansson, L.; Hailer, N. P.; Rahme, H., High incidence of periprosthetic joint infection with propionibacterium acnes after the use of a stemless shoulder prosthesis with metaphyseal screw fixation - a retrospective cohort study of 241 patients. *BMC Musculoskelet. Disord.* **2017,** *18* (1), 203.10.1186/s12891-017-1555-8
83. Arciola, C. R.; Campoccia, D.; Montanaro, L., Implant infections: adhesion, biofilm formation and immune evasion. *Nat. Rev. Microbiol.* **2018**.10.1038/s41579-018-0019-y
84. Phillips, J. E.; Crane, T. P.; Noy, M.; Elliott, T. S. J.; Grimer, R. J., The incidence of deep prosthetic infections in a specialist orthopaedic hospital. *J. Bone Joint Surg. Br.* **2006,** *88-B* (7), 943-948.10.1302/0301-620X.88B7
85. Ribeiro, M.; Monteiro, F. J.; Ferraz, M. P., Infection of orthopedic implants with emphasis on bacterial adhesion process and techniques used in studying bacterial-material interactions. *Biomatter.* **2012,** *2* (4), 176-94.10.4161/biom.22905
86. Brady, R. A.; Calhoun, J. H.; Leid, J. G.; Shirtliff, M. E., Infections of Orthopaedic Implants and Devices. *Springer Ser. Biofilms* **2008**.10.1007/7142_2008_251
87. Nickinson, R. S.; Board, T. N.; Gambhir, A. K.; Porter, M. L.; Kay, P. R., The microbiology of the infected knee arthroplasty. *Int. Orthop.* **2010,** *34* (4), 505-10.10.1007/s00264-009-0797-y
88. Glage, S.; Paret, S.; Winkel, A.; Stiesch, M.; Bleich, A.; Krauss, J. K.; Schwabe, K., A new model for biofilm formation and inflammatory tissue reaction: intraoperative infection of

a cranial implant with Staphylococcus aureus in rats. *Acta Neurochir.* **2017,** *159* (9), 1747-1756.10.1007/s00701-017-3244-7
89. Chu, C.-B.; Zeng, H.; Shen, D.-X.; Wang, H.; Wang, J.-F.; Cui, F.-Z., A new rabbit model of implant-related biofilm infection: development and evaluation. *Front. Mater. Sci.* **2015,** *10* (1), 80-89.10.1007/s11706-016-0324-1
90. Bresco, M. S.; Harris, L. G.; Thompson, K.; Stanic, B.; Morgenstern, M.; O'Mahony, L.; Richards, R. G.; Moriarty, T. F., Pathogenic mechanisms and host interactions in staphylococcus epidermidis device-related infection. *Front. Microbiol.* **2017,** *8*, 1401.10.3389/fmicb.2017.01401
91. Basile, A. R.; Basile, F.; Basile, A. V. D., Late infection following breast augmentation with textured silicone gel-filled implants. *Aesthet. Surg. J.* **2005,** *25* (3), 249-54.10.1016/j.asj.2005.02.006
92. Alexander, J. W., History of the Medical Use of Silver. *Surg. Infect.* **2009,** *10* (3), 289-292.10.1089/sur.2008.9941
93. Sondi, I.; Salopek-Sondi, B., Silver nanoparticles as antimicrobial agent: a case study on E. coli as a model for Gram-negative bacteria. *Journal of Colloid and Interface Science* **2004,** *275* (1), 177-182.https://doi.org/10.1016/j.jcis.2004.02.012
94. Li, W.-R.; Xie, X.-B.; Shi, Q.-S.; Zeng, H.-Y.; Ou-Yang, Y.-S.; Chen, Y.-B., Antibacterial activity and mechanism of silver nanoparticles on Escherichia coli. *Applied Microbiology and Biotechnology* **2010,** *85* (4), 1115-1122.10.1007/s00253-009-2159-5
95. Ahumada, M.; Bohne, C.; Oake, J.; Alarcon, E. I., Protein capped nanosilver free radical oxidation: role of biomolecule capping on nanoparticle colloidal stability and protein oxidation. *Chem Commun (Camb)* **2018,** *54* (37), 4724-4727.10.1039/c7cc08629f
96. Alarcon, E. I.; Udekwu, K.; Skog, M.; Pacioni, N. L.; Stamplecoskie, K. G.; Gonzalez-Bejar, M.; Polisetti, N.; Wickham, A.; Richter-Dahlfors, A.; Griffith, M.; Scaiano, J. C., The biocompatibility and antibacterial properties of collagen-stabilized, photochemically prepared silver nanoparticles. *Biomaterials* **2012,** *33* (19), 4947-56.10.1016/j.biomaterials.2012.03.033
97. Choi, O.; Deng, K. K.; Kim, N.-J.; Ross, L.; Surampalli, R. Y.; Hu, Z., The inhibitory effects of silver nanoparticles, silver ions, and silver chloride colloids on microbial growth. *Water Research* **2008,** *42* (12), 3066-3074.https://doi.org/10.1016/j.watres.2008.02.021
98. Lazurko, C.; Ahumada, M.; Valenzuela-Henríquez, F.; Alarcon, E. I., NANoPoLC algorithm for correcting nanoparticle concentration by sample polydispersity. *Nanoscale* **2018,** *10* (7), 3166-3170.10.1039/C7NR08672E
99. Stoehr, L. C.; Gonzalez, E.; Stampfl, A.; Casals, E.; Duschl, A.; Puntes, V.; Oostingh, G. J., Shape matters: effects of silver nanospheres and wires on human alveolar epithelial cells. *Part Fibre Toxicol* **2011,** *8*, 36.10.1186/1743-8977-8-36
100. Powers, C. M.; Badireddy, A. R.; Ryde, I. T.; Seidler, F. J.; Slotkin, T. A., Silver nanoparticles compromise neurodevelopment in PC12 cells: critical contributions of silver ion, particle size, coating, and composition. *Environ Health Perspect* **2011,** *119* (1), 37-44.10.1289/ehp.1002337
101. Rai, M. K.; Deshmukh, S. D.; Ingle, A. P.; Gade, A. K., Silver nanoparticles: the powerful nanoweapon against multidrug-resistant bacteria. *J Appl Microbiol* **2012,** *112* (5), 841-52.10.1111/j.1365-2672.2012.05253.x
102. Mchugh, G. L.; Moellering, R.; Hopkins, C.; Swartz, M., Salmonella typhimurium resistant to silver nitrate, chloramphenicol, and ampicillin.: A New Threat in Burn Units ? *The Lancet* **1975,** *305* (7901), 235-240.https://doi.org/10.1016/S0140-6736(75)91138-1

103. Bridges, K.; Kidson, A.; Lowbury, E. J.; Wilkins, M. D., Gentamicin- and silver-resistant pseudomonas in a burns unit. *British Medical Journal* **1979,** *1* (6161), 446
104. Zhang, C.; Liang, Z.; Hu, Z., Bacterial response to a continuous long-term exposure of silver nanoparticles at sub-ppm silver concentrations in a membrane bioreactor activated sludge system. *Water Research* **2014,** *50*, 350-358.https://doi.org/10.1016/j.watres.2013.10.047
105. Alt, V.; Bechert, T.; Steinrucke, P.; Wagener, M.; Seidel, P.; Dingeldein, E.; Domann, E.; Schnettler, R., An in vitro assessment of the antibacterial properties and cytotoxicity of nanoparticulate silver bone cement. *Biomaterials* **2004,** *25* (18), 4383-91.10.1016/j.biomaterials.2003.10.078
106. Pacioni, N. L.; Borsarelli, C. D.; Rey, V.; Veglia, A. V., Synthetic Routes for the Preparation of Silver Nanoparticles. In *Silver Nanoparticle Applications: In the Fabrication and Design of Medical and Biosensing Devices*, Alarcon, E. I.; Griffith, M.; Udekwu, K. I., Eds. Springer International Publishing: Cham, 2015; pp 13-46.10.1007/978-3-319-11262-6_2
107. Ravve, A., Photosensitizers and Photoinitiators. In *Light-Associated Reactions of Synthetic Polymers*, Ravve, A., Ed. Springer New York: New York, NY, 2006; pp 23-122.10.1007/0-387-36414-5_2
108. Turkevich, J.; Stevenson, P. C.; Hillier, J., A study of the nucleation and growth processes in the synthesis of colloidal gold. *Discuss. Faraday Soc.* **1951,** *11*, 55-75.10.1039/DF9511100055
109. Lee, P. C.; Meisel, D., Adsorption and Surface-Enhanced Raman of Dyes on Silver and Gold Sols. *J. Phys. Chem.* **1982,** *86*, 3391–3395
110. Pillai, Z. S.; Kamat, P. V., What factors control the size and shape of silver nanoparticles in the citrate ion reduction method? *J. Phys. Chem. B* **2004,** *108*, 945–951
111. McLaughlin, S.; Ahumada, M.; Franco, W.; Mah, T. F.; Seymour, R.; Suuronen, E. J.; Alarcon, E. I., Sprayable peptide-modified silver nanoparticles as a barrier against bacterial colonization. *Nanoscale* **2016,** *8* (46), 19200-19203.10.1039/c6nr07976h
112. Vignoni, M.; de Alwis Weerasekera, H.; Simpson, M. J.; Phopase, J.; Mah, T. F.; Griffith, M.; Alarcon, E. I.; Scaiano, J. C., LL37 peptide@silver nanoparticles: combining the best of the two worlds for skin infection control. *Nanoscale* **2014,** *6* (11), 5725-8.10.1039/c4nr01284d
113. Albers, C. E.; Hofstetter, W.; Siebenrock, K. A.; Landmann, R.; Klenke, F. M., In vitro cytotoxicity of silver nanoparticles on osteoblasts and osteoclasts at antibacterial concentrations. *Nanotoxicology* **2013,** *7* (1), 30-6.10.3109/17435390.2011.626538
114. Simpson, M. J.; Poblete, H.; Griffith, M.; Alarcon, E. I.; Scaiano, J. C., Impact of dye-protein interaction and silver nanoparticles on rose bengal photophysical behavior and protein photocrosslinking. *Photochem Photobiol* **2013,** *89* (6), 1433-41.10.1111/php.12119
115. Martinez-Gutierrez, F.; Olive, P. L.; Banuelos, A.; Orrantia, E.; Nino, N.; Sanchez, E. M.; Ruiz, F.; Bach, H.; Av-Gay, Y., Synthesis, characterization, and evaluation of antimicrobial and cytotoxic effect of silver and titanium nanoparticles. *Nanomedicine* **2010,** *6* (5), 681-8.10.1016/j.nano.2010.02.001
116. Travan, A.; Pelillo, C.; Donati, I.; Marsich, E.; Benincasa, M.; Scarpa, T.; Semeraro, S.; Turco, G.; Gennaro, R.; Paoletti, S., Non-cytotoxic Silver Nanoparticle Polysaccharide Nanocomposites with Antimicrobial Activity. *Biomacromolecules* **2009,** *10* (6), 1429–1435
117. Ajitha, B.; Kumar Reddy, Y. A.; Reddy, P. S.; Jeon, H.-J.; Ahn, C. W., Role of capping agents in controlling silver nanoparticles size, antibacterial activity and potential application

as optical hydrogen peroxide sensor. *RSC Advances* **2016,** *6* (42), 36171-36179.10.1039/c6ra03766f
118. Alarcon, E. I.; Udekwu, K. I.; Noel, C. W.; Gagnon, L. B.; Taylor, P. K.; Vulesevic, B.; Simpson, M. J.; Gkotzis, S.; Islam, M. M.; Lee, C. J.; Richter-Dahlfors, A.; Mah, T. F.; Suuronen, E. J.; Scaiano, J. C.; Griffith, M., Safety and efficacy of composite collagen-silver nanoparticle hydrogels as tissue engineering scaffolds. *Nanoscale* **2015,** *7* (44), 18789-98.10.1039/c5nr03826j
119. Pallavicini, P.; Arciola, C. R.; Bertoglio, F.; Curtosi, S.; Dacarro, G.; D'Agostino, A.; Ferrari, F.; Merli, D.; Milanese, C.; Rossi, S.; Taglietti, A.; Tenci, M.; Visai, L., Silver nanoparticles synthesized and coated with pectin: An ideal compromise for anti-bacterial and anti-biofilm action combined with wound-healing properties. *J Colloid Interface Sci* **2017,** *498*, 271-281.10.1016/j.jcis.2017.03.062
120. De Giglio, E.; Cafagna, D.; Cometa, S.; Allegretta, A.; Pedico, A.; Giannossa, L. C.; Sabbatini, L.; Mattioli-Belmonte, M.; Iatta, R., An innovative, easily fabricated, silver nanoparticle-based titanium implant coating: development and analytical characterization. *Anal Bioanal Chem* **2013,** *405* (2-3), 805-16.10.1007/s00216-012-6293-z
121. Masurkar, S. A.; Chaudhari, P. R.; Shidore, V. B.; Kamble, S. P., Effect of biologically synthesised silver nanoparticles on Staphylococcus aureus biofilm quenching and prevention of biofilm formation. *IET Nanobiotechnol* **2012,** *6* (3), 110-4.10.1049/iet-nbt.2011.0061
122. Fayaz, A. M.; Balaji, K.; Girilal, M.; Yadav, R.; Kalaichelvan, P. T.; Venketesan, R., Biogenic synthesis of silver nanoparticles and their synergistic effect with antibiotics: a study against gram-positive and gram-negative bacteria. *Nanomedicine* **2010,** *6* (1), 103-9.10.1016/j.nano.2009.04.006
123. Wu, X.; Li, H.; Xiao, N., Advancement of Near-infrared (NIR) laser interceded surface enactment of proline functionalized graphene oxide with silver nanoparticles for proficient antibacterial, antifungal and wound recuperating therapy in nursing care in hospitals. *J. Photochem Photobiol B* **2018,** *187*, 89-95.10.1016/j.jphotobiol.2018.07.015
124. Wehling, J.; Koser, J.; Lindner, P.; Luder, C.; Beutel, S.; Kroll, S.; Rezwan, K., Silver nanoparticle-doped zirconia capillaries for enhanced bacterial filtration. *Mater Sci Eng C Mater Biol Appl* **2015,** *48*, 179-87.10.1016/j.msec.2014.12.001
125. Gillett, A. R.; Baxter, S. N.; Hodgson, S. D.; Smith, G. C.; Thomas, P. J., Using sub-micron silver-nanoparticle based films to counter biofilm formation by Gram-negative bacteria. *Applied Surface Science* **2018,** *442*, 288-297.10.1016/j.apsusc.2018.02.116
126. Divakar, D. D.; Jastaniyah, N. T.; Altamimi, H. G.; Alnakhli, Y. O.; Muzaheed; Alkheraif, A. A.; Haleem, S., Enhanced antimicrobial activity of naturally derived bioactive molecule chitosan conjugated silver nanoparticle against dental implant pathogens. *Int J Biol Macromol* **2018,** *108*, 790-797.10.1016/j.ijbiomac.2017.10.166
127. Cheng, H.; Li, Y.; Huo, K.; Gao, B.; Xiong, W., Long-lasting in vivo and in vitro antibacterial ability of nanostructured titania coating incorporated with silver nanoparticles. *J Biomed Mater Res A* **2014,** *102* (10), 3488-99.10.1002/jbm.a.35019
128. Actis, L.; Srinivasan, A.; Lopez-Ribot, J. L.; Ramasubramanian, A. K.; Ong, J. L., Effect of silver nanoparticle geometry on methicillin susceptible and resistant Staphylococcus aureus, and osteoblast viability. *J Mater Sci Mater Med* **2015,** *26* (7), 215.10.1007/s10856-015-5538-8
129. Thomas, R.; Soumya, K. R.; Mathew, J.; Radhakrishnan, E. K., Inhibitory effect of silver nanoparticle fabricated urinary catheter on colonization efficiency of Coagulase

Negative Staphylococci. *J Photochem Photobiol B* **2015,** *149*, 68-77.10.1016/j.jphotobiol.2015.04.034
130. Gorzelanny, C.; Kmeth, R.; Obermeier, A.; Bauer, A. T.; Halter, N.; Kumpel, K.; Schneider, M. F.; Wixforth, A.; Gollwitzer, H.; Burgkart, R.; Stritzker, B.; Schneider, S. W., Silver nanoparticle-enriched diamond-like carbon implant modification as a mammalian cell compatible surface with antimicrobial properties. *Sci Rep* **2016,** *6*, 22849.10.1038/srep22849
131. Velusamy, P.; Su, C. H.; Venkat Kumar, G.; Adhikary, S.; Pandian, K.; Gopinath, S. C.; Chen, Y.; Anbu, P., Biopolymers Regulate Silver Nanoparticle under Microwave Irradiation for Effective Antibacterial and Antibiofilm Activities. *PLoS One* **2016,** *11* (6), e0157612.10.1371/journal.pone.0157612
132. Zhong, X.; Song, Y.; Yang, P.; Wang, Y.; Jiang, S.; Zhang, X.; Li, C., Titanium Surface Priming with Phase-Transited Lysozyme to Establish a Silver Nanoparticle-Loaded Chitosan/Hyaluronic Acid Antibacterial Multilayer via Layer-by-Layer Self-Assembly. *PLoS One* **2016,** *11* (1), e0146957.10.1371/journal.pone.0146957
133. da Silva Ferreira, V.; ConzFerreira, M. E.; Lima, L. M.; Frases, S.; de Souza, W.; Sant'Anna, C., Green production of microalgae-based silver chloride nanoparticles with antimicrobial activity against pathogenic bacteria. *Enzyme Microb Technol* **2017,** *97*, 114-121.10.1016/j.enzmictec.2016.10.018
134. Kora, A. J.; Sashidhar, R. B., Biogenic silver nanoparticles synthesized with rhamnogalacturonan gum: Antibacterial activity, cytotoxicity and its mode of action. *Arabian Journal of Chemistry* **2018,** *11* (3), 313-323.10.1016/j.arabjc.2014.10.036
135. Dhayalan, M.; Denison, M. I. J.; Ayyar, M.; Gandhi, N. N.; Krishnan, K.; Abdulhadi, B., Biogenic synthesis, characterization of gold and silver nanoparticles from Coleus forskohlii and their clinical importance. *J Photochem Photobiol B* **2018,** *183*, 251-257.10.1016/j.jphotobiol.2018.04.042
136. Ojo, O. A.; Oyinloye, B. E.; Ojo, A. B.; Ajiboye, B. O.; Olayide, I. I.; Idowu, O.; Olasehinde, O.; Fadugba, A.; Adewunmi, F., Green-route mediated synthesis of silver nanoparticles (AgNPs) from Syzygium cumini (L.) Skeels polyphenolic-rich leaf extracts and investigation of their antimicrobial activity. *IET Nanobiotechnology* **2018,** *12* (3), 305-310.10.1049/iet-nbt.2017.0127
137. Ferraris, S.; Spriano, S.; Miola, M.; Bertone, E.; Allizond, V.; Cuffini, A. M.; Banche, G., Surface modification of titanium surfaces through a modified oxide layer and embedded silver nanoparticles: Effect of reducing/stabilizing agents on precipitation and properties of the nanoparticles. *Surface and Coatings Technology* **2018,** *344*, 177-189.10.1016/j.surfcoat.2018.03.020
138. Lee, S. J.; Heo, M.; Lee, D.; Han, S.; Moon, J.-H.; Lim, H.-N.; Kwon, I. K., Preparation and characterization of antibacterial orthodontic resin containing silver nanoparticles. *Applied Surface Science* **2018,** *432*, 317-323.10.1016/j.apsusc.2017.04.030
139. Xu, T.; Zhang, J.; Zhu, Y.; Zhao, W.; Pan, C.; Ma, H.; Zhang, L., A poly(hydroxyethyl methacrylate)-Ag nanoparticle porous hydrogel for simultaneous in vivo prevention of the foreign-body reaction and bacterial infection. *Nanotechnology* **2018,** *29* (39), 395101.10.1088/1361-6528/aad257
140. Jo, Y. K.; Seo, J. H.; Choi, B. H.; Kim, B. J.; Shin, H. H.; Hwang, B. H.; Cha, H. J., Surface-independent antibacterial coating using silver nanoparticle-generating engineered mussel glue. *ACS Appl Mater Interfaces* **2014,** *6* (22), 20242-53.10.1021/am505784k

141. Gunell, M.; Haapanen, J.; Brobbey, K. J.; Saarinen, J. J.; Toivakka, M.; Makela, J. M.; Huovinen, P.; Eerola, E., Antimicrobial characterization of silver nanoparticle-coated surfaces by "touch test" method. *Nanotechnol Sci Appl* **2017,** *10*, 137-145.10.2147/NSA.S139505
142. Velmurugan, P.; Lee, S. M.; Cho, M.; Park, J. H.; Seo, S. K.; Myung, H.; Bang, K. S.; Oh, B. T., Antibacterial activity of silver nanoparticle-coated fabric and leather against odor and skin infection causing bacteria. *Appl. Microbiol Biotechnol* **2014,** *98* (19), 8179-89.10.1007/s00253-014-5945-7
143. Lv, X.; Wang, H.; Su, A.; Chu, Y., A novel approach of silver-sericin nanoparticles synthesis and their potential as microbicide candidates. *J Microbiol Biotechnol* **2018**.10.4014/jmb.1803.02054
144. Thiyagarajan, K.; Bharti, V. K.; Tyagi, S.; Tyagi, P. K.; Ahuja, A.; Kumar, K.; Raj, T.; Kumar, B., Synthesis of non-toxic, biocompatible, and colloidal stable silver nanoparticle using egg-white protein as capping and reducing agents for sustainable antibacterial application. *RSC Advances* **2018,** *8* (41), 23213-23229.10.1039/c8ra03649g
145. Alarcon, E. I.; Vulesevic, B.; Argawal, A.; Ross, A.; Bejjani, P.; Podrebarac, J.; Ravichandran, R.; Phopase, J.; Suuronen, E. J.; Griffith, M., Coloured cornea replacements with anti-infective properties: expanding the safe use of silver nanoparticles in regenerative medicine. *Nanoscale* **2016,** *8* (12), 6484-9.10.1039/c6nr01339b
146. Zhao, L.; Wang, H.; Huo, K.; Cui, L.; Zhang, W.; Ni, H.; Zhang, Y.; Wu, Z.; Chu, P. K., Antibacterial nano-structured titania coating incorporated with silver nanoparticles. *Biomaterials* **2011,** *32* (24), 5706-16.10.1016/j.biomaterials.2011.04.040
147. Azeez, M. A.; Lateef, A.; Asafa, T. B.; Yekeen, T. A.; Akinboro, A.; Oladipo, I. C.; Gueguim-Kana, E. e. B.; Beukes, L. S., Biomedical Applications of Cocoa Bean Extract-Mediated Silver Nanoparticles as Antimicrobial, Larvicidal and Anticoagulant Agents. *J. Clust. Sci.* **2017,** *28* (1), 149-164.10.1007/s10876-016-1055-2
148. Singhal, G.; Bhavesh, R.; Kasariya, K.; Sharma, A. R.; Singh, R. P., Biosynthesis of silver nanoparticles using Ocimum sanctum (Tulsi) leaf extract and screening its antimicrobial activity. *J. Nanopart. Res.* **2011,** *13* (7), 2981-2988.10.1007/s11051-010-0193-y
149. Zhang, H.; Peng, M.; Cheng, T.; Zhao, P.; Qiu, L.; Zhou, J.; Lu, G.; Chen, J., Silver nanoparticles-doped collagen–alginate antimicrobial biocomposite as potential wound dressing. *J. Mater. Sci.* **2018,** *53* (21), 14944-14952.10.1007/s10853-018-2710-9
150. Harris, M., http://www.airbrushmakeupsalon.com/airbrush-makeup-review-belloccio-airbrush-makeup-the-big-review/. **2012**,
151. Chang, C. Y., Surface Sensing for Biofilm Formation in Pseudomonas aeruginosa. *Front. Microbiol.* **2017,** *8*.10.3389/fmicb.2017.02671
152. Klockgether, J.; Munder, A.; Neugebauer, J.; Davenport, C. F.; Stanke, F.; Larbig, K. D.; Heeb, S.; Schock, U.; Pohl, T. M.; Wiehlmann, L.; Tummler, B., Genome diversity of Pseudomonas aeruginosa PAO1 laboratory strains. *J Bacteriol* **2010,** *192* (4), 1113-21.10.1128/JB.01515-09
153. Mathee, K., Forensic investigation into the origin of Psuedomonas aeuginosa PA14-old but not lost. *J. Med. Microbiol.* **2018,** *67*, 1019-1021.10.1099/jmm.0.000778
154. Christensen, G. D.; Bisno, A. L.; Parisi, J. T.; McLaughlin, B.; Hester, M. G.; Luther, R. W., Nosocomial septicemia due to multiply antibiotic-resistant Staphylococcus epidermidis. *Ann. Intern. Med.* **1982,** *96*, 1-10
155. Stieber, B.; Sabat, A.; Monecke, S.; Slickers, P.; Akkerboom, V.; Muller, E.; Friedrich, A. W.; Ehricht, R., PVL overexpression due to genomic rearrangements and mutations in the

S. aureus reference strain ATCC25923. *BMC Res. Notes* **2017,** *10* (1), 576.10.1186/s13104-017-2891-3
156. Xiao, S. J.; Textor, M.; Spencer, N. D.; Wieland, M.; Keller, B.; Sigrist, H., Immobilization of the cell-adhesive peptide Arg–Gly–Asp–Cys (RGDC) on titanium surfaces by covalent chemical attachment. *J. Mater. Sci. Mater. Med.* **1997,** *8* (12), 867-872.10.1023/A:1018501804943
157. Cushing, B. L.; Kolesnichenko, V. L.; O'Connor, C. J., Recent Advances in the Liquid-Phase Syntheses of Inorganic Nanoparticles. *Chem. Rev.* **2004,** *104* (9), 3893-3946.10.1021/cr030027b
158. Elias, C. N.; Lima, J. H. C.; Valiev, R.; Meyers, M. A., Biomedical applications of titanium and its alloys. *JOM* **2008,** *60* (3), 46-49.10.1007/s11837-008-0031-1
159. Hang, R.; Gao, A.; Bai, L.; Chu, P. K. H., Titania Nanotubes as Silver Nanoparticle Carriers to Prevent Implant-Associated Infection. In *Silver Nanoparticles for Antibacterial Devices*, CRC Press/Taylor & Francis: 2017; pp 85-110
160. Brown, S. A.; Lemons, J. E., *Medical Applications of Titanium and Its Alloys: The Material and Biological Issues*. ASTM International: West Conshohocken, PA, 1996.10.1520/STP1272-EB
161. Whitcher, J. P.; Srinivasan, M.; Upadhyay, M. P., Corneal blindness: a global perspective. *Bulletin of the World Health Organization* **2001,** *79* (3), 214-221
162. Griffith, M.; Polisetti, N.; Kuffova, L.; Gallar, J.; Forrester, J.; Vemuganti, G. K.; Fuchsluger, T. A., Regenerative approaches as alternatives to donor allografting for restoration of corneal function. *Ocul. Surf.* **2012,** *10* (3), 170-83.10.1016/j.jtos.2012.04.004
163. Simpson, F. C.; Griffith, M., Regenerative Medicine in the Cornea. *Current Ophthalmology Reports* **2017,** *5* (3), 187-192.10.1007/s40135-017-0140-5
164. Domingos, R.; Baalousha, M.; Ju-Nam, Y.; Reid, M.; Tufenkji, N.; R Lead, J.; Leppard, G.; Wilkinson, K., *Characterizing Manufactured Nanoparticles in the Environment: Multimethod Determination of Particle Sizes*. Environ. Sci. Technol.: 2009; Vol. 43, p 7277-7284.10.1021/es900249m
165. Jiang, J.; Oberdörster, G.; Biswas, P., Characterization of size, surface charge, and agglomeration state of nanoparticle dispersions for toxicological studies. *J. Nanopart. Res.* **2009,** *11* (1), 77-89.10.1007/s11051-008-9446-4
166. Kermanizadeh, A.; Pojana, G.; Gaiser, B. K.; Birkedal, R.; Bilanicova, D.; Wallin, H.; Jensen, K. A.; Sellergren, B.; Hutchison, G. R.; Marcomini, A.; Stone, V., In vitro assessment of engineered nanomaterials using a hepatocyte cell line: cytotoxicity, pro-inflammatory cytokines and functional markers. *Nanotoxicology* **2013,** *7* (3), 301-13.10.3109/17435390.2011.653416